Technical Summary

A report accepted by Working Group I of the IPCC but not approved in detail

"Acceptance" of IPCC Reports at a Session of the Working Group or Panel signifies that the material has not been subject to line by line discussion and agreement, but nevertheless presents a comprehensive, objective and balanced view of the subject matter.

Co-ordinating Lead Authors

D.L. Albritton (USA), L.G. Meira Filho (Brazil)

Lead Authors

U. Cubasch (Germany), X. Dai (China), Y. Ding (China), D.J. Griggs (UK), B. Hewitson (South Africa), J.T. Houghton (UK), I. Isaksen (Norway), T. Karl (USA), M. McFarland (USA), V.P. Meleshko (Russia), J.F.B. Mitchell (UK), M. Noguer (UK), B.S. Nyenzi (Tanzania), M. Oppenheimer (USA), J.E. Penner (USA), S. Pollonais (Trinidad and Tobago), T. Stocker (Switzerland), K.E. Trenberth (USA)

Contributing Authors

M.R. Allen, (UK), A.P.M. Baede (Netherlands), J.A. Church (Australia), D.H. Ehhalt (Germany), C.K. Folland (UK), F. Giorgi (Italy), J.M. Gregory (UK), J.M. Haywood (UK), J.I. House (Germany), M. Hulme (UK), V.J. Jaramillo (Mexico), A. Jayaraman (India), C.A. Johnson (UK), S. Joussaume (France), D.J. Karoly (Australia), H. Kheshgi (USA), C. Le Quéré (France), L.J. Mata (Germany), B.J. McAvaney (Australia), L.O. Mearns (USA), G.A. Meehl (USA), B. Moore III (USA), R.K. Mugara (Zambia), M. Prather (USA), C. Prentice (Germany), V. Ramaswamy (USA), S.C.B. Raper (UK), M.J. Salinger (New Zealand), R. Scholes (S. Africa), S. Solomon (USA), R. Stouffer (USA), M-X. Wang (China), R.T. Watson (USA), K-S. Yap (Malaysia)

Review Editors

F. Joos (Switzerland), A. Ramirez-Rojas (Venzuela), J.M.R. Stone (Canada), J. Zillman (Australia)

Technical Summary of the Working Group I Report

A. Introduction

A.1 The IPCC and its Working Groups

The Intergovernmental Panel on Climate Change (IPCC) was established by the World Meteorological Organisation (WMO) and the United Nations Environment Programme (UNEP) in 1988. The aim was, and remains, to provide an assessment of the understanding of all aspects of climate change[1], including how human activities can cause such changes and can be impacted by them. It had become widely recognised that human-influenced emissions of greenhouse gases have the potential to alter the climate system (see Box 1), with possible deleterious or beneficial effects. It was also recognised that addressing such global issues required organisation on a global scale, including assessment of the understanding of the issue by the worldwide expert communities.

At its first session, the IPCC was organised into three Working Groups. The current remits of the Working Groups are for Working Group I to address the scientific aspects of the climate system and climate change, Working Group II to address the impacts of and adaptations to climate change, and Working Group III to address the options for the mitigation of climate change. The IPCC provided its first major assessment report in 1990 and its second major assessment report in 1996.

The IPCC reports are (i) up-to-date descriptions of the knowns and unknowns of the climate system and related factors, (ii) based on the knowledge of the international expert communities, (iii) produced by an open and peer-reviewed professional process, and (iv) based upon scientific publications whose findings are summarised in terms useful to decision makers. While the assessed information is policy relevant, the IPCC does not establish or advocate public policy.

The scope of the assessments of Working Group I includes observations of the current changes and trends in the climate system, a reconstruction of past changes and trends, an understanding of the processes involved in those changes, and the incorporation of this knowledge into models that can attribute the causes of changes and that can provide simulation of natural and human-induced future changes in the climate system.

A.2 The First and Second Assessment Reports of Working Group I

In the First Assessment Report in 1990, Working Group I broadly described the status of the understanding of the climate system and climate change that had been gained over the preceding decades of research. Several major points were emphasised. The greenhouse effect is a natural feature of the planet, and its fundamental physics is well understood. The atmospheric abundances of greenhouse gases were increasing, due largely to human activities. Continued future growth in greenhouse gas emissions was predicted to lead to significant increases in the average surface temperature of the planet, increases that would exceed the natural variation of the past several millennia and that could be reversed only slowly. The past century had, at that time, seen a surface warming of nearly 0.5°C, which was broadly consistent with that predicted by climate models for the greenhouse gas increases, but was also comparable to what was then known about natural variation. Lastly, it was pointed out that the current level of understanding at that time and the existing capabilities of climate models limited the prediction of changes in the climate of specific regions.

Based on the results of additional research and Special Reports produced in the interim, IPCC Working Group I assessed the new state of understanding in its Second Assessment Report (SAR[2]) in 1996. The report underscored that greenhouse gas abundances continued to increase in the atmosphere and that very substantial cuts in emissions would be required for stabilisation of greenhouse gas concentrations in the atmosphere (which is the ultimate goal of Article 2 of the Framework Convention on Climate Change). Further, the general increase in

[1] *Climate change* in IPCC usage refers to any change in climate over time, whether due to natural variability or as a result of human activity. This usage differs from that in the Framework Convention on Climate Change, where *climate change* refers to a change of climate that is attributed directly or indirectly to human activity that alters the composition of the global atmosphere and that is in addition to natural climate variability observed over comparable time periods. For a definition of scientific and technical terms: see the Glossary in Appendix I.

[2] The IPCC Second Assessment Report is referred to in this Technical Summary as the SAR.

global temperature continued, with recent years being the warmest since at least 1860. The ability of climate models to simulate observed events and trends had improved, particularly with the inclusion of sulphate aerosols and stratospheric ozone as radiative forcing agents in climate models. Utilising this simulative capability to compare to the observed patterns of regional temperature changes, the report concluded that the ability to quantify the human influence on global climate was limited. The limitations arose because the expected signal was still emerging from the noise of natural variability and because of uncertainties in other key factors. Nevertheless, the report also concluded that "the balance of evidence suggests a discernible human influence on global climate". Lastly, based on a range of scenarios of future greenhouse gas abundances, a set of responses of the climate system was simulated.

A.3 The Third Assessment Report: This Technical Summary

The third major assessment report of IPCC Working Group I builds upon these past assessments and incorporates the results of the past five years of climate research. This Technical Summary is based on the underlying information of the chapters, which is cross-referenced in the Source Notes in the Appendix. This Summary aims to describe the major features (see Figure 1) of the understanding of the climate system and climate change at the outset of the 21st century. Specifically:

- What does the observational record show with regard to past climate changes, both globally and regionally and both on the average and in the extremes? (Section B)

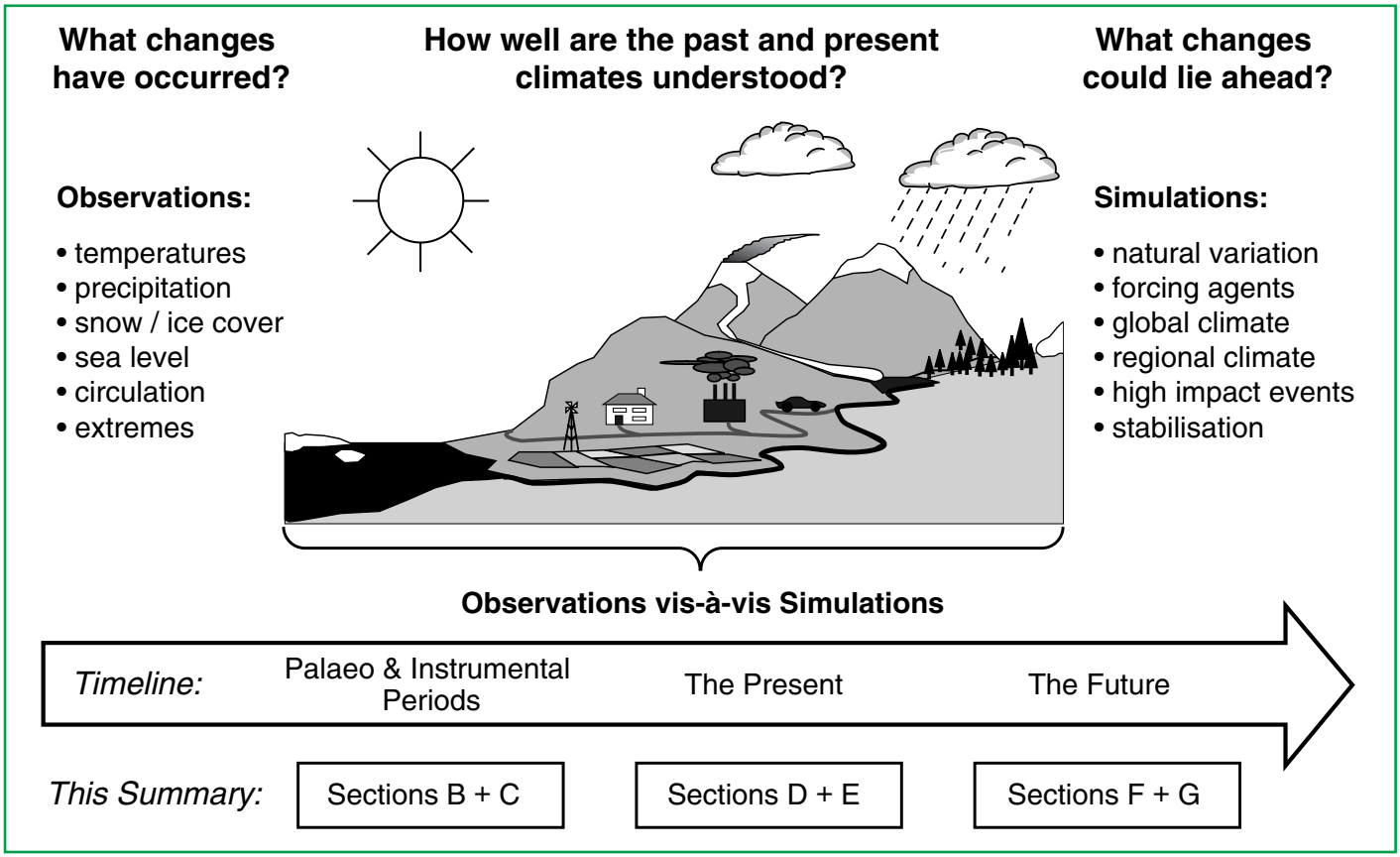

Figure 1: Key questions about the climate system and its relation to humankind. This Technical Summary, which is based on the underlying information in the chapters, is a status report on the answers, presented in the structure indicated.

- How quantitative is the understanding of the agents that cause climate to change, including both those that are natural (e.g., solar variation) and human-related (e.g., greenhouse gases) phenomena? (Section C)
- What is the current ability to simulate the responses of the climate system to these forcing agents? In particular, how well are key physical and biogeochemical processes described by present global climate models? (Section D)
- Based on today's observational data and today's climate predictive capabilities, what does the comparison show regarding a human influence on today's climate? (Section E)
- Further, using current predictive tools, what could the possible climate future be? Namely, for a wide spectrum of projections for several climate-forcing agents, what does current understanding project for global temperatures, regional patterns of precipitation, sea levels, and changes in extremes? (Section F)

Finally, what are the most urgent research activities that need to be addressed to improve our understanding of the climate system and to reduce our uncertainty regarding future climate change?

The Third Assessment Report of IPCC Working Group I is the product of hundreds of scientists from the developed and developing world who contributed to its preparation and review. What follows is a summary of their understanding of the climate system.

Box 1: What drives changes in climate?

The Earth absorbs radiation from the Sun, mainly at the surface. This energy is then redistributed by the atmospheric and oceanic circulations and radiated back to space at longer (infrared) wavelengths. For the annual mean and for the Earth as a whole, the incoming solar radiation energy is balanced approximately by the outgoing terrestrial radiation. Any factor that alters the radiation received from the Sun or lost to space, or that alters the redistribution of energy within the atmosphere and between the atmosphere, land, and ocean, can affect climate. A change in the net radiative energy available to the global Earth-atmosphere system is termed here, and in previous IPCC reports, a radiative forcing. Positive radiative forcings tend to warm the Earth's surface and lower atmosphere. Negative radiative forcings tend to cool them.

Increases in the concentrations of greenhouse gases will reduce the efficiency with which the Earth's surface radiates to space. More of the outgoing terrestrial radiation from the surface is absorbed by the atmosphere and re-emitted at higher altitudes and lower temperatures. This results in a positive radiative forcing that tends to warm the lower atmosphere and surface. Because less heat escapes to space, this is the enhanced greenhouse effect – an enhancement of an effect that has operated in the Earth's atmosphere for billions of years due to the presence of naturally occurring greenhouse gases: water vapour, carbon dioxide, ozone, methane and nitrous oxide. The amount of radiative forcing depends on the size of the increase in concentration of each greenhouse gas, the radiative properties of the gases involved, and the concentrations of other greenhouse gases already present in the atmosphere. Further, many greenhouse gases reside in the atmosphere for centuries after being emitted, thereby introducing a long-term commitment to positive radiative forcing.

Anthropogenic aerosols (microscopic airborne particles or droplets) in the troposphere, such as those derived from fossil fuel and biomass burning, can reflect solar radiation, which leads to a cooling tendency in the climate system. Because it can absorb solar radiation, black carbon (soot) aerosol tends to warm the climate system. In addition, changes in aerosol concentrations can alter cloud amount and cloud reflectivity through their effect on cloud properties and lifetimes. In most cases, tropospheric aerosols tend to produce a negative radiative forcing and a cooler climate. They have a much shorter lifetime (days to weeks) than most greenhouse

gases (decades to centuries), and, as a result, their concentrations respond much more quickly to changes in emissions.

Volcanic activity can inject large amounts of sulphur-containing gases (primarily sulphur dioxide) into the stratosphere, which are transformed into sulphate aerosols. Individual eruptions can produce a large, but transitory, negative radiative forcing, tending to cool the Earth's surface and lower atmosphere over periods of a few years.

The Sun's output of energy varies by small amounts (0.1%) over an 11-year cycle and, in addition, variations over longer periods may occur. On time-scales of tens to thousands of years, slow variations in the Earth's orbit, which are well understood, have led to changes in the seasonal and latitudinal distribution of solar radiation. These changes have played an important part in controlling the variations of climate in the distant past, such as the glacial and inter-glacial cycles.

When radiative forcing changes, the climate system responds on various time-scales. The longest of these are due to the large heat capacity of the deep ocean and dynamic adjustment of the ice sheets. This means that the transient response to a change (either positive or negative) may last for thousands of years. Any changes in the radiative balance of the Earth, including those due to an increase in greenhouse gases or in aerosols, will alter the global hydrological cycle and atmospheric and oceanic circulation, thereby affecting weather patterns and regional temperatures and precipitation.

Any human-induced changes in climate will be embedded in a background of natural climatic variations that occur on a whole range of time- and space-scales. Climate variability can occur as a result of natural changes in the forcing of the climate system, for example variations in the strength of the incoming solar radiation and changes in the concentrations of aerosols arising from volcanic eruptions. Natural climate variations can also occur in the absence of a change in external forcing, as a result of complex interactions between components of the climate system, such as the coupling between the atmosphere and ocean. The El Niño-Southern Oscillation (ENSO) phenomenon is an example of such natural "internal" variability on interannual time-scales. To distinguish anthropogenic climate changes from natural variations, it is necessary to identify the anthropogenic "signal" against the background "noise" of natural climate variability.

B. The Observed Changes in the Climate System

Is the Earth's climate changing? The answer is unequivocally "Yes". A suite of observations supports this conclusion and provides insight about the rapidity of those changes. These data are also the bedrock upon which to construct the answer to the more difficult question: "*Why* is it changing?", which is addressed in later Sections.

This Section provides an updated summary of the observations that delineate how the climate system has changed in the past. Many of the variables of the climate system have been measured directly, i.e., the "instrumental record". For example, widespread direct measurements of surface temperature began around the middle of the 19th century. Near global observations of other surface "weather" variables, such as precipitation and winds, have been made for about a hundred years. Sea level measurements have been made for over 100 years in some places, but the network of tide gauges with long records provides only limited global coverage. Upper air observations have been made systematically only since the late 1940s. There are also long records of surface oceanic observations made from ships since the mid-19th century and by dedicated buoys since about the late 1970s. Sub-surface oceanic temperature measurements with near global coverage are now available from the late 1940s. Since the late 1970s, other data from Earth-observation satellites have been used to provide a wide range of global observations of various components of the climate system. In addition, a growing set of palaeoclimatic data, e.g., from trees, corals, sediments, and ice, are giving information about the Earth's climate of centuries and millennia before the present.

This Section places particular emphasis on current knowledge of past changes in key climate variables: temperature, precipitation and atmospheric moisture, snow cover, extent of land and sea ice, sea level, patterns in atmospheric and oceanic circulation, extreme weather and climate events, and overall features of the climate variability. The concluding part of this Section compares the observed trends in these various climate indicators to see if a collective picture emerges. The degree of this internal consistency is a critical factor in assessing the level of confidence in the current understanding of the climate system.

B.1 Observed Changes in Temperature

Temperatures in the instrumental record for land and oceans

The global average surface temperature has increased by 0.6 ± 0.2°C[3] since the late 19th century. It is very likely that the 1990s was the warmest decade and 1998 the warmest year in the instrumental record since 1861 (see Figure 2). The main cause of the increased estimate of global warming of 0.15°C since the SAR is related to the record warmth of the additional six years (1995 to 2000) of data. A secondary reason is related to improved methods of estimating change. The current, slightly larger uncertainty range (±0.2°C, 95% confidence interval) is also more objectively based. Further, the scientific basis for confidence in the estimates of the increase in global temperature since the late 19th century has been strengthened since the SAR. This is due to the improvements derived from several new studies. These include an independent test of the corrections used for time-dependent biases in the sea surface temperature data and new analyses of the effect of urban "heat island" influences on global land-temperature trends. As indicated in Figure 2, most of the increase in global temperature since the late 19th century has occurred in two distinct periods: 1910 to 1945 and since 1976. The rate of increase of temperature for both periods is about 0.15°C/decade. Recent warming has been greater over land compared to oceans; the increase in sea surface temperature over the period 1950 to 1993 is about half that of the mean land-surface air temperature. The high global temperature associated with the 1997 to 1998 El Niño event stands out as an extreme event, even taking into account the recent rate of warming.

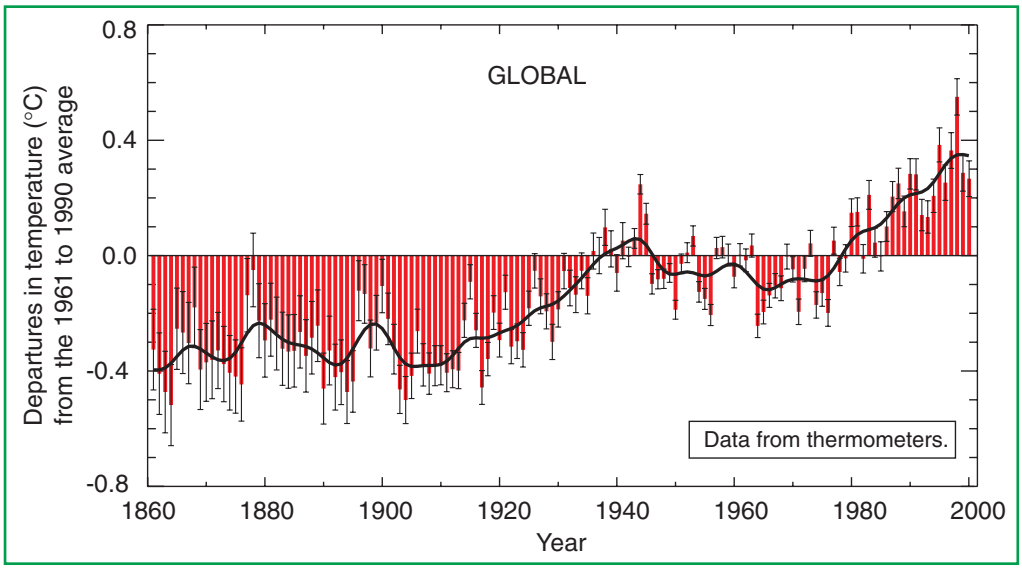

Figure 2: Combined annual land-surface air and sea surface temperature anomalies (°C) 1861 to 2000, relative to 1961 to 1990. Two standard error uncertainties are shown as bars on the annual number. [Based on Figure 2.7c]

The regional patterns of the warming that occurred in the early part of the 20th century were different than those that occurred in the latter part. Figure 3 shows the regional patterns of the warming that have occurred over the full 20th century, as well as for three component time periods. The most recent period of warming (1976 to 1999) has been almost global, but the largest increases in temperature have occurred over the mid- and high latitudes of the continents in the Northern Hemisphere. Year-round cooling is evident in the north-western North Atlantic and the central North Pacific Oceans, but the North Atlantic cooling trend has recently reversed. The recent regional patterns of temperature change have been shown to be related, in part, to various phases of atmospheric-oceanic oscillations, such as the North Atlantic-Arctic Oscillation and possibly the Pacific Decadal Oscillation. Therefore, regional temperature trends over a few decades can be strongly influenced by regional variability in the climate system and can depart appreciably from a global average. The 1910 to 1945 warming was initially concentrated in the North Atlantic. By contrast, the period 1946 to 1975 showed significant cooling in the North Atlantic, as well as much of the Northern Hemisphere, and warming in much of the Southern Hemisphere.

New analyses indicate that global ocean heat content has increased significantly since the late 1950s. More than half of the increase in heat content has occurred in the upper 300 m

[3] Generally, temperature trends are rounded to the nearest 0.05°C per unit of time, the periods often being limited by data availability.

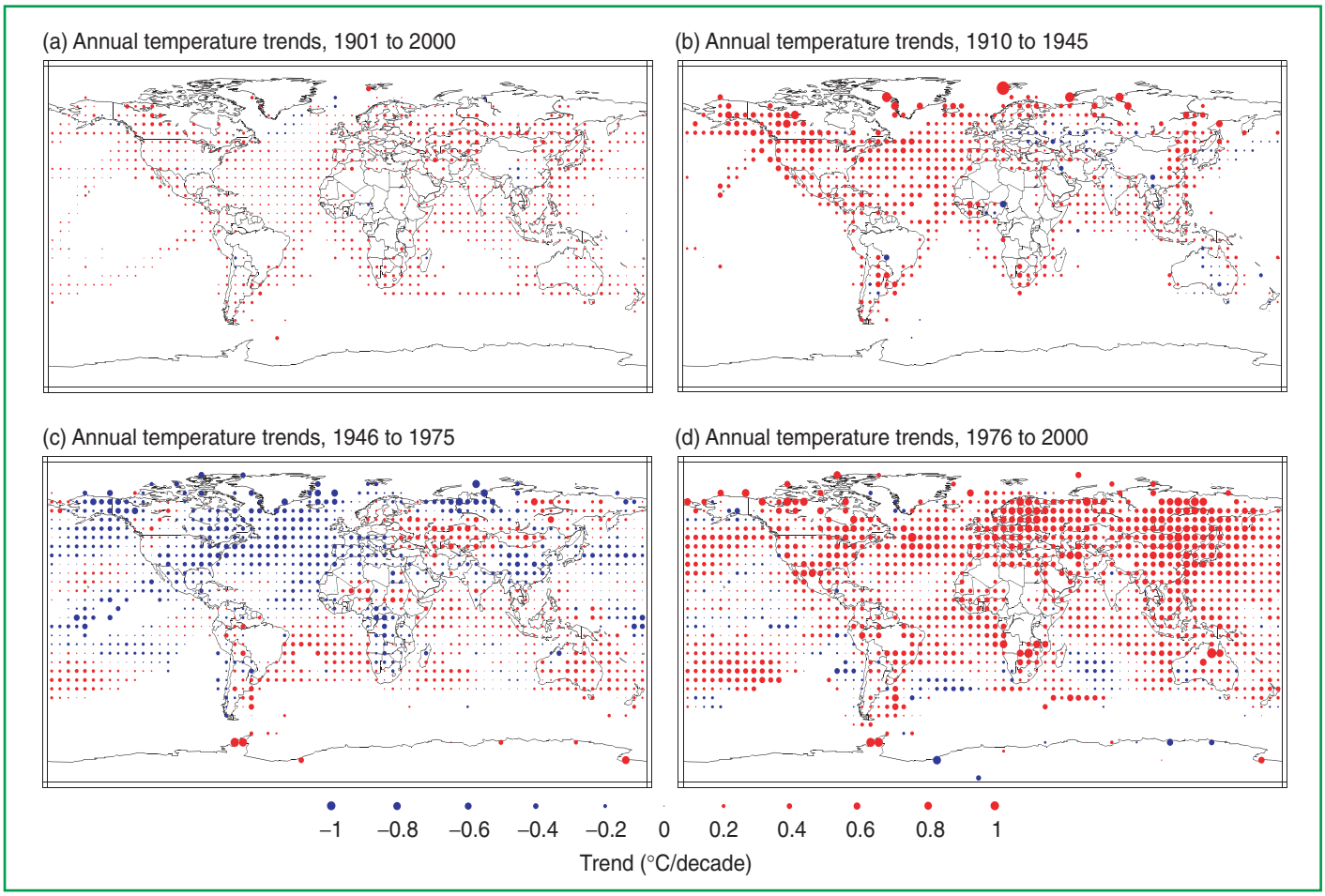

Figure 3: Annual temperature trends for the periods 1901 to 1999, 1910 to 1945, 1946 to 1975 and 1976 to 1999 respectively. Trends are represented by the area of the circle with red representing increases, blue representing decreases, and green little or no change. Trends were calculated from annually averaged gridded anomalies with the requirement that the calculation of annual anomalies include a minimum of 10 months of data. For the period 1901 to 1999, trends were calculated only for those grid boxes containing annual anomalies in at least 66 of the 100 years. The minimum number of years required for the shorter time periods (1910 to 1945, 1946 to 1975, and 1976 to 1999) was 24, 20, and 16 years respectively. [Based on Figure 2.9]

of the ocean, equivalent to a rate of temperature increase in this layer of about 0.04°C/decade.

New analyses of daily maximum and minimum land-surface temperatures for 1950 to 1993 continue to show that this measure of diurnal temperature range is decreasing very widely, although not everywhere. On average, minimum temperatures are increasing at about twice the rate of maximum temperatures (0.2 versus 0.1°C/decade).

Temperatures above the surface layer from satellite and weather balloon records

Surface, balloon and satellite temperature measurements show that the troposphere and Earth's surface have warmed and that the stratosphere has cooled. Over the shorter time period for which there have been both satellite and weather balloon data (since 1979), the balloon and satellite records show significantly less lower-tropospheric warming than observed at the surface. Analyses of temperature trends since 1958 for the lowest 8 km of the atmosphere and at the surface are in

good agreement, as shown in Figure 4a, with a warming of about 0.1°C per decade. However, since the beginning of the satellite record in 1979, the temperature data from both satellites and weather balloons show a warming in the global middle-to-lower troposphere at a rate of approximately 0.05 ± 0.10°C per decade. The global average surface temperature has increased significantly by 0.15 ± 0.05°C/decade. The difference in the warming rates is statistically significant. By contrast, during the period 1958 to 1978, surface temperature trends were near zero, while trends for the lowest 8 km of the atmosphere were near 0.2°C/decade. About half of the observed difference in warming since 1979 is likely[4] to be due to the combination of the differences in spatial coverage of the surface and tropospheric observations and the physical effects of the sequence of volcanic eruptions and a substantial El Niño (see Box 4 for a general description of ENSO) that occurred within this period. The remaining difference is very likely real and not an observing bias. It arises primarily due to differences in the rate of temperature change over the tropical and sub-tropical regions, which were faster in the lowest 8 km of the atmosphere before about 1979, but which have been slower since then. There are no significant differences in warming rates over mid-latitude continental regions in the Northern Hemisphere. In the upper troposphere, no significant global temperature trends have been detected since the early 1960s. In the stratosphere, as shown in Figure 4b, both satellites and balloons show substantial cooling, punctuated by sharp warming episodes of one to two years long that are due to volcanic eruptions.

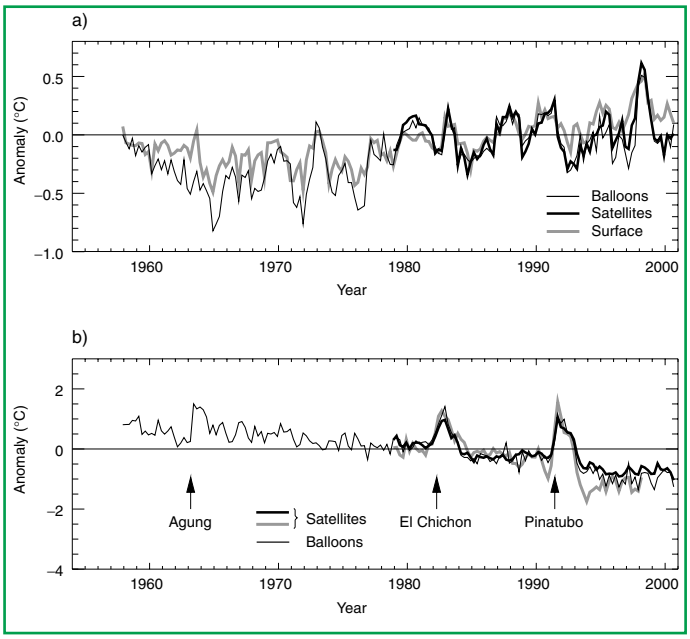

Figure 4: (a) Time-series of seasonal temperature anomalies of the troposphere based on balloons and satellites in addition to the surface. (b) Time-series of seasonal temperature anomalies of the lower stratosphere from balloons and satellites. [Based on Figure 2.12]

Surface temperatures during the pre-instrumental period from the proxy record

*It is likely that the rate and duration of the warming of the 20th century is larger than any other time during the last 1,000 years. The 1990s are likely to have been the warmest decade of the millennium in the Northern Hemisphere, and 1998 is likely to have been the warmest yea*r. There has been a considerable advance in understanding of temperature change that occurred over the last millennium, especially from the synthesis of individual temperature reconstructions. This new detailed temperature record for the Northern Hemisphere is shown in Figure 5. The data show a relatively warm period associated with the 11th to 14th centuries and a relatively cool period associated with the 15th to 19th centuries in the Northern Hemisphere. However, evidence does not support these "Medieval Warm Period" and "Little Ice Age" periods, respectively, as being globally synchronous. As Figure 5 indicates, the rate and duration of warming of the Northern Hemisphere in the 20th century appears to have been unprecedented during the millennium, and it cannot simply be considered as a recovery from the "Little Ice Age" of the 15th to 19th centuries. These analyses are complemented by sensitivity analysis of the spatial representativeness of available palaeoclimatic data, indicating that the warmth of the recent decade is outside the 95% confidence interval of temperature uncertainty, even during the warmest periods of the last millennium. Moreover, several different analyses have now been completed, each suggesting

[4] In this Technical Summary and in the Summary for Policymakers, the following words have been used to indicate approximate judgmental estimates of confidence: *virtually certain* (greater than 99% chance that a result is true); *very likely* (90–99% chance); *likely* (66–90% chance); *medium likelihood* (33–66% chance); *unlikely* (10–33% chance); *very unlikely* (1–10% chance); *exceptionally unlikely* (less than 1% chance). The reader is referred to individual chapters for more details.

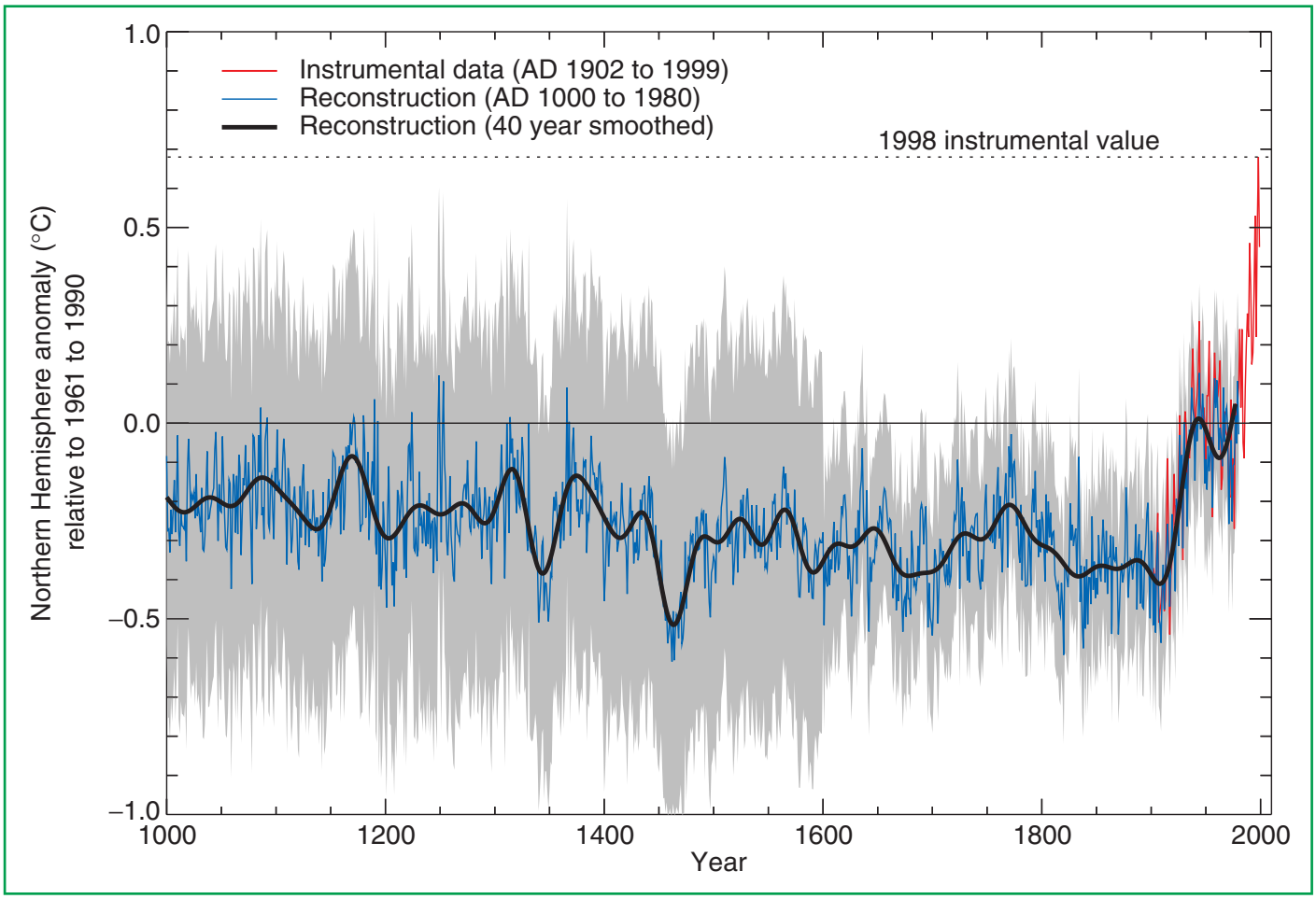

Figure 5: Millennial Northern Hemisphere (NH) temperature reconstruction (blue – tree rings, corals, ice cores, and historical records) and instrumental data (red) from AD 1000 to 1999. Smoother version of NH series (black), and two standard error limits (gray shaded) are shown. [Based on Figure 2.20]

that the Northern Hemisphere temperatures of the past decade have been warmer than any other time in the past six to ten centuries. This is the time-span over which temperatures with annual resolution can be calculated using hemispheric-wide tree-ring, ice-cores, corals, and and other annually-resolved proxy data. Because less data are available, less is known about annual averages prior to 1,000 years before the present and for conditions prevailing in most of the Southern Hemisphere prior to 1861.

It is likely that large rapid decadal temperature changes occurred during the last glacial and its deglaciation (between about 100,000 and 10,000 years ago), particularly in high latitudes of the Northern Hemisphere. In a few places during the deglaciation, local increases in temperature of 5 to 10°C are likely to have occurred over periods as short as a few decades. During the last 10,000 years, there is emerging evidence of significant rapid regional temperature changes, which are part of the natural variability of climate.

B.2 Observed Changes in Precipitation and Atmospheric Moisture

Since the time of the SAR, annual land precipitation has continued to increase in the middle and high latitudes of the Northern Hemisphere (very likely to be 0.5 to 1%/decade), except over Eastern Asia. Over the sub-tropics (10°N to 30°N), land-surface rainfall has decreased on average (likely to be about 0.3%/decade), although this has shown signs of recovery in recent years. Tropical land-surface precipitation measurements indicate that precipitation likely has increased by about 0.2 to 0.3%/decade over the 20th century, but increases are not evident over the past few decades and the amount of tropical land (versus ocean) area for the latitudes 10°N to 10°S is relatively small. Nonetheless, direct measurements of precipitation and model reanalyses of inferred precipitation indicate that rainfall has also increased over large parts of the tropical oceans. Where and when available, changes in annual streamflow often relate well to changes in total precipitation. The increases in precipitation over Northern Hemisphere mid- and high latitude land areas have a strong correlation to long-term increases in total cloud amount. In contrast to the Northern Hemisphere, no comparable systematic changes in precipitation have been detected in broad latitudinal averages over the Southern Hemisphere.

It is likely that total atmospheric water vapour has increased several per cent per decade over many regions of the Northern Hemisphere. Changes in water vapour over approximately the past 25 years have been analysed for selected regions using *in situ* surface observations, as well as lower-tropospheric measurements from satellites and weather balloons. A pattern of overall surface and lower-tropospheric water vapour increases over the past few decades is emerging from the most reliable data sets, although there are likely to be time-dependent biases in these data and regional variations in the trends. Water vapour in the lower stratosphere is also likely to have increased by about 10% per decade since the beginning of the observational record (1980).

Changes in total cloud amounts over Northern Hemisphere mid- and high latitude continental regions indicate a likely increase in cloud cover of about 2% since the beginning of the 20th century, which has now been shown to be positively correlated with decreases in the diurnal temperature range. Similar changes have been shown over Australia, the only Southern Hemisphere continent where such an analysis has been completed. Changes in total cloud amount are uncertain both over sub-tropical and tropical land areas, as well as over the oceans.

B.3 Observed Changes in Snow Cover and Land- and Sea-Ice Extent

Decreasing snow cover and land-ice extent continue to be positively correlated with increasing land-surface temperatures. Satellite data show that there are very likely to have been decreases of about 10% in the extent of snow cover since the late 1960s. There is a highly significant correlation between increases in Northern Hemisphere land temperatures and the decreases. There is now ample evidence to support a major retreat of alpine and continental glaciers in response to 20th century warming. In a few maritime regions, increases in precipitation due to regional atmospheric circulation changes have overshadowed increases in temperature in the past two decades, and glaciers have re-advanced. Over the past 100 to 150 years, ground-based observations show that there is very likely to have been a reduction of about two weeks in the annual duration of lake and river ice in the mid- to high latitudes of the Northern Hemisphere.

Northern Hemisphere sea-ice amounts are decreasing, but no significant trends in Antarctic sea-ice extent are apparent. A retreat of sea-ice extent in the Arctic spring and summer of 10 to 15% since the 1950s is consistent with an increase in spring temperatures and, to a lesser extent, summer temperatures in the high latitudes. There is little indication of reduced Arctic sea-ice extent during winter when temperatures have increased in the surrounding region. By contrast, there is no readily apparent relationship between decadal changes of Antarctic temperatures and sea-ice extent since 1973. After an initial decrease in the mid-1970s, Antarctic sea-ice extent has remained stable, or even slightly increased.

New data indicate that there likely has been an approximately 40% decline in Arctic sea-ice thickness in late summer to early autumn between the period of 1958 to 1976 and the mid-1990s, and a substantially smaller decline in winter. The relatively short record length and incomplete sampling limit the interpretation of these data. Interannual variability and inter-decadal variability could be influencing these changes.

B.4 Observed Changes in Sea Level

Changes during the instrumental record

Based on tide gauge data, the rate of global mean sea level rise during the 20th century is in the range 1.0 to 2.0 mm/yr, with a central value of 1.5 mm/yr (the central value should not be interpreted as a best estimate). (See Box 2 for the factors that influence sea level.) As Figure 6 indicates, the longest instrumental records (two or three centuries at most) of local sea level come from tide gauges. Based on the very few long tide-gauge records, the average rate of sea level rise has been larger during the 20th century than during the 19th century. No significant acceleration in the rate of sea level rise during the 20th century has been detected. This is not inconsistent with model results due to the possibility of compensating factors and the limited data.

Changes during the pre-instrumental record

Since the last glacial maximum about 20,000 years ago, the sea level in locations far from present and former ice sheets has risen by over 120 m as a result of loss of mass from these ice sheets. Vertical land movements, both upward and downward, are still occurring in response to these large transfers of mass from ice sheets to oceans. The most rapid rise in global sea level was between 15,000 and 6,000 years

Box 2: What causes sea level to change?

The level of the sea at the shoreline is determined by many factors in the global environment that operate on a great range of time-scales, from hours (tidal) to millions of years (ocean basin changes due to tectonics and sedimentation). On the time-scale of decades to centuries, some of the largest influences on the average levels of the sea are linked to climate and climate change processes.

Firstly, as ocean water warms, it expands. On the basis of observations of ocean temperatures and model results, thermal expansion is believed to be one of the major contributors to historical sea level changes. Further, thermal expansion is expected to contribute the largest component to sea level rise over the next hundred years. Deep ocean temperatures change only slowly; therefore, thermal expansion would continue for many centuries even if the atmospheric concentrations of greenhouse gases were to stabilise.

The amount of warming and the depth of water affected vary with location. In addition, warmer water expands more than colder water for a given change in temperature. The geographical distribution of sea level change results from the geographical variation of thermal expansion, changes in salinity, winds, and ocean circulation. The range of regional variation is substantial compared with the global average sea level rise.

Sea level also changes when the mass of water in the ocean increases or decreases. This occurs when ocean water is exchanged with the water stored on land. The major land store is the water frozen in glaciers or ice sheets. Indeed, the main reason for the lower sea level during the last glacial period was the amount of water stored in the large extension of the ice sheets on the continents of the Northern Hemisphere. After thermal expansion, the melting of mountain glaciers and ice caps is expected to make the largest contribution to the rise of sea level over the next hundred years. These glaciers and ice caps make up only a few per cent of the world's land-ice area, but they are more sensitive to climate change than the larger ice sheets in Greenland and Antarctica, because the ice sheets are in colder climates with low precipitation and low melting rates. Consequently, the large ice sheets are expected to make only a small net contribution to sea level change in the coming decades.

Sea level is also influenced by processes that are not explicitly related to climate change. Terrestrial water storage (and hence, sea level) can be altered by extraction of ground water, building of reservoirs, changes in surface runoff, and seepage into deep aquifers from reservoirs and irrigation. These factors may be offsetting a significant fraction of the expected acceleration in sea level rise from thermal expansion and glacial melting. In addition, coastal subsidence in river delta regions can also influence local sea level. Vertical land movements caused by natural geological processes, such as slow movements in the Earth's mantle and tectonic displacements of the crust, can have effects on local sea level that are comparable to climate-related impacts. Lastly, on seasonal, interannual, and decadal time-scales, sea level responds to changes in atmospheric and ocean dynamics, with the most striking example occurring during El Niño events.

ago, with an average rate of about 10 mm/yr. Based on geological data, eustatic sea level (i.e., corresponding to a change in ocean volume) may have risen at an average rate of 0.5 mm/yr over the past 6,000 years and at an average rate of 0.1 to 0.2 mm/yr over the last 3,000 years. This rate is about one tenth of that occurring during the 20th century. Over the past 3,000 to 5,000 years, oscillations in global sea level on time-scales of 100 to 1,000 years are unlikely to have exceeded 0.3 to 0.5 m.

B.5 Observed Changes in Atmospheric and Oceanic Circulation Patterns

The behaviour of ENSO (see Box 4 for a general description), has been unusual since the mid-1970s compared with the previous 100 years, with warm phase ENSO episodes being relatively more frequent, persistent, and intense than the opposite cool phase. This recent behaviour of ENSO is reflected in variations in precipitation and temperature over much of the global tropics and sub-tropics. The overall effect

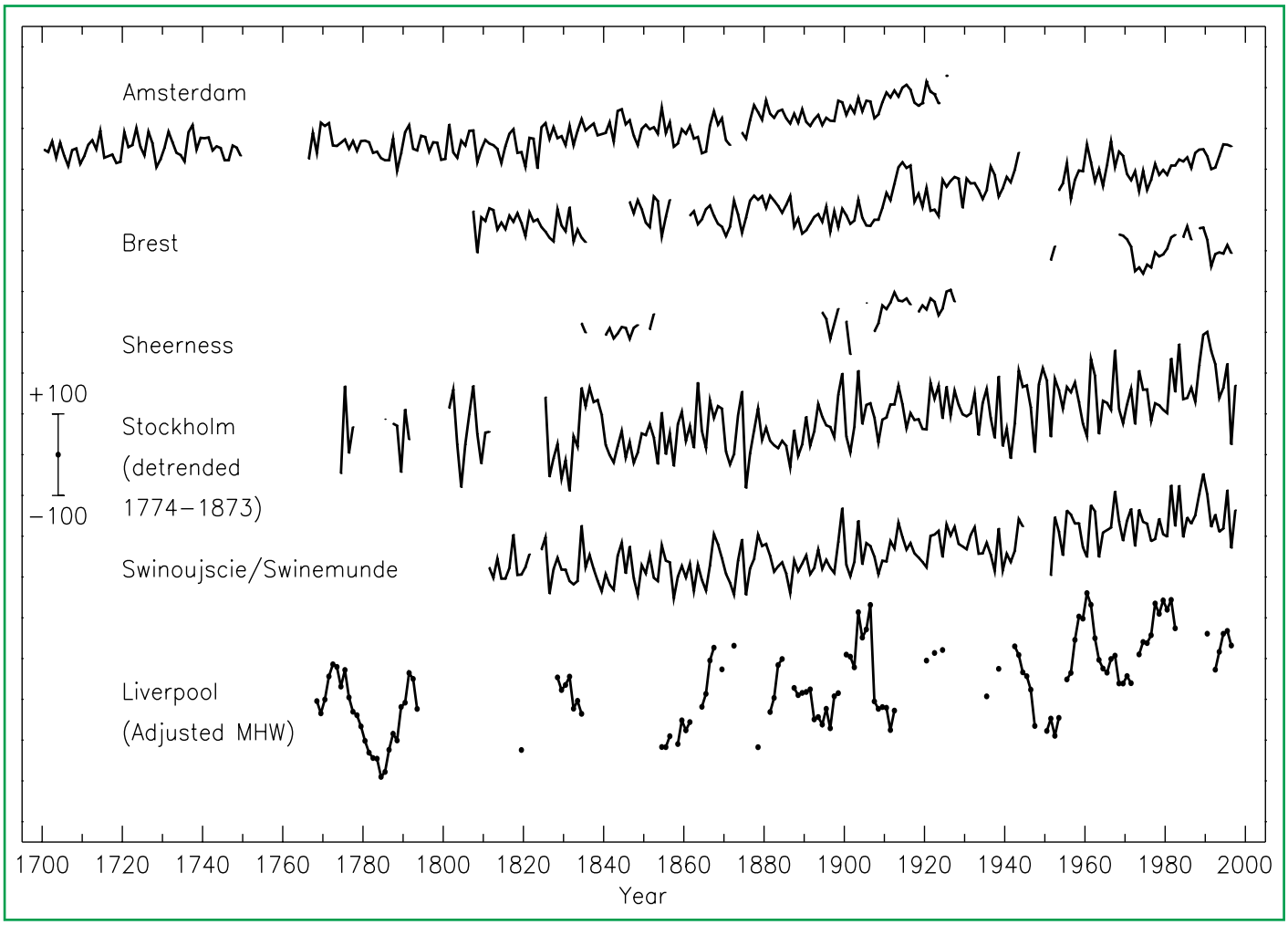

Figure 6: Time-series of relative sea level for the past 300 years from Northern Europe: Amsterdam, Netherlands; Brest, France; Sheerness, UK; Stockholm, Sweden (detrended over the period 1774 to 1873 to remove to first order the contribution of post-glacial rebound); Swinoujscie, Poland (formerly Swinemunde, Germany); and Liverpool, UK. Data for the latter are of "Adjusted Mean High Water" rather than Mean Sea Level and include a nodal (18.6 year) term. The scale bar indicates ±100 mm. [Based on Figure 11.7]

is likely to have been a small contribution to the increase in global temperatures during the last few decades. The Inter-decadal Pacific Oscillation and the Pacific Decadal Oscillation are associated with decadal to multidecadal climate variability over the Pacific basin. It is likely that these oscillations modulate ENSO-related climate variability.

Other important circulation features that affect the climate in large regions of the globe are being characterised. The North Atlantic Oscillation (NAO) is linked to the strength of the westerlies over the Atlantic and extra-tropical Eurasia. During winter the NAO displays irregular oscillations on interannual to multi-decadal time-scales. Since the 1970s, the winter NAO has often been in a phase that contributes to stronger westerlies, which correlate with cold season warming over Eurasia. New evidence indicates that the NAO and changes in Arctic sea ice are likely to be closely coupled. The NAO is now believed to be part of a wider scale atmospheric Arctic Oscillation that affects much of the extratropical Northern Hemisphere. A similar Antarctic Oscillation has been in an enhanced positive phase during the last 15 years, with stronger westerlies over the Southern Oceans.

B.6 Observed Changes in Climate Variability and Extreme Weather and Climate Events

New analyses show that in regions where total precipitation has increased, it is very likely that there have been even more pronounced increases in heavy and extreme precipitation events. The converse is also true. In some regions, however, heavy and extreme events (i.e., defined to be within the upper or lower ten percentiles) have increased despite the fact that total precipitation has decreased or remained constant. This is attributed to a decrease in the frequency of precipitation events. Overall, it is likely that for many mid- and high latitude areas, primarily in the Northern Hemisphere, statistically significant increases have occurred in the proportion of total annual precipitation derived from heavy and extreme precipitation events; it is likely that there has been a 2 to 4% increase in the frequency of heavy precipitation events over the latter half of the 20th century. Over the 20th century (1900 to 1995), there were relatively small increases in global land areas experiencing severe drought or severe wetness. In some regions, such as parts of Asia and Africa, the frequency and intensity of drought have been observed to increase in recent decades. In many regions, these changes are dominated by inter-decadal and multi-decadal climate variability, such as the shift in ENSO towards more warm events. In many regions, inter-daily temperature variability has decreased, and increases in the daily minimum temperature are lengthening the freeze-free period in most mid- and high latitude regions. Since 1950 it is very likely that there has been a significant reduction in the frequency of much-below-normal seasonal mean temperatures across much of the globe, but there has been a smaller increase in the frequency of much-above-normal seasonal temperatures.

There is no compelling evidence to indicate that the characteristics of tropical and extratropical storms have changed. Changes in tropical storm intensity and frequency are dominated by interdecadal to multidecadal variations, which may be substantial, e.g., in the tropical North Atlantic. Owing to incomplete data and limited and conflicting analyses, it is uncertain as to whether there have been any long-term and large-scale increases in the intensity and frequency of extra-tropical cyclones in the Northern Hemisphere. Regional increases have been identified in the North Pacific, parts of North America, and Europe over the past several decades. In the Southern Hemisphere, fewer analyses have been completed, but they suggest a decrease in extra-tropical cyclone activity since the 1970s. Recent analyses of changes in severe local weather (e.g., tornadoes, thunderstorm days, and hail) in a few selected regions do not provide compelling evidence to suggest long-term changes. In general, trends in severe weather events are notoriously difficult to detect because of their relatively rare occurrence and large spatial variability.

B.7 The Collective Picture: A Warming World and Other Changes in the Climate System

As summarised above, a suite of climate changes is now well-documented, particularly over the recent decades to century time period, with its growing set of direct measurements. Figure 7 illustrates these trends in temperature indicators (Figure 7a) and hydrological and storm-related indicators (Figure 7b), as well as also providing an indication of certainty about the changes.

Taken together, these trends illustrate a collective picture of a warming world:

- Surface temperature measurements over the land and oceans (with two separate estimates over the latter) have been measured and adjusted independently. All data sets show quite similar upward trends globally, with two major warming periods globally: 1910 to 1945 and since 1976. There is an emerging tendency for global land-surface air temperatures to warm faster than the global ocean-surface temperatures.
- Weather balloon measurements show that lower-tropospheric temperatures have been increasing since 1958, though only slightly since 1979. Since 1979, satellite data are available and show similar trends to balloon data.
- The decrease in the continental diurnal temperature range coincides with increases in cloud amount, precipitation, and increases in total water vapour.
- The nearly worldwide decrease in mountain glacier extent and ice mass is consistent with worldwide surface temperature increases. A few recent exceptions in coastal regions are consistent with atmospheric circulation variations and related precipitation increases.
- The decreases in snow cover and the shortening seasons of lake and river ice relate well to increases in Northern Hemispheric land-surface temperatures.
- The systematic decrease in spring and summer sea-ice extent and thickness in the Arctic is consistent with increases in temperature over most of the adjacent land and ocean.
- Ocean heat content has increased, and global average sea level has risen.
- The increases in total tropospheric water vapour in the last 25 years are qualitatively consistent with increases in tropospheric temperatures and an enhanced hydrologic cycle, resulting in more extreme and heavier precipitation events in many areas with increasing precipitation, e.g., middle and high latitudes of the Northern Hemisphere.

Some important aspects of climate appear not to have changed.

- A few areas of the globe have not warmed in recent decades, mainly over some parts of the Southern Hemisphere oceans and parts of Antarctica.
- No significant trends in Antarctic sea-ice extent are apparent over the period of systematic satellite measurements (since 1978).
- Based on limited data, the observed variations in the intensity and frequency of tropical and extra-tropical cyclones and severe local storms show no clear trends in the last half of the 20th century, although multi-decadal fluctuations are sometimes apparent.

The variations and trends in the examined indicators imply that it is virtually certain that there has been a generally increasing trend in global surface temperature over the 20th century, although short-term and regional deviations from this trend occur.

(a) Temperature Indicators

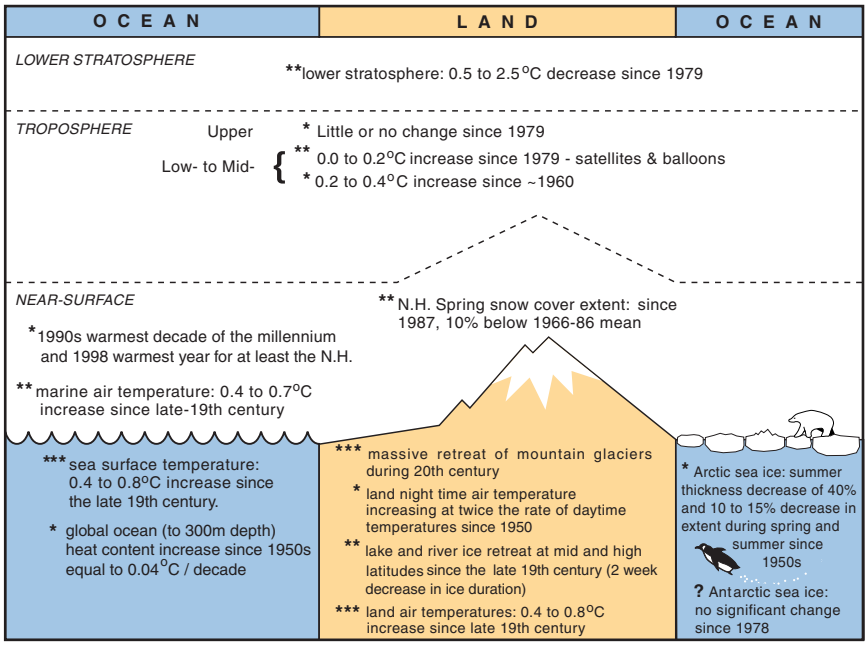

Likelihood:
- *** **Virtually certain (probability > 99%)**
- ** **Very likely (probability ≥ 90% but ≤ 99%)**
- * **Likely (probability > 66% but < 90%)**
- ? **Medium likelihood (probability > 33% but ≤ 66%)**

Figure 7a: Schematic of observed variations of the temperature indicators. [Based on Figure 2.39a]

(b) Hydrological and Storm related Indicators

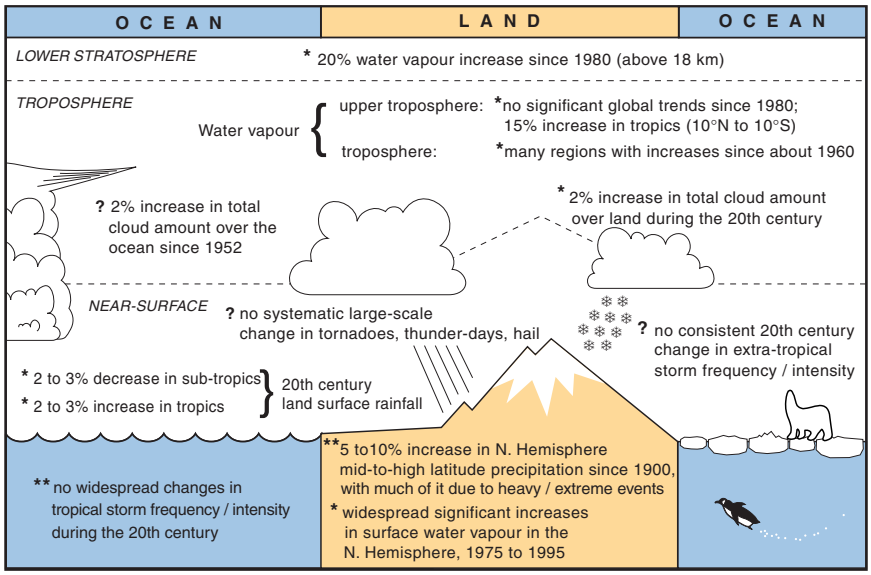

Likelihood:
- *** **Virtually certain (probability > 99%)**
- ** **Very likely (probability ≥ 90% but ≤ 99%)**
- * **Likely (probability > 66% but < 90%)**
- ? **Medium likelihood (probability > 33% but ≤ 66%)**

Figure 7b: Schematic of observed variations of the hydrological and storm-related indicators. [Based on Figure 2.39b]

C. The Forcing Agents That Cause Climate Change

In addition to the past variations and changes in the Earth's climate, observations have also documented the changes that have occurred in agents that can cause climate change. Most notable among these are increases in the atmospheric concentrations of greenhouse gases and aerosols (microscopic airborne particles or droplets) and variations in solar activity, both of which can alter the Earth's radiation budget and hence climate. These observational records of climate-forcing agents are part of the input needed to understand the past climate changes noted in the preceding Section and, very importantly, to predict what climate changes could lie ahead (see Section F).

Like the record of past climate changes, the data sets for forcing agents are of varying length and quality. Direct measurements of solar irradiance exist for only about two decades. The sustained direct monitoring of the atmospheric concentrations of carbon dioxide (CO_2) began about the middle of the 20th century and, in later years, for other long-lived, well-mixed gases such as methane. Palaeo-atmospheric data from ice cores reveal the concentration changes occurring in earlier millennia for some greenhouse gases. In contrast, the time-series measurements for the forcing agents that have relatively short residence times in the atmosphere (e.g., aerosols) are more recent and are far less complete, because they are harder to measure and are spatially heterogeneous. Current data sets show the human influence on atmospheric concentrations of both the long-lived greenhouse gases and short-lived forcing agents during the last part of the past millennium. Figure 8 illustrates the effects of the large growth over the Industrial Era in the anthropogenic emissions of greenhouse gases and sulphur dioxide, the latter being a precursor of aerosols.

A change in the energy available to the global Earth-atmosphere system due to changes in these forcing agents is termed radiative forcing (Wm^{-2}) of the climate system (see Box 1). Defined in this manner, radiative forcing of climate change constitutes an index of the relative global mean impacts on the surface-troposphere system due to different natural and anthropogenic causes. This Section updates the knowledge of the radiative forcing of climate change that has occurred from pre-industrial times to the present. Figure 9 shows the estimated radiative forcings from the beginning of the Industrial Era (1750) to 1999 for the quantifiable natural and anthropogenic

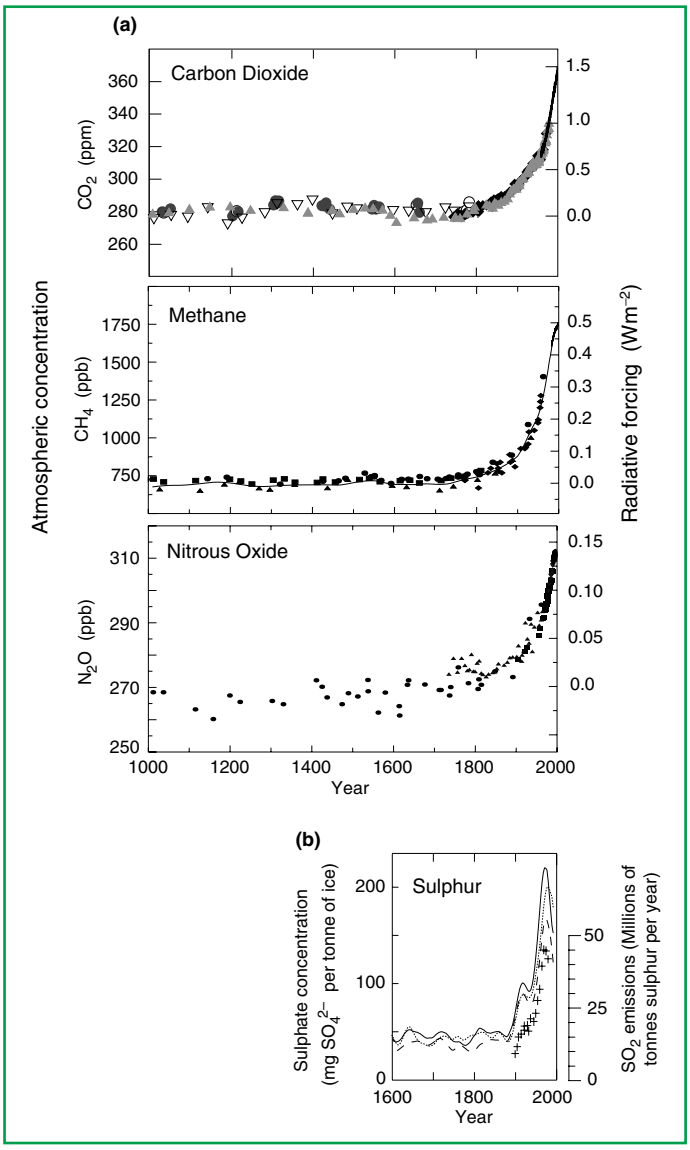

Figure 8: Records of changes in atmospheric composition. (a) Atmospheric concentrations of CO_2, CH_4 and N_2O over the past 1,000 years. Ice core and firn data for several sites in Antarctica and Greenland (shown by different symbols) are supplemented with the data from direct atmospheric samples over the past few decades (shown by the line for CO_2 and incorporated in the curve representing the global average of CH_4). The estimated radiative forcing from these gases is indicated on the right-hand scale. (b) Sulphate concentration in several Greenland ice cores with the episodic effects of volcanic eruptions removed (lines) and total SO_2 emissions from sources in the US and Europe (crosses). [Based on (a) Figure 3.2b (CO_2), Figure 4.1a and b (CH_4) and Figure 4.2 (N_2O) and (b) Figure 5.4a]

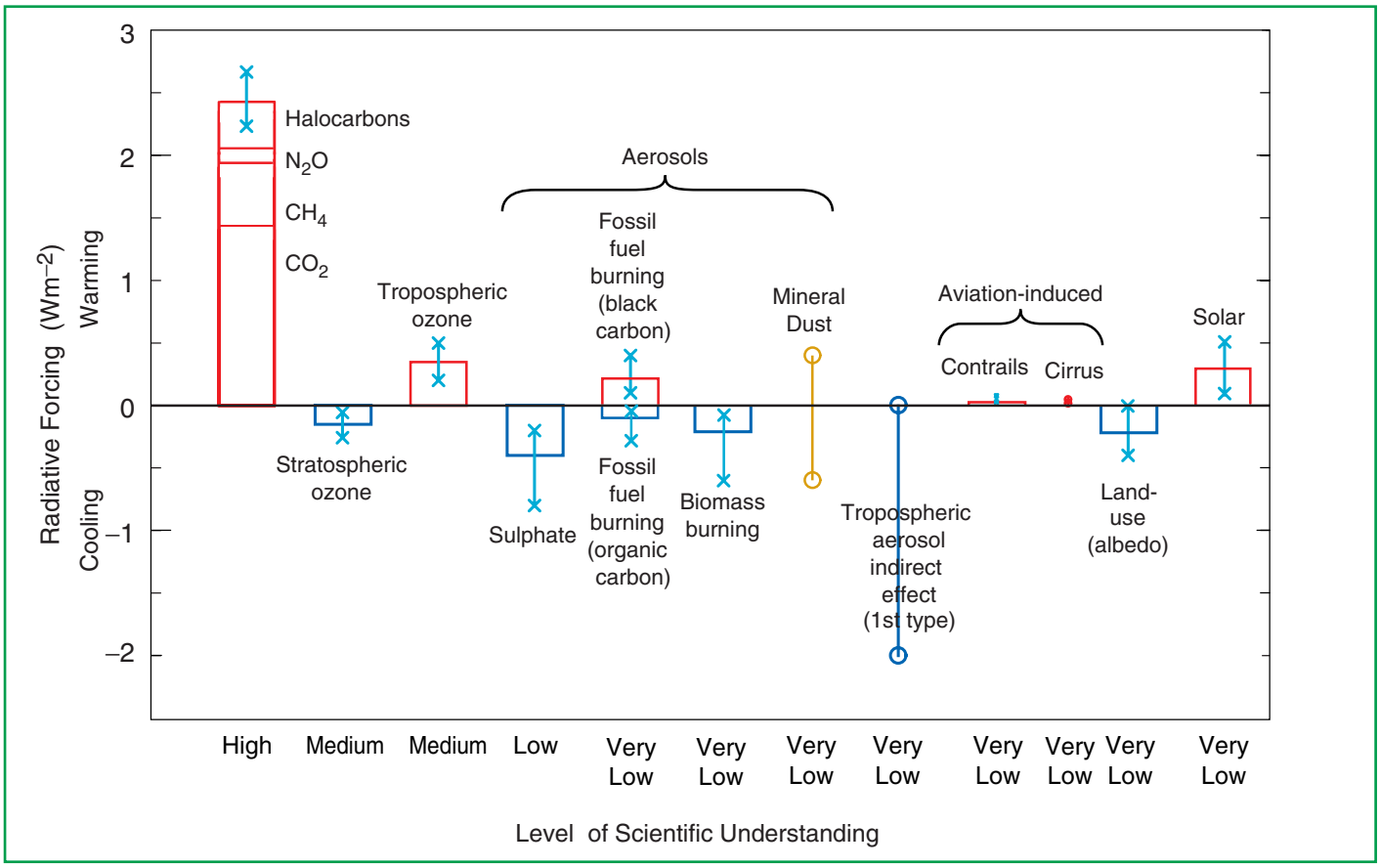

Figure 9: Global, annual-mean radiative forcings (Wm^{-2}) due to a number of agents for the period from pre-industrial (1750) to present (late 1990s; about 2000) (numerical values are also listed in Table 6.11 of Chapter 6). For detailed explanations, see Chapter 6.13. The height of the rectangular bar denotes a central or best estimate value, while its absence denotes no best estimate is possible. The vertical line about the rectangular bar with "x" delimiters indicates an estimate of the uncertainty range, for the most part guided by the spread in the published values of the forcing. A vertical line without a rectangular bar and with "o" delimiters denotes a forcing for which no central estimate can be given owing to large uncertainties. The uncertainty range specified here has no statistical basis and therefore differs from the use of the term elsewhere in this document. A "level of scientific understanding" index is accorded to each forcing, with high, medium, low and very low levels, respectively. This represents the subjective judgement about the reliability of the forcing estimate, involving factors such as the assumptions necessary to evaluate the forcing, the degree of knowledge of the physical/chemical mechanisms determining the forcing, and the uncertainties surrounding the quantitative estimate of the forcing (see Table 6.12). The well-mixed greenhouse gases are grouped together into a single rectangular bar with the individual mean contributions due to CO_2, CH_4, N_2O and halocarbons shown (see Tables 6.1 and 6.11). Fossil fuel burning is separated into the "black carbon" and "organic carbon" components with its separate best estimate and range. The sign of the effects due to mineral dust is itself an uncertainty. The indirect forcing due to tropospheric aerosols is poorly understood. The same is true for the forcing due to aviation via its effects on contrails and cirrus clouds. Only the "first" type of indirect effect due to aerosols as applicable in the context of liquid clouds is considered here. The "second" type of effect is conceptually important, but there exists very little confidence in the simulated quantitative estimates. The forcing associated with stratospheric aerosols from volcanic eruptions is highly variable over the period and is not considered for this plot (however, see Figure 6.8). All the forcings shown have distinct spatial and seasonal features (Figure 6.7) such that the global, annual means appearing on this plot do not yield a complete picture of the radiative perturbation. They are only intended to give, in a relative sense, a first-order perspective on a global, annual mean scale and cannot be readily employed to obtain the climate response to the total natural and/or anthropogenic forcings. As in the SAR, it is emphasised that the positive and negative global mean forcings cannot be added up and viewed *a priori* as providing offsets in terms of the complete global climate impact. [Based on Figure 6.6]

forcing agents. Although not included in the figure due to their episodic nature, volcanic eruptions are the source of another important natural forcing. Summaries of the information about each forcing agent follow in the sub-sections below.

The forcing agents included in Figure 9 vary greatly in their form, magnitude and spatial distribution. Some of the greenhouse gases are emitted directly into the atmosphere; some are chemical products from other emissions. Some greenhouse gases have long atmospheric residence times and, as a result, are well-mixed throughout the atmosphere. Others are short-lived and have heterogeneous regional concentrations. Most of the gases originate from both natural and anthropogenic sources. Lastly, as shown in Figure 9, the radiative forcings of individual agents can be positive (i.e., a tendency to warm the Earth's surface) or negative (i.e., a tendency to cool the Earth's surface).

C.1 Observed Changes in Globally Well-Mixed Greenhouse Gas Concentrations and Radiative Forcing

Over the millennium before the Industrial Era, the atmospheric concentrations of greenhouse gases remained relatively constant. Since then, however, the concentrations of many greenhouse gases have increased directly or indirectly because of human activities.

Table 1 provides examples of several greenhouse gases and summarises their 1750 and 1998 concentrations, their change during the 1990s, and their atmospheric lifetimes. The contribution of a species to radiative forcing of climate change depends on the molecular radiative properties of the gas, the size of the increase in atmospheric concentration, and the residence time of the species in the atmosphere, once emitted. *The latter – the atmospheric residence time of the greenhouse gas – is a highly policy relevant characteristic. Namely, emissions of a greenhouse gas that has a long atmospheric residence time is a quasi-irreversible commitment to sustained radiative forcing over decades, centuries, or millennia, before natural processes can remove the quantities emitted.*

Table 1: Examples of greenhouse gases that are affected by human activities. [Based upon Chapter 3 and Table 4.1]

	CO_2 (Carbon Dioxide)	CH_4 (Methane)	N_2O (Nitrous Oxide)	CFC-11 (Chlorofluoro-carbon-11)	HFC-23 (Hydrofluoro-carbon-23)	CF_4 (Perfluoro-methane)
Pre-industrial concentration	about 280 ppm	about 700 ppb	about 270 ppb	zero	zero	40 ppt
Concentration in 1998	365 ppm	1745 ppb	314 ppb	268 ppt	14 ppt	80 ppt
Rate of concentration change[b]	1.5 ppm/yr[a]	7.0 ppb/yr[a]	0.8 ppb/yr	–1.4 ppt/yr	0.55 ppt/yr	1 ppt/yr
Atmospheric lifetime	5 to 200 yr[c]	12 yr[d]	114 yr[d]	45 yr	260 yr	>50,000 yr

[a] Rate has fluctuated between 0.9 ppm/yr and 2.8 ppm/yr for CO_2 and between 0 and 13 ppb/yr for CH_4 over the period 1990 to 1999.

[b] Rate is calculated over the period 1990 to 1999.

[c] No single lifetime can be defined for CO_2 because of the different rates of uptake by different removal processes.

[d] This lifetime has been defined as an "adjustment time" that takes into account the indirect effect of the gas on its own residence time.

Carbon dioxide (CO_2)

The atmospheric concentration of CO_2 has increased from 280 ppm[5] in 1750 to 367 ppm in 1999 (31%, Table 1). Today's CO_2 concentration has not been exceeded during the past 420,000 years and likely not during the past 20 million years. The rate of increase over the past century is unprecedented, at least during the past 20,000 years (Figure 10). The CO_2 isotopic composition and the observed decrease in Oxygen (O_2) demonstrates that the observed increase in CO_2 is predominately due to the oxidation of organic carbon by fossil-fuel combustion and deforestation. An expanding set of palaeo-atmospheric data from air trapped in ice over hundreds of millennia provide a context for the increase in CO_2 concentrations during the Industrial Era (Figure 10). Compared to the relatively stable CO_2 concentrations (280 ± 10 ppm) of the preceding several thousand years, the increase during the Industrial Era is dramatic. The average rate of increase since 1980 is 0.4%/yr. The increase is a consequence of CO_2 emissions. Most of the emissions during the past 20 years are due to fossil fuel burning, the rest (10 to 30%) is predominantly due to land-use change, especially deforestation. As shown in Figure 9, CO_2 is the dominant human-influenced greenhouse gas, with a current radiative forcing of 1.46 Wm^{-2}, being 60% of the total from the changes in concentrations of all of the long-lived and globally mixed greenhouse gases.

Direct atmospheric measurements of CO_2 concentrations made over the past 40 years show that year to year fluctuations in the rate of increase of atmospheric CO_2 are large. In the 1990s, the annual rates of CO_2 increase in the atmosphere varied from 0.9 to 2.8 ppm/yr, equivalent to 1.9 to 6.0 PgC/yr. Such annual changes can be related statistically to short-term climate variability, which alters the rate at which atmospheric CO_2 is taken up and released by the oceans and land. The highest rates of increase in atmospheric CO_2 have typically been in strong El Niño years (Box 4). These higher rates of increase can be plausibly explained by reduced terrestrial uptake (or terrestrial outgassing) of CO_2 during El Niño years, overwhelming the tendency of the ocean to take up more CO_2 than usual.

Partitioning of anthropogenic CO_2 between atmospheric increases and land and ocean uptake for the past two decades can now be calculated from atmospheric observations. Table 2 presents a global CO_2 budget for the 1980s (which proves to be similar to the one constructed with the help of ocean model results in the SAR) and for the 1990s. Measurements of the decrease in atmospheric oxygen (O_2) as well as the increase in CO_2 were used in the construction of these new budgets. Results from this approach are consistent with other analyses based on the isotopic composition of atmospheric CO_2 and with independent estimates based on measurements of CO_2 and $^{13}CO_2$ in seawater. The 1990s budget is based on newly available measurements and updates the budget for

Table 2: Global CO_2 budgets (in PgC/yr) based on measurements of atmospheric CO_2 and O_2. Positive values are fluxes to the atmosphere; negative values represent uptake from the atmosphere. [Based upon Tables 3.1 and 3.3]

	SAR[a,b]	This Report[a]	
	1980 to 1989	1980 to 1989	1990 to 1999
Atmospheric increase	3.3 ± 0.1	3.3 ± 0.1	3.2 ± 0.1
Emissions (fossil fuel, cement)[c]	5.5 ± 0.3	5.4 ± 0.3	6.3 ± 0.4
Ocean-atmosphere flux	−2.0 ± 0.5	−1.9 ± 0.6	−1.7 ± 0.5
Land-atmosphere flux[d]	−0.2 ± 0.6	−0.2 ± 0.7	−1.4 ± 0.7

[a] Note that the uncertainties cited in this table are ±1 standard error. The uncertainties cited in the SAR were ±1.6 standard error (i.e., approximately 90% confidence interval). Uncertainties cited from the SAR were adjusted to ±1 standard error. Error bars denote uncertainty, not interannual variability, which is substantially greater.

[b] Previous IPCC carbon budgets calculated ocean uptake from models and the land-atmosphere flux was inferred by difference.

[c] The fossil fuel emissions term for the 1980s has been revised slightly downward since the SAR.

[d] The land-atmosphere flux represents the balance of a positive term due to land-use change and a residual terrestrial sink. The two terms cannot be separated on the basis of current atmospheric measurements. Using independent analyses to estimate the land-use change component for 1980 to 1989, the residual terrestrial sink can be inferred as follows: Land-use change 1.7 PgC/yr (0.6 to 2.5); Residual terrestrial sink –1.9 PgC/yr (–3.8 to 0.3). Comparable data for the 1990s are not yet available.

[5] Atmospheric abundances of trace gases are reported here as the mole fraction (molar mixing ratio) of the gas relative to dry air (ppm = 10^{-6}, ppb = 10^{-9}, ppt = 10^{-12}). Atmospheric burden is reported as the total mass of the gas (e.g., Mt = Tg = 10^{12} g). The global carbon cycle is expressed in PgC = GtC.

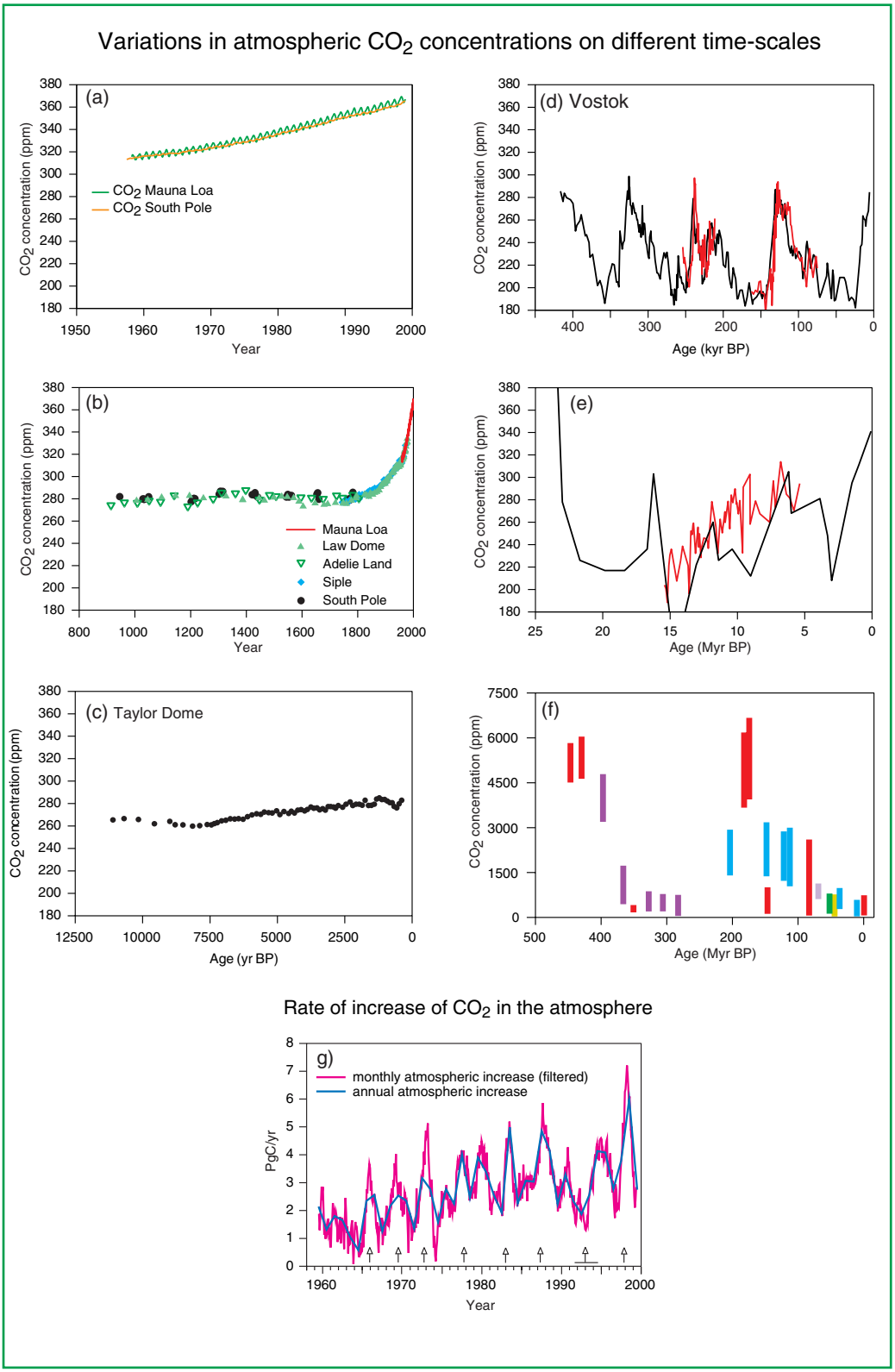

Figure 10: Variations in atmospheric CO_2 concentration on different time-scales. (a) Direct measurements of atmospheric CO_2. (b) CO_2 concentration in Antarctic ice cores for the past millenium. Recent atmospheric measurements (Mauna Loa) are shown for comparison. (c) CO_2 concentration in the Taylor Dome Antarctic ice core. (d) CO_2 concentration in the Vostok Antarctic ice core. (Different colours represent results from different studies.) (e to f) Geochemically inferred CO_2 concentrations. (Coloured bars and lines represent different published studies) (g) Annual atmospheric increases in CO_2. Monthly atmospheric increases have been filtered to remove the seasonal cycle. Vertical arrows denote El Niño events. A horizontal line defines the extended El Niño of 1991 to 1994. [Based on Figures 3.2 and 3.3]

1989 to 1998 derived using SAR methodology for the IPCC Special Report on Land Use, Land-Use Change and Forestry (2000). The terrestrial biosphere as a whole has gained carbon during the 1980s and 1990s; i.e., the CO_2 released by land-use change (mainly tropical deforestation) was more than compensated by other terrestrial sinks, which are likely located in both the northern extra-tropics and in the tropics. There remain large uncertainties associated with estimating the CO_2 release due to land-use change (and, therefore, with the magnitude of the residual terrestrial sink).

Process-based modelling (terrestrial and ocean carbon models) has allowed preliminary quantification of mechanisms in the global carbon cycle. Terrestrial model results indicate that enhanced plant growth due to higher CO_2 (CO_2 fertilisation) and anthropogenic nitrogen deposition contribute significantly to CO_2 uptake, i.e., are potentially responsible for the residual terrestrial sink described above, along with other proposed mechanisms, such as changes in land-management practices. The modelled effects of climate change during the 1980s on the terrestrial sink are small and of uncertain sign.

Methane (CH_4)

Atmospheric methane (CH_4) concentrations have increased by about 150% (1,060 ppb) since 1750. The present CH_4 concentration has not been exceeded during the past 420,000 years. Methane (CH_4) is a greenhouse gas with both natural (e.g., wetlands) and human-influenced sources (e.g., agriculture, natural gas activities, and landfills). Slightly more than half of current CH_4 emissions are anthropogenic. It is removed from the atmosphere by chemical reactions. As Figure 11 shows, systematic, globally representative measurements of the concentration of CH_4 in the atmosphere have been made since 1983, and the record of atmospheric concentrations has been extended to earlier times from air extracted from ice cores and firn layers. The current direct radiative forcing of 0.48 Wm^{-2} from CH_4 is 20% of the total from all of the long-lived and globally mixed greenhouse gases (see Figure 9).

The atmospheric abundance of CH_4 continues to increase, from about 1,610 ppb in 1983 to 1,745 ppb in 1998, but the observed annual increase has declined during this period. The increase was highly variable during the 1990s; it was near zero in 1992 and as large as 13 ppb during 1998. There is no clear quantitative explanation for this variability. Since

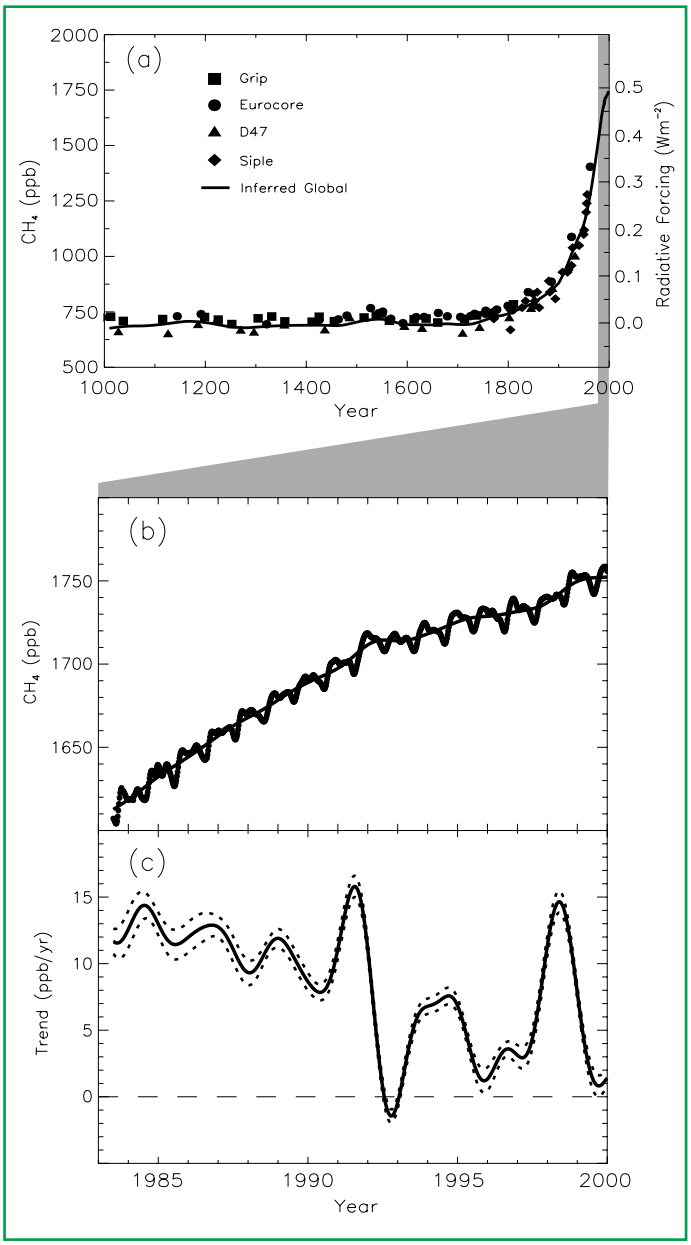

Figure 11: (a) Change in CH_4 abundance (mole fraction, in ppb = 10^{-9}) determined from ice cores, firn, and whole air samples plotted for the last 1000 years. Radiative forcing, approximated by a linear scale since the pre-industrial era, is plotted on the right axis. (b) Globally averaged CH_4 (monthly varying) and deseasonalised CH_4 (smooth line) abundance plotted for 1983 to 1999. (c) Instantaneous annual growth rate (ppb/yr) in global atmospheric CH_4 abundance from 1983 through 1999 calculated as the derivative of the deseasonalised trend curve above. Uncertainties (dotted lines) are ±1 standard deviation. [Based on Figure 4.1]

the SAR, quantification of certain anthropogenic sources of CH_4, such as that from rice production, has improved.

The rate of increase in atmospheric CH_4 is due to a small imbalance between poorly characterised sources and sinks, which makes the prediction of future concentrations problematic. Although the major contributors to the global CH_4 budget likely have been identified, most of them are quite uncertain quantitatively because of the difficulty in assessing emission rates of highly variable biospheric sources. The limitations of poorly quantified and characterised CH_4 source strengths inhibit the prediction of future CH_4 atmospheric concentrations (and hence its contribution to radiative forcing) for any given anthropogenic emission scenario, particularly since both natural emissions and the removal of CH_4 can be influenced substantially by climate change.

Nitrous oxide (N_2O)

The atmospheric concentration of nitrous oxide (N_2O) has steadily increased during the Industrial Era and is now 16% (46 ppb) larger than in 1750. The present N_2O concentration has not been exceeded during at least the past thousand years. Nitrous oxide is another greenhouse gas with both natural and anthropogenic sources, and it is removed from the atmosphere by chemical reactions. Atmospheric concentrations of N_2O continue to increase at a rate of 0.25%/yr (1980 to 1998). Significant interannual variations in the upward trend of N_2O concentrations are observed, e.g., a 50% reduction in annual growth rate from 1991 to 1993. Suggested causes are several-fold: a decrease in use of nitrogen-based fertiliser, lower biogenic emissions, and larger stratospheric losses due to volcanic-induced circulation changes. Since 1993, the growth of N_2O concentrations has returned to rates closer to those observed during the 1980s. While this observed multi-year variance has provided some potential insight into what processes control the behaviour of atmospheric N_2O, the multi-year trends of this greenhouse gas remain largely unexplained.

The global budget of nitrous oxide is in better balance than in the SAR, but uncertainties in the emissions from individual sources are still quite large. Natural sources of N_2O are estimated to be approximately 10 TgN/yr (1990), with soils being about 65% of the sources and oceans about 30%. New, higher estimates of the emissions from anthropogenic sources (agriculture, biomass burning, industrial activities, and livestock management) of approximately 7 TgN/yr have brought the source/sink estimates closer in balance, compared with the SAR. However, the predictive understanding associated with this significant, long-lived greenhouse gas has not improved significantly since the last assessment. The radiative forcing is estimated at 0.15 Wm^{-2}, which is 6% of the total from all of the long-lived and globally mixed greenhouse gases (see Figure 9).

Halocarbons and related compounds

The atmospheric concentrations of many of those gases that are both ozone-depleting and greenhouse gases are either decreasing (CFC-11, CFC-113, CH_3CCl_3 and CCl_4) or increasing more slowly (CFC-12) in response to reduced emissions under the regulations of the Montreal Protocol and its Amendments. Many of these halocarbons are also radiatively effective, long-lived greenhouse gases. Halocarbons are carbon compounds that contain fluorine, chlorine, bromine or iodine. For most of these compounds, human activities are the sole source. Halocarbons that contain chlorine (e.g., chlorofluorocarbons - CFCs) and bromine (e.g., halons) cause depletion of the stratospheric ozone layer and are controlled under the Montreal Protocol. The combined tropospheric abundance of ozone-depleting gases peaked in 1994 and is slowly declining. The atmospheric abundances of some of the major greenhouse halocarbons have peaked, as shown for CFC-11 in Figure 12. The concentrations of CFCs and chlorocarbons in the troposphere are consistent with reported emissions. Halocarbons contribute a radiative forcing of 0.34 Wm^{-2}, which is 14% of the radiative forcing from all of the globally mixed greenhouse gases (Figure 9).

The observed atmospheric concentrations of the substitutes for the CFCs are increasing, and some of these compounds are greenhouse gases. The abundances of the hydrochlorofluoro-carbons (HCFCs) and hydrofluorocarbons (HFCs) are increasing as a result of continuation of earlier uses and of their use as substitutes for the CFCs. For example, the concentration of HFC-23 has increased by more than a factor of three between 1978 and 1995. Because current concentrations are relatively low, the present contribution of HFCs to radiative forcing is relatively small. The present contribution of HCFCs to radiative forcing is also relatively small, and future emissions of these gases are limited by the Montreal Protocol.

The perfluorocarbons (PFCs, e.g., CF_4 and C_2F_6) and sulphur hexafluoride (SF_6) have anthropogenic sources, have extremely

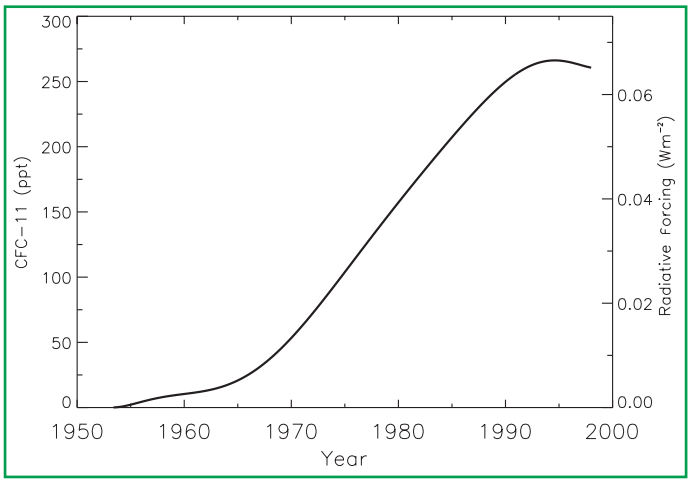

Figure 12: Global mean CFC-11 ($CFCl_3$) tropospheric abundance (ppt) from 1950 to 1998 based on smoothed measurements and emission models. CFC-11's radiative forcing is shown on the right axis. [Based on Figure 4.6]

long atmospheric residence times, and are strong absorbers of infrared radiation. Therefore, these compounds, even with relatively small emissions, have the potential to influence climate far into the future. Perfluoromethane (CF_4) resides in the atmosphere for at least 50,000 years. It has a natural background; however, current anthropogenic emissions exceed natural ones by a factor of 1,000 or more and are responsible for the observed increase. Sulphur hexafluoride (SF_6) is 22,200 times more effective a greenhouse gas than CO_2 on a per-kg basis. The current atmospheric concentrations are very small (4.2 ppt), but have a significant growth rate (0.24 ppt/yr). There is good agreement between the observed atmospheric growth rate of SF_6 and the emissions based on revised sales and storage data.

C.2 Observed Changes in Other Radiatively Important Gases

Atmospheric ozone (O_3)

Ozone (O_3) is an important greenhouse gas present in both the stratosphere and troposphere. The role of ozone in the atmospheric radiation budget is strongly dependent on the altitude at which changes in ozone concentrations occur. The changes in ozone concentrations are also spatially variable. Further, ozone is not a directly emitted species, but rather it is formed in the atmosphere from photochemical processes involving both natural and human-influenced precursor species. Once formed, the residence time of ozone in the atmosphere is relatively short, varying from weeks to months. As a result, estimation of ozone's radiative role is more complex and much less certain than for the above long-lived and globally well-mixed greenhouse gases.

The observed losses of stratospheric ozone layer over the past two decades have caused a negative forcing of 0.15 ± 0.1 Wm^{-2} (i.e., a tendency toward cooling) of the surface troposphere system. It was reported in Climate Change 1992: The Supplementary Report to the IPCC Scientific Assessment, that depletion of the ozone layer by anthropogenic halocarbons introduces a negative radiative forcing. The estimate shown in Figure 9 is slightly larger in magnitude than that given in the SAR, owing to the ozone depletion that has continued over the past five years, and it is more certain as a result of an increased number of modelling studies. Studies with General Circulation Models indicate that, despite the inhomogeneity in ozone loss (i.e., lower stratosphere at high latitudes), such a negative forcing does relate to a surface temperature decrease in proportion to the magnitude of the negative forcing. Therefore, this negative forcing over the past two decades has offset some of the positive forcing that is occurring from the long-lived and globally well-mixed greenhouse gases (Figure 9). A major source of uncertainty in the estimation of the negative forcing is due to incomplete knowledge of ozone depletion near the tropopause. Model calculations indicate that increased penetration of ultraviolet radiation to the troposphere, as a result of stratospheric ozone depletion, leads to enhanced removal rates of gases like CH_4, thus amplifying the negative forcing due to ozone depletion. As the ozone layer recovers in future decades because of the effects of the Montreal Protocol, relative to the present, future radiative forcing associated with stratospheric ozone is projected to become positive.

The global average radiative forcing due to increases in tropospheric ozone since pre-industrial times is estimated to have enhanced the anthropogenic greenhouse gas forcing by 0.35 ± 0.2 Wm^{-2}. This makes tropospheric ozone the third most important greenhouse gas after CO_2 and CH_4. Ozone is formed by photochemical reactions and its future change will be determined by, among other things, emissions of CH_4 and

pollutants (as noted below). Ozone concentrations respond relatively quickly to changes in the emissions of pollutants. On the basis of limited observations and several modelling studies, tropospheric ozone is estimated to have increased by about 35% since the Pre-industrial Era, with some regions experiencing larger and some with smaller increases. There have been few observed increases in ozone concentrations in the global troposphere since the mid-1980s at most of the few remote locations where it is regularly measured. The lack of observed increase over North America and Europe is related to the lack of a sustained increase in ozone-precursor emissions from those continents. However, some Asian stations indicate a possible rise in tropospheric ozone, which could be related to the increase in East Asian emissions. As a result of more modelling studies than before, there is now an increased confidence in the estimates of tropospheric ozone forcing. The confidence, however, is still much less than that for the well-mixed greenhouse gases, but more so than that for aerosol forcing. Uncertainties arise because of limited information on pre-industrial ozone distributions and limited information to evaluate modelled global trends in the modern era (i.e., post-1960).

Gases with only indirect radiative influences

Several chemically reactive gases, including reactive nitrogen species (NO_x), carbon monoxide (CO), and the volatile organic compounds (VOCs), control, in part, the oxidising capacity of the troposphere, as well as the abundance of ozone. These pollutants act as indirect greenhouse gases through their influence not only on ozone, but also on the lifetimes of CH_4 and other greenhouse gases. The emissions of NO_x and CO are dominated by human activities.

Carbon monoxide is identified as an important indirect greenhouse gas. Model calculations indicate that emission of 100 Mt of CO is equivalent in terms of greenhouse gas perturbations to the emission of about 5 Mt of CH_4. The abundance of CO in the Northern Hemisphere is about twice that in the Southern Hemisphere and has increased in the second half of the 20th century along with industrialisation and population.

The reactive nitrogen species NO and NO_2, (whose sum is denoted NO_x), are key compounds in the chemistry of the troposphere, but their overall radiative impact remains difficult to quantify. The importance of NO_x in the radiation budget is because increases in NO_x concentrations perturb several greenhouse gases; for example, decreases in methane and the HFCs and increases in tropospheric ozone. Deposition of the reaction products of NO_x fertilises the biosphere, thereby decreasing atmospheric CO_2. While difficult to quantify, increases in NO_x that are projected to the year 2100 would cause significant changes in greenhouse gases.

C.3 Observed and Modelled Changes in Aerosols

Aerosols (very small airborne particles and droplets) are known to influence significantly the radiative budget of the Earth/atmosphere. Aerosol radiative effects occur in two distinct ways: (i) the direct effect, whereby aerosols themselves scatter and absorb solar and thermal infrared radiation, and (ii) the indirect effect, whereby aerosols modify the microphysical and hence the radiative properties and amount of clouds. Aerosols are produced by a variety of processes, both natural (including dust storms and volcanic activity) and anthropogenic (including fossil fuel and biomass burning). The atmospheric concentrations of tropospheric aerosols are thought to have increased over recent years due to increased anthropogenic emissions of particles and their precursor gases, hence giving rise to radiative forcing. Most aerosols are found in the lower troposphere (below a few kilometres), but the radiative effect of many aerosols is sensitive to the vertical distribution. Aerosols undergo chemical and physical changes while in the atmosphere, notably within clouds, and are removed largely and relatively rapidly by precipitation (typically within a week). Because of this short residence time and the inhomogeneity of sources, aerosols are distributed inhomogeneously in the troposphere, with maxima near the sources. The radiative forcing due to aerosols depends not only on these spatial distributions, but also on the size, shape, and chemical composition of the particles and various aspects (e.g., cloud formation) of the hydrological cycle as well. As a result of all of these factors, obtaining accurate estimates of this forcing has been very challenging, from both the observational and theoretical standpoints.

*Nevertheless, substantial progress has been achieved in better defining the **direct effect** of a wider set of different aerosols.* The SAR considered the direct effects of only three anthropogenic aerosol species: sulphate aerosols, biomass-burning aerosols, and fossil fuel black carbon (or soot). Observations have now shown the importance of organic materials in both fossil fuel carbon aerosols and biomass-burning carbon aerosols. Since

the SAR, the inclusion of estimates for the abundance of fossil fuel organic carbon aerosols has led to an increase in the predicted total optical depth (and consequent negative forcing) associated with industrial aerosols. Advances in observations and in aerosol and radiative models have allowed quantitative estimates of these separate components, as well as an estimate for the range of radiative forcing associated with mineral dust, as shown in Figure 9. Direct radiative forcing is estimated to be –0.4 Wm^{-2} for sulphate, –0.2 Wm^{-2} for biomass-burning aerosols, –0.1 Wm^{-2} for fossil fuel organic carbon, and +0.2 Wm^{-2} for fossil fuel black carbon aerosols. Uncertainties remain relatively large, however. These arise from difficulties in determining the concentration and radiative characteristics of atmospheric aerosols and the fraction of the aerosols that are of anthropogenic origin, particularly the knowledge of the sources of carbonaceous aerosols. This leads to considerable differences (i.e., factor of two to three range) in the burden and substantial differences in the vertical distribution (factor of ten). Anthropogenic dust aerosol is also poorly quantified. Satellite observations, combined with model calculations, are enabling the identification of the spatial signature of the total aerosol radiative effect in clear skies; however, the quantitative amount is still uncertain.

*Estimates of the **indirect radiative** forcing by anthropogenic aerosols remain problematic, although observational evidence points to a negative aerosol-induced indirect forcing in warm clouds.* Two different approaches exist for estimating the indirect effect of aerosols: empirical methods and mechanistic methods. The former have been applied to estimate the effects of industrial aerosols, while the latter have been applied to estimate the effects of sulphate, fossil fuel carbonaceous aerosols, and biomass aerosols. In addition, models for the indirect effect have been used to estimate the effects of the initial change in droplet size and concentrations (a first indirect effect), as well as the effects of the subsequent change in precipitation efficiency (a second indirect effect). The studies represented in Figure 9 provide an expert judgement for the range of the first of these; the range is now slightly wider than in the SAR; the radiative perturbation associated with the second indirect effect is of the same sign and could be of similar magnitude compared to the first effect.

The indirect radiative effect of aerosols is now understood to also encompass effects on ice and mixed-phase clouds, but the magnitude of any such indirect effect is not known, although it is likely to be positive. It is not possible to estimate the number of anthropogenic ice nuclei at the present time. Except at cold temperatures (below –45°C) where homogeneous nucleation is expected to dominate, the mechanisms of ice formation in these clouds are not yet known.

C.4 Observed Changes in Other Anthropogenic Forcing Agents

Land-use (albedo) change

Changes in land use, deforestation being the major factor, appear to have produced a negative radiative forcing of –0.2 ± 0.2 Wm^{-2} (Figure 8). The largest effect is estimated to be at the high latitudes. This is because deforestation has caused snow-covered forests with relatively low albedo to be replaced with open, snow-covered areas with higher albedo. The estimate given above is based on simulations in which pre-industrial vegetation is replaced by current land-use patterns. However, the level of understanding is very low for this forcing, and there have been far fewer investigations of this forcing compared to investigations of other factors considered in this report.

C.5 Observed and Modelled Changes in Solar and Volcanic Activity

Radiative forcing of the climate system due to solar irradiance change is estimated to be 0.3 ± 0.2 Wm^{-2} for the period 1750 to the present (Figure 8), and most of the change is estimated to have occurred during the first half of the 20th century. The fundamental source of all energy in the Earth's climate system is radiation from the Sun. Therefore, variation in solar output is a radiative forcing agent. The absolute value of the spectrally integrated total solar irradiance (TSI) incident on the Earth is not known to better than about 4 Wm^{-2}, but satellite observations since the late 1970s show relative variations over the past two solar 11-year activity cycles of about 0.1%, which is equivalent to a variation in radiative forcing of about 0.2 Wm^{-2}. Prior to these satellite observations, reliable direct measurements of solar irradiance are not available. Variations over longer periods may have been larger, but the techniques used to reconstruct historical values of TSI from proxy observations (e.g., sunspots) have not been adequately verified. Solar variation varies more substantially in the ultraviolet region, and studies with climate models suggest that inclusion of spectrally resolved solar irradiance variations and solar-

induced stratospheric ozone changes may improve the realism of model simulations of the impact of solar variability on climate. Other mechanisms for the amplification of solar effects on climate have been proposed, but do not have a rigorous theoretical or observational basis.

Stratospheric aerosols from explosive volcanic eruptions lead to negative forcing that lasts a few years. Several explosive eruptions occurred in the periods 1880 to 1920 and 1960 to 1991, and no explosive eruptions since 1991. Enhanced stratospheric aerosol content due to volcanic eruptions, together with the small solar irradiance variations, result in a net negative natural radiative forcing over the past two, and possibly even the past four, decades.

C.6 Global Warming Potentials

Radiative forcings and Global Warming Potentials (GWPs) are presented in Table 3 for an expanded set of gases. GWPs are a measure of the relative radiative effect of a given substance compared to CO_2, integrated over a chosen time horizon. New categories of gases in Table 3 include fluorinated organic molecules, many of which are ethers that are proposed as halocarbon substitutes. Some of the GWPs have larger uncertainties than that of others, particularly for those gases where detailed laboratory data on lifetimes are not yet available. The direct GWPs have been calculated relative to CO_2 using an improved calculation of the CO_2 radiative forcing, the SAR response function for a CO_2 pulse, and new values for the radiative forcing and lifetimes for a number of halocarbons. Indirect GWPs, resulting from indirect radiative forcing effects, are also estimated for some new gases, including carbon monoxide. The direct GWPs for those species whose lifetimes are well characterised are estimated to be accurate within ±35%, but the indirect GWPs are less certain.

D. The Simulation of the Climate System and its Changes

The preceding two Sections reported on the climate from the distant past to the present day through the observations of climate variables and the forcing agents that cause climate to change. This Section bridges to the climate of the future by describing the only tool that provides quantitative estimates of future climate changes, namely, numerical models. The basic understanding of the energy balance of the Earth system means that quite simple models can provide a broad quantitative estimate of some globally averaged variables, but more accurate estimates of feedbacks and of regional detail can only come from more elaborate climate models. The complexity of the processes in the climate system prevents the use of extrapolation of past trends or statistical and other purely empirical techniques for projections. Climate models can be used to simulate the climate responses to different input scenarios of future forcing agents (Section F). Similarly, projection of the fate of emitted CO_2 (i.e., the relative sequestration into the various reservoirs) and other greenhouse gases requires an understanding of the biogeochemical processes involved and incorporating these into a numerical carbon cycle model.

A climate model is a simplified mathematical representation of the Earth's climate system (see Box 3). The degree to which the model can simulate the responses of the climate system hinges to a very large degree on the level of understanding of the physical, geophysical, chemical and biological processes that govern the climate system. Since the SAR, researchers have made substantial improvements in the simulation of the Earth's climate system with models. First, the current understanding of some of the most important processes that govern the climate system and how well they are represented in present climate models are summarised here. Then, this Section presents an assessment of the overall ability of present models to make useful projections of future climate.

D.1 Climate Processes and Feedbacks

Processes in the climate system determine the natural variability of the climate system and its response to perturbations, such as the increase in the atmospheric concentrations of greenhouse gases. Many basic climate processes of importance are well-known and modelled exceedingly well. Feedback processes amplify (a positive feedback) or reduce (a negative

Table 3: Direct Global Warming Potentials (GWPs) relative to carbon dioxide (for gases for which the lifetimes have been adequately characterised). GWPs are an index for estimating relative global warming contribution due to atmospheric emission of a kg of a particular greenhouse gas compared to emission of a kg of carbon dioxide. GWPs calculated for different time horizons show the effects of atmospheric lifetimes of the different gases. [Based upon Table 6.7]

Gas		Lifetime (years)	Global Warming Potential (Time Horizon in years)		
			20 yrs	100 yrs	500 yrs
Carbon dioxide	CO_2		1	1	1
Methane[a]	CH_4	12.0[b]	62	23	7
Nitrous oxide	N_2O	114[b]	275	296	156
Hydrofluorocarbons					
HFC-23	CHF_3	260	9400	12000	10000
HFC-32	CH_2F_2	5.0	1800	550	170
HFC-41	CH_3F	2.6	330	97	30
HFC-125	CHF_2CF_3	29	5900	3400	1100
HFC-134	CHF_2CHF_2	9.6	3200	1100	330
HFC-134a	CH_2FCF_3	13.8	3300	1300	400
HFC-143	CHF_2CH_2F	3.4	1100	330	100
HFC-143a	CF_3CH_3	52	5500	4300	1600
HFC-152	CH_2FCH_2F	0.5	140	43	13
HFC-152a	CH_3CHF_2	1.4	410	120	37
HFC-161	CH_3CH_2F	0.3	40	12	4
HFC-227ea	CF_3CHFCF_3	33	5600	3500	1100
HFC-236cb	$CH_2FCF_2CF_3$	13.2	3300	1300	390
HFC-236ea	CHF_2CHFCF_3	10	3600	1200	390
HFC-236fa	$CF_3CH_2CF_3$	220	7500	9400	7100
HFC-245ca	$CH_2FCF_2CHF_2$	5.9	2100	640	200
HFC-245fa	$CHF_2CH_2CF_3$	7.2	3000	950	300
HFC-365mfc	$CF_3CH_2CF_2CH_3$	9.9	2600	890	280
HFC-43-10mee	$CF_3CHFCHFCF_2CF_3$	15	3700	1500	470
Fully fluorinated species					
SF_6		3200	15100	22200	32400
CF_4		50000	3900	5700	8900
C_2F_6		10000	8000	11900	18000
C_3F_8		2600	5900	8600	12400
C_4F_{10}		2600	5900	8600	12400
c-C_4F_8		3200	6800	10000	14500
C_5F_{12}		4100	6000	8900	13200
C_6F_{14}		3200	6100	9000	13200
Ethers and Halogenated Ethers					
CH_3OCH_3		0.015	1	1	<<1
HFE-125	CF_3OCHF_2	150	12900	14900	9200
HFE-134	CHF_2OCHF_2	26.2	10500	6100	2000
HFE-143a	CH_3OCF_3	4.4	2500	750	230
HCFE-235da2	$CF_3CHClOCHF_2$	2.6	1100	340	110
HFE-245fa2	$CF_3CH_2OCHF_2$	4.4	1900	570	180
HFE-254cb2	$CHF_2CF_2OCH_3$	0.22	99	30	9
HFE-7100	$C_4F_9OCH_3$	5.0	1300	390	120
HFE-7200	$C_4F_9OC_2H_5$	0.77	190	55	17
H-Galden 1040x	$CHF_2OCF_2OC_2F_4OCHF_2$	6.3	5900	1800	560
HG-10	$CHF_2OCF_2OCHF_2$	12.1	7500	2700	850
HG-01	$CHF_2OCF_2CF_2OCHF_2$	6.2	4700	1500	450

[a] The methane GWPs include an indirect contribution from stratospheric H_2O and O_3 production.

[b] The values for methane and nitrous oxide are adjustment times, which incorporate the indirect effects of emission of each gas on its own lifetime.

Box 3: Climate Models: How are they built and how are they applied?

Comprehensive climate models are based on physical laws represented by mathematical equations that are solved using a three-dimensional grid over the globe. For climate simulation, the major components of the climate system must be represented in sub-models (atmosphere, ocean, land surface, cryosphere and biosphere), along with the processes that go on within and between them. Most results in this report are derived from the results of models, which include some representation of all these components. Global climate models in which the atmosphere and ocean components have been coupled together are also known as Atmosphere-Ocean General Circulation Models (AOGCMs). In the atmospheric module, for example, equations are solved that describe the large-scale evolution of momentum, heat and moisture. Similar equations are solved for the ocean. Currently, the resolution of the atmospheric part of a typical model is about 250 km in the horizontal and about 1 km in the vertical above the boundary layer. The resolution of a typical ocean model is about 200 to 400 m in the vertical, with a horizontal resolution of about 125 to 250 km. Equations are typically solved for every half hour of a model integration. Many physical processes, such as those related to clouds or ocean convection, take place on much smaller spatial scales than the model grid and therefore cannot be modelled and resolved explicitly. Their average effects are approximately included in a simple way by taking advantage of physically based relationships with the larger-scale variables. This technique is known as parametrization.

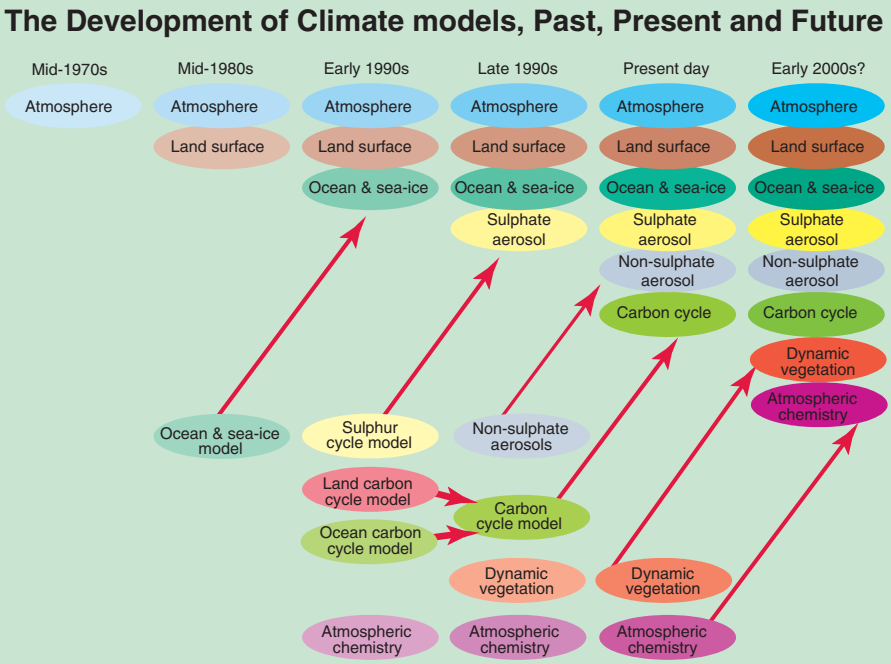

Box 3, Figure 1: The development of climate models over the last 25 years showing how the different components are first developed separately and later coupled into comprehensive climate models.

In order to make quantitative projections of future climate change, it is necessary to use climate models that simulate all the important processes governing the future evolution of the climate. Climate models have developed over the past few decades as computing power has increased. During that time, models of the main components, atmosphere, land, ocean and sea ice have been developed separately and then gradually integrated. This coupling of the various components is a difficult process. Most recently, sulphur cycle components have been incorporated to represent the emissions of sulphur and how they are oxidised to form aerosol particles. Currently in progress, in a few models, is the coupling of the land carbon cycle and the ocean carbon cycle. The atmospheric chemistry component currently is modelled outside the main climate model. The ultimate aim is, of course, to model as much as possible of the whole of the Earth's climate system so that all the components can interact and, thus, the predictions of climate change will continuously take into account the effect of feedbacks among components. The Figure above shows the past, present and possible future evolution of climate models.

Some models offset errors and surface flux imbalances through "flux adjustments", which are empirically determined systematic adjustments at the atmosphere-ocean interface held fixed in time in order to bring the simulated climate closer to the observed state. A strategy has been designed for carrying out climate experiments that removes much of the effects of some model errors on results. What is often done is that first a "control" climate simulation is run with the model. Then, the climate change experiment simulation is run, for example, with increased CO_2 in the model atmosphere. Finally, the difference is taken to provide an estimate of the change in climate due to the perturbation. The differencing technique removes most of the effects of any artificial adjustments in the model, as well as systematic errors that are common to both runs. However, a comparison of different model results makes it apparent that the nature of some errors still influences the outcome.

Many aspects of the Earth's climate system are chaotic – its evolution is sensitive to small perturbations in initial conditions. This sensitivity limits predictability of the detailed evolution of weather to about two weeks. However, predictability of climate is not so limited because of the systematic influences on the atmosphere of the more slowly varying components of the climate system. Nevertheless, to be able to make reliable forecasts in the presence of both initial condition and model uncertainty, it is desirable to repeat the prediction many times from different perturbed initial states and using different global models. These ensembles are the basis of probability forecasts of the climate state.

Comprehensive AOGCMs are very complex and take large computer resources to run. To explore different scenarios of emissions of greenhouse gases and the effects of assumptions or approximations in parameters in the model more thoroughly, simpler models are also widely used. The simplifications may include coarser resolution and simplified dynamics and physical processes. Together, simple, intermediate, and comprehensive models form a "hierarchy of climate models", all of which are necessary to explore choices made in parametrizations and assess the robustness of climate changes.

feedback) changes in response to an initial perturbation and hence are very important for accurate simulation of the evolution of climate.

Water vapour

A major feedback accounting for the large warming predicted by climate models in response to an increase in CO_2 is the increase in atmospheric water vapour. An increase in the temperature of the atmosphere increases its water-holding capacity; however, since most of the atmosphere is undersaturated, this does not automatically mean that water vapour, itself, must increase. Within the boundary layer (roughly the lowest 1 to 2 km of the atmosphere), water vapour increases with increasing temperature. In the free troposphere above the boundary layer, where the water vapour greenhouse effect is most important, the situation is harder to quantify. Water vapour feedback, as derived from current models, approximately doubles the warming from what it would be for fixed water vapour. Since the SAR, major improvements have occurred in the treatment of water vapour in models, although detrainment of moisture from clouds remains quite uncertain and discrepancies exist between model water vapour distributions and those observed. Models are capable of simulating the moist and very dry regions observed in the tropics and sub-tropics and how they evolve with the seasons and from year to year. While reassuring, this does not provide a check of the feedbacks, although the balance of evidence favours a positive clear-sky water vapour feedback of the magnitude comparable to that found in simulations.

Clouds

As has been the case since the first IPCC Assessment Report in 1990, probably the greatest uncertainty in future projections of climate arises from clouds and their interactions with radiation. Clouds can both absorb and reflect solar radiation (thereby cooling the surface) and absorb and emit long wave radiation (thereby warming the surface). The competition between these effects depends on cloud height, thickness and radiative properties. The radiative properties and evolution of clouds depend on the distribution of atmospheric water vapour, water drops, ice particles, atmospheric aerosols and cloud thickness. The physical basis of cloud parametrizations is greatly improved in models through inclusion of bulk representation of cloud microphysical properties in a cloud water budget equation, although considerable uncertainty remains. Clouds represent a significant source of potential error in climate simulations. The possibility that models underestimate systematically solar

absorption in clouds remains a controversial matter. The sign of the net cloud feedback is still a matter of uncertainty, and the various models exhibit a large spread. Further uncertainties arise from precipitation processes and the difficulty in correctly simulating the diurnal cycle and precipitation amounts and frequencies.

Stratosphere

There has been a growing appreciation of the importance of the stratosphere in the climate system because of changes in its structure and recognition of the vital role of both radiative and dynamical processes. The vertical profile of temperature change in the atmosphere, including the stratosphere, is an important indicator in detection and attribution studies. Most of the observed decreases in lower-stratospheric temperatures have been due to ozone decreases, of which the Antarctic "ozone hole" is a part, rather than increased CO_2 concentrations. Waves generated in the troposphere can propagate into the stratosphere where they are absorbed. As a result, stratospheric changes alter where and how these waves are absorbed, and the effects can extend downward into the troposphere. Changes in solar irradiance, mainly in the ultraviolet (UV), lead to photochemically-induced ozone changes and, hence, alter the stratospheric heating rates, which can alter the tropospheric circulation. Limitations in resolution and relatively poor representation of some stratospheric processes adds uncertainty to model results.

Ocean

Major improvements have taken place in modelling ocean processes, in particular heat transport. These improvements, in conjunction with an increase in resolution, have been important in reducing the need for flux adjustment in models and in producing realistic simulations of natural large-scale circulation patterns and improvements in simulating El Niño (see Box 4). Ocean currents carry heat from the tropics to higher latitudes. The ocean exchanges heat, water (through evaporation and precipitation) and CO_2 with the atmosphere. Because of its huge mass and high heat capacity, the ocean slows climate change and influences the time-scales of variability in the ocean-atmosphere system. Considerable progress has been made in the understanding of ocean processes relevant for climate change. Increases in resolution, as well as improved representation (parametrization) of important sub-grid scale processes (e.g., mesoscale eddies), have increased the realism of simulations. Major uncertainties still exist with the representation of small-scale processes, such as overflows (flow through narrow channels, e.g., between Greenland and Iceland), western boundary currents (i.e., large-scale narrow currents along coastlines), convection and mixing. Boundary currents in climate simulations are weaker and wider than in nature, although the consequences of this for climate are not clear.

Cryosphere

The representation of sea-ice processes continues to improve, with several climate models now incorporating physically based treatments of ice dynamics. The representation of land-ice processes in global climate models remains rudimentary. The cryosphere consists of those regions of Earth that are seasonally or perennially covered by snow and ice. Sea ice is important because it reflects more incoming solar radiation than the sea surface (i.e., it has a higher albedo), and it insulates the sea from heat loss during the winter. Therefore, reduction of sea ice gives a positive feedback on climate warming at high latitudes. Furthermore, because sea ice contains less salt than sea water, when sea ice is formed the salt content (salinity) and density of the surface layer of the ocean is increased. This promotes an exchange of water with deeper layers of the ocean, affecting ocean circulation. The formation of icebergs and the melting of ice shelves returns fresh water from the land to the ocean, so that changes in the rates of these processes could affect ocean circulation by changing the surface salinity. Snow has a higher albedo than the land surface; hence, reductions in snow cover lead to a similar positive albedo feedback, although weaker than for sea ice. Increasingly complex snow schemes and sub-grid scale variability in ice cover and thickness, which can significantly influence albedo and atmosphere-ocean exchanges, are being introduced in some climate models.

Land surface

Research with models containing the latest representations of the land surface indicates that the direct effects of increased CO_2 on the physiology of plants could lead to a relative reduction in evapotranspiration over the tropical continents, with associated regional warming and drying over that predicted for conventional greenhouse warming effects. Land surface changes provide important feedbacks as anthropogenic climate changes (e.g., increased temperature, changes in precipitation, changes in net radiative heating, and the direct effects of CO_2) will influence the state of the land surface (e.g., soil moisture, albedo, roughness and vegetation). Exchanges of

energy, momentum, water, heat and carbon between the land surface and the atmosphere can be defined in models as functions of the type and density of the local vegetation and the depth and physical properties of the soil, all based on land-surface data bases that have been improved using satellite observations. Recent advances in the understanding of vegetation photosynthesis and water use have been used to couple the terrestrial energy, water and carbon cycles within a new generation of land surface parametrizations, which have been tested against field observations and implemented in a few GCMs, with demonstrable improvements in the simulation of land-atmosphere fluxes. However, significant problems remain to be solved in the areas of soil moisture processes, runoff prediction, land-use change and the treatment of snow and sub-grid scale heterogeneity.

Changes in land-surface cover can affect global climate in several ways. Large-scale deforestation in the humid tropics (e.g., South America, Africa, and Southeast Asia) has been identified as the most important ongoing land-surface process, because it reduces evaporation and increases surface temperature. These effects are qualitatively reproduced by most models. However, large uncertainties still persist on the quantitative impact of large-scale deforestation on the hydrological cycle, particularly over Amazonia.

Carbon cycle

Recent improvements in process-based terrestrial and ocean carbon cycle models and their evaluation against observations have given more confidence in their use for future scenario studies. CO_2 naturally cycles rapidly among the atmosphere, oceans and land. However, the removal of the CO_2 perturbation added by human activities from the atmosphere takes far longer. This is because of processes that limit the rate at which ocean and terrestrial carbon stocks can increase. Anthropogenic CO_2 is taken up by the ocean because of its high solubility (caused by the nature of carbonate chemistry), but the rate of uptake is limited by the finite speed of vertical mixing. Anthropogenic CO_2 is taken up by terrestrial ecosystems through several possible mechanisms, for example, land management, CO_2 fertilisation (the enhancement of plant growth as a result of increased atmospheric CO_2 concentration) and increasing anthropogenic inputs of nitrogen. This uptake is limited by the relatively small fraction of plant carbon that can enter long-term storage (wood and humus). The fraction of emitted CO_2 that can be taken up by the oceans and land is expected to decline with increasing CO_2 concentrations. Process-based models of the ocean and land carbon cycles (including representations of physical, chemical and biological processes) have been developed and evaluated against measurements pertinent to the natural carbon cycle. Such models have also been set up to mimic the human perturbation of the carbon cycle and have been able to generate time-series of ocean and land carbon uptake that are broadly consistent with observed global trends. There are still substantial differences among models, especially in how they treat the physical ocean circulation and in regional responses of terrestrial ecosystem processes to climate. Nevertheless, current models consistently indicate that when the effects of climate change are considered, CO_2 uptake by oceans and land becomes smaller.

D.2 The Coupled Systems

As noted in Section D.1, many feedbacks operate within the individual components of the climate system (atmosphere, ocean, cryosphere and land surface). However, many important processes and feedbacks occur through the coupling of the climate system components. Their representation is important to the prediction of large-scale responses.

Modes of natural variability

There is an increasing realisation that natural circulation patterns, such as ENSO and NAO, play a fundamental role in global climate and its interannual and longer-term variability. The strongest natural fluctuation of climate on interannual time-scales is the ENSO phenomenon (see Box 4). It is an inherently coupled atmosphere-ocean mode with its core activity in the tropical Pacific, but with important regional climate impacts throughout the world. Global climate models are only now beginning to exhibit variability in the tropical Pacific that resembles ENSO, mainly through increased meridional resolution at the equator. Patterns of sea surface temperature and atmospheric circulation similar to those occurring during ENSO on interannual time-scales also occur on decadal and longer time-scales.

The North Atlantic Oscillation (NAO) is the dominant pattern of northern wintertime atmospheric circulation variability and is increasingly being simulated realistically. The NAO is closely related to the Arctic Oscillation (AO), which has an additional annular component around the Arctic. There is strong evidence that the NAO arises mainly from internal atmospheric processes involving the entire troposphere-stratosphere system.

Box 4: The El Niño-Southern Oscillation (ENSO)

The strongest natural fluctuation of climate on interannual time-scales is the El Niño-Southern Oscillation (ENSO) phenomenon. The term "El Niño" originally applied to an annual weak warm ocean current that ran southwards along the coast of Peru about Christmas-time and only subsequently became associated with the unusually large warmings. The coastal warming, however, is often associated with a much more extensive anomalous ocean warming to the International Dateline, and it is this Pacific basinwide phenomenon that forms the link with the anomalous global climate patterns. The atmospheric component tied to "El Niño" is termed the "Southern Oscillation". Scientists often call this phenomenon, where the atmosphere and ocean collaborate together, ENSO (El Niño-Southern Oscillation).

ENSO is a natural phenomenon, and there is good evidence from cores of coral and glacial ice in the Andes that it has been going on for millennia. The ocean and atmospheric conditions in the tropical Pacific are seldom average, but instead fluctuate somewhat irregularly between El Niño events and the opposite "La Niña" phase, consisting of a basinwide cooling of the tropical Pacific, with a preferred period of about three to six years. The most intense phase of each event usually lasts about a year.

A distinctive pattern of sea surface temperatures in the Pacific Ocean sets the stage for ENSO events. Key features are the "warm pool" in the tropical western Pacific, where the warmest ocean waters in the world reside, much colder waters in the eastern Pacific, and a cold tongue along the equator that is most pronounced about October and weakest in March. The atmospheric easterly trade winds in the tropics pile up the warm waters in the west, producing an upward slope of sea level along the equator of 0.60 m from east to west. The winds drive the surface ocean currents, which determine where the surface waters flow and diverge. Thus, cooler nutrient-rich waters upwell from below along the equator and western coasts of the Americas, favouring development of phytoplankton, zooplankton, and hence fish. Because convection and thunder-storms preferentially occur over warmer waters, the pattern of sea surface temperatures determines the distribution of rainfall in the tropics, and this in turn determines the atmospheric heating patterns through the release of latent heat. The heating drives the large-scale monsoonal-type circulations in the tropics, and consequently determines the winds. This strong coupling between the atmosphere and ocean in the tropics gives rise to the El Niño phenomenon.

During El Niño, the warm waters from the western tropical Pacific migrate eastward as the trade winds weaken, shifting the pattern of tropical rainstorms, further weakening the trade winds, and thus reinforcing the changes in sea temperatures. Sea level drops in the west, but rises in the east by as much as 0.25 m, as warm waters surge eastward along the equator. However, the changes in atmospheric circulation are not confined to the tropics, but extend globally and influence the jet streams and storm tracks in mid-latitudes. Approximately reverse patterns occur during the opposite La Niña phase of the phenomenon.

Changes associated with ENSO produce large variations in weather and climate around the world from year to year. These often have a profound impact on humanity and society because of associated droughts, floods, heat waves and other changes that can severely disrupt agriculture, fisheries, the environment, health, energy demand, air quality and also change the risks of fire. ENSO also plays a prominent role in modulating exchanges of CO_2 with the atmosphere. The normal upwelling of cold nutrient-rich and CO_2-rich waters in the tropical Pacific is suppressed during El Niño.

Fluctuations in Atlantic Sea Surface Temperatures (SSTs) are related to the strength of the NAO, and a modest two-way interaction between the NAO and the Atlantic Ocean, leading to decadal variability, is emerging as important in projecting climate change.

Climate change may manifest itself both as shifting means, as well as changing preference of specific climate regimes, as evidenced by the observed trend toward positive values for the last 30 years in the NAO index and the climate "shift" in the tropical Pacific about 1976. While coupled models simulate features of observed natural climate variability, such as the NAO and ENSO, which suggests that many of the relevant processes are included in the models, further progress is needed to depict these natural modes accurately. Moreover,

because ENSO and NAO are key determinants of regional climate change and can possibly result in abrupt and counter intuitive changes, there has been an increase in uncertainty in those aspects of climate change that critically depend on regional changes.

The thermohaline circulation (THC)

The thermohaline circulation (THC) is responsible for the major part of the meridional heat transport in the Atlantic Ocean. The THC is a global-scale overturning in the ocean driven by density differences arising from temperature and salinity effects. In the Atlantic, heat is transported by warm surface waters flowing northward and cold saline waters from the North Atlantic returning at depth. Reorganisations in the Atlantic THC can be triggered by perturbations in the surface buoyancy, which is influenced by precipitation, evaporation, continental runoff, sea-ice formation, and the exchange of heat, processes that could all change with consequences for regional and global climate. Interactions between the atmosphere and the ocean are also likely to be of considerable importance on decadal and longer time-scales, where the THC is involved. The interplay between the large-scale atmospheric forcing, with warming and evaporation in low latitudes and cooling and increased precipitation at high latitudes, forms the basis of a potential instability of the present Atlantic THC. ENSO may also influence the Atlantic THC by altering the fresh water balance of the tropical Atlantic, therefore providing a coupling between low and high latitudes. Uncertainties in the representation of small-scale flows over sills and through narrow straits and of ocean convection limit the ability of models to simulate situations involving substantial changes in the THC. The less saline North Pacific means that a deep THC does not occur in the Pacific.

Non-linear events and rapid climate change

The possibility for rapid and irreversible changes in the climate system exists, but there is a large degree of uncertainty about the mechanisms involved and hence also about the likelihood or time-scales of such transitions. The climate system involves many processes and feedbacks that interact in complex non-linear ways. This interaction can give rise to thresholds in the climate system that can be crossed if the system is perturbed sufficiently. There is evidence from polar ice cores suggesting that atmospheric regimes can change within a few years and that large-scale hemispheric changes can evolve as fast as a few decades. For example, the possibility of a threshold for a rapid transition of the Atlantic THC to a collapsed state has been demonstrated with a hierarchy of models. It is not yet clear what this threshold is and how likely it is that human activity would lead it to being exceeded (see Section F.6). Atmospheric circulation can be characterised by different preferred patterns; e.g., arising from ENSO and the NAO/AO, and changes in their phase can occur rapidly. Basic theory and models suggest that climate change may be first expressed in changes in the frequency of occurrence of these patterns. Changes in vegetation, through either direct anthropogenic deforestation or those caused by global warming, could occur rapidly and could induce further climate change. It is supposed that the rapid creation of the Sahara about 5,500 years ago represents an example of such a non-linear change in land cover.

D.3 Regionalisation Techniques

Regional climate information was only addressed to a limited degree in the SAR. Techniques used to enhance regional detail have been substantially improved since the SAR and have become more widely applied. They fall into three categories: high and variable resolution AOGCMs; regional (or nested limited area) climate models (RCMs); and empirical/statistical and statistical/dynamical methods. The techniques exhibit different strengths and weaknesses and their use at the continental scale strongly depends on the needs of specific applications.

Coarse resolution AOGCMs simulate atmospheric general circulation features well in general. At the regional scale, the models display area-average biases that are highly variable from region to region and among models, with sub-continental area averaged seasonal temperature biases typically ±4ºC and precipitation biases between –40 and +80%. These represent an important improvement compared to AOGCMs evaluated in the SAR.

The development of high resolution/variable resolution Atmospheric General Circulation Models (AGCMs) since the SAR generally shows that the dynamics and large-scale flow in the models improves as resolution increases. In some cases, however, systematic errors are worsened compared to coarser resolution models, although only very few results have been documented.

High resolution RCMs have matured considerably since the SAR. Regional models consistently improve the spatial detail of simulated climate compared to AGCMs. RCMs driven by

observed boundary conditions evidence area-averaged temperature biases (regional scales of 10^5 to 10^6 km^2) generally below 2ºC, while precipitation biases are below 50%. Regionalisation work indicates at finer scales that the changes can be substantially different in magnitude or sign from the large area-average results. A relatively large spread exists among models, although attribution of the cause of these differences is unclear.

D.4 Overall Assessment of Abilities

Coupled models have evolved and improved significantly since the SAR. In general, they provide credible simulations of climate, at least down to sub-continental scales and over temporal scales from seasonal to decadal. Coupled models, as a class, are considered to be suitable tools to provide useful projections of future climates. These models cannot yet simulate all aspects of climate (e.g., they still cannot account fully for the observed trend in the surface-troposphere temperature differences since 1979). Clouds and humidity also remain sources of significant uncertainty, but there have been incremental improvements in simulations of these quantities. No single model can be considered "best", and it is important to utilise results from a range of carefully evaluated coupled models to explore effects of different formulations. The rationale for increased confidence in models arises from model performance in the following areas.

Flux adjustment

The overall confidence in model projections is increased by the improved performance of several models that do not use flux adjustment. These models now maintain stable, multi-century simulations of surface climate that are considered to be of sufficient quality to allow their use for climate change projections. The changes whereby many models can now run without flux adjustment have come from improvements in both the atmospheric and oceanic components. In the model atmosphere, improvements in convection, the boundary layer, clouds, and surface latent heat fluxes are most notable. In the model ocean, the improvements are in resolution, boundary layer mixing, and in the representation of eddies. The results from climate change studies with flux adjusted and non-flux adjusted models are broadly in agreement; nonetheless, the development of stable non-flux adjusted models increases confidence in their ability to simulate future climates.

Climate of the 20th century

Confidence in the ability of models to project future climates is increased by the ability of several models to reproduce warming trends in the 20th century surface air temperature when driven by increased greenhouse gases and sulphate aerosols. This is illustrated in Figure 13. However, only idealized scenarios of sulphate aerosols have been used and contributions from some additional processes and forcings may not have been included in the models. Some modelling studies suggest that inclusion of additional forcings like solar variability and volcanic aerosols may improve some aspects of the simulated climate variability of the 20th century.

Extreme events

Analysis of and confidence in extreme events simulated within climate models are still emerging, particularly for storm tracks and storm frequency. "Tropical-cyclone-like" vortices are being simulated in climate models, although enough uncertainty remains over their interpretation to warrant caution in projections of tropical cyclone changes. However, in general, the analysis of extreme events in both observations (see Section B.6) and coupled models is underdeveloped.

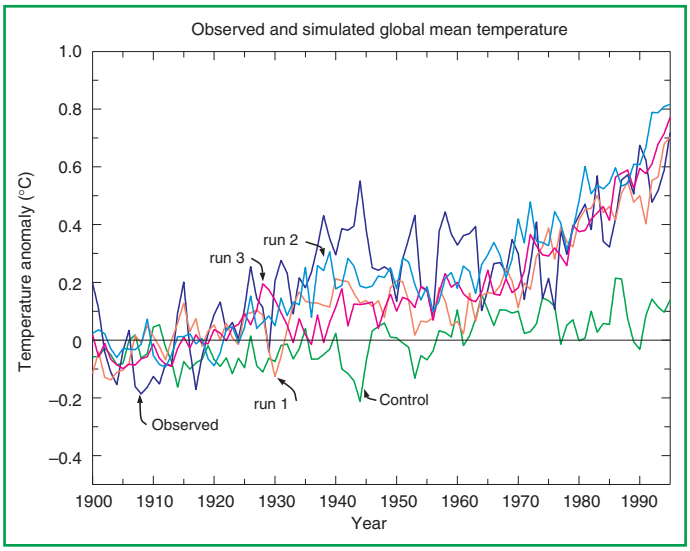

Figure 13: Observed and modelled global annual mean temperature anomalies (°C) relative to the average of the observations over the period 1900 to 1930. The control and three independent simulations with the same greenhouse gas plus aerosol forcing and slightly different initial conditions are shown from an AOGCM. The three greenhouse gas plus aerosol simulations are labeled 'run 1', 'run 2', and 'run 3' respectively. [Based on Figure 8.15]

Interannual variability

The performance of coupled models in simulating ENSO has improved; however, its variability is displaced westward and its strength is generally underestimated. When suitably initialised with surface wind and sub-surface ocean data, some coupled models have had a degree of success in predicting ENSO events.

Model intercomparisons

The growth in systematic intercomparisons of models provides the core evidence for the growing capabilities of climate models. For example, the Coupled Model Intercomparison Project (CMIP) is enabling a more comprehensive and systematic evaluation and intercomparison of coupled models run in a standardised configuration and responding to standardised forcing. Some degree of quantification of improvements in coupled model performance has now been demonstrated. The Palaeoclimate Model Intercomparison Project (PMIP) provides intercomparisons of models for the mid-Holocene (6,000 years before present) and for the Last Glacial Maximum (21,000 years before present). The ability of these models to simulate some aspects of palaeoclimates, compared to a range of palaeoclimate proxy data, gives confidence in models (at least the atmospheric component) over a range of difference forcings.

E. The Identification of a Human Influence on Climate Change

Sections B and C characterised the observed past changes in climate and in forcing agents, respectively. Section D examined the capabilities of climate models to predict the response of the climate system to such changes in forcing. This Section uses that information to examine the question of whether a human influence on climate change to date can be identified.

This is an important point to address. The SAR concluded that "the balance of evidence suggests that there is a discernible human influence on global climate". It noted that the detection and attribution of anthropogenic climate change signals will be accomplished through a gradual accumulation of evidence. The SAR also noted uncertainties in a number of factors, including internal variability and the magnitude and patterns of forcing and response, which prevented them from drawing a stronger conclusion.

E.1 The Meaning of Detection and Attribution

Detection *is the process of demonstrating that an observed change is significantly different (in a statistical sense) than can be explained by natural variability.* ***Attribution*** *is the process of establishing cause and effect with some defined level of confidence, including the assessment of competing hypotheses.* The response to anthropogenic changes in climate forcing occurs against a backdrop of natural internal and externally forced climate variability. Internal climate variability, i.e., climate variability not forced by external agents, occurs on all time-scales from weeks to centuries and even millennia. Slow climate components, such as the ocean, have particularly important roles on decadal and century time-scales because they integrate weather variability. Thus, the climate is capable of producing long time-scale variations of considerable magnitude without external influences. Externally forced climate variations (signals) may be due to changes in natural forcing factors, such as solar radiation or volcanic aerosols, or to changes in anthropogenic forcing factors, such as increasing concentrations of greenhouse gases or aerosols. The presence of this natural climate variability means that the detection and attribution of anthropogenic climate change is a statistical "signal to noise" problem. *Detection* studies demonstrate whether or not an observed change is highly unusual in a statistical sense, but this does not necessarily

imply that we understand its causes. The *attribution* of climate change to anthropogenic causes involves statistical analysis and the careful assessment of multiple lines of evidence to demonstrate, within a pre-specified margin of error, that the observed changes are:

- unlikely to be due entirely to internal variability;
- consistent with the estimated responses to the given combination of anthropogenic and natural forcing; and
- not consistent with alternative, physically plausible explanations of recent climate change that exclude important elements of the given combination of forcings.

E.2 A Longer and More Closely Scrutinised Observational Record

Three of the last five years (1995, 1997 and 1998) were the warmest globally in the instrumental record. The impact of observational sampling errors has been estimated for the global and hemispheric mean temperature record. There is also a better understanding of the errors and uncertainties in the satellite-based (Microwave Sounding Unit, MSU) temperature record. Discrepancies between MSU and radiosonde data have largely been resolved, although the observed trend in the difference between the surface and lower tropospheric temperatures cannot fully be accounted for (see Section B). New reconstructions of temperature over the last 1,000 years indicate that the temperature changes over the last hundred years are unlikely to be entirely natural in origin, even taking into account the large uncertainties in palaeo-reconstructions (see Section B).

E.3 New Model Estimates of Internal Variability

The warming over the past 100 years is very unlikely to be due to internal variability alone, as estimated by current models. The instrumental record is short and covers the period of human influence and palaeo-records include natural forced variations, such as those due to variations in solar irradiance and in the frequency of major volcanic eruptions. These limitations leave few alternatives to using long "control" simulations with coupled models for the estimation of internal climate variability. Since the SAR, more models have been used to estimate the magnitude of internal climate variability, a representative sample of which is given in Figure 14. As can be seen, there is a wide range of global scale internal variability in these models. Estimates of the longer time-scale variability relevant to detection and attribution studies is uncertain, but, on interannual and decadal time-scales, some models show similar or larger variability than observed, even though models do not include variance from external sources. Conclusions on detection of an anthropogenic signal are insensitive to the model used to estimate internal variability, and recent changes cannot be accounted for as pure internal variability, even if the amplitude of simulated internal variations is increased by a factor of two or perhaps more. Most recent detection and attribution studies find no evidence that model-estimated internal variability at the surface is inconsistent with the residual variability that remains in the observations after removal of the estimated anthropogenic signals on the large spatial and long time-scales used in detection and attribution studies. Note, however, the ability to detect inconsistencies is limited. As Figure 14 indicates, no model control simulation shows a trend in surface air temperature as large as the observed trend over the last 1,000 years.

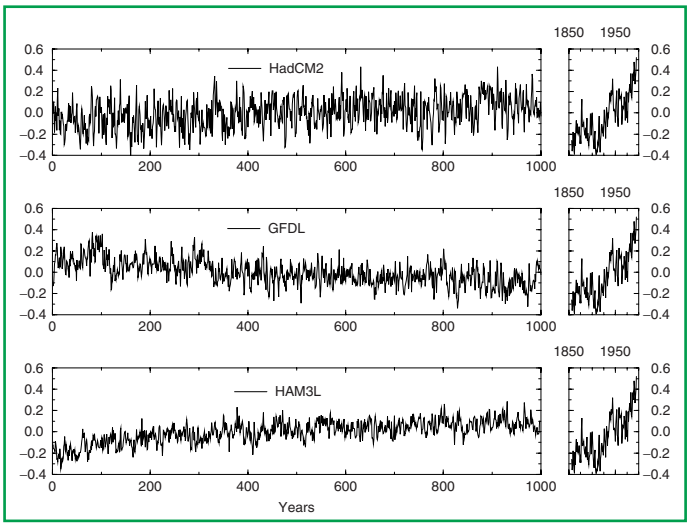

Figure 14: Global mean surface air temperature anomalies from 1,000 year control simulations with three different climate models, – Hadley, Geophysical Fluid Dynamics Laboratory and Hamburg, compared to the recent instrumental record. No model control simulation shows a trend in surface air temperature as large as the observed trend. If internal variability is correct in these models, the recent warming is likely not due to variability produced within the climate system alone. [Based on Figure 12.1]

E.4 New Estimates of Responses to Natural Forcing

Assessments based on physical principles and model simulations indicate that natural forcing alone is unlikely to explain the recent observed global warming or the observed changes in vertical temperature structure of the atmosphere. Fully coupled ocean-atmosphere models have used reconstructions of solar and volcanic forcings over the last one to three centuries to estimate the contribution of natural forcing to climate variability and change. Although the reconstruction of natural forcings is uncertain, including their effects produces an increase in variance at longer (multi-decadal) time-scales. This brings the low-frequency variability closer to that deduced from palaeo-reconstructions. It is likely that the net natural forcing (i.e., solar plus volcanic) has been negative over the past two decades, and possibly even the past four decades. Statistical assessments confirm that simulated natural variability, both internal and naturally forced, is unlikely to explain the warming in the latter half of the 20th century (see Figure 15). However, there is evidence for a detectable volcanic influence on climate and evidence that suggests a detectable solar influence, especially in the early part of the 20th century. Even if the models underestimate the magnitude of the response to solar or volcanic forcing, the spatial and temporal patterns are such that these effects alone cannot explain the observed temperature changes over the 20th century.

E.5 Sensitivity to Estimates of Climate Change Signals

There is a wide range of evidence of qualitative consistencies between observed climate changes and model responses to anthropogenic forcing. Models and observations show increasing global temperature, increasing land-ocean temperature contrast, diminishing sea-ice extent, glacial retreat, and increases in precipitation at high latitudes in the Northern Hemisphere. Some qualitative inconsistencies remain, including the fact that models predict a faster rate of warming in the mid- to upper troposphere than is observed in either satellite or radiosonde tropospheric temperature records.

All simulations with greenhouse gases and sulphate aerosols that have been used in detection studies have found that a significant anthropogenic contribution is required to account for surface and tropospheric trends over at least the last 30 years. Since the SAR, more simulations with increases in greenhouse gases and some representation of aerosol effects have become available. Several studies have included an explicit representation of greenhouse gases (as opposed to an equivalent increase in CO_2). Some have also included tropospheric ozone changes, an interactive sulphur cycle, an explicit radiative treatment of the scattering of sulphate aerosols, and improved estimates of the changes in stratospheric ozone. Overall, while detection of the climate response to these other anthropogenic factors is often ambiguous, detection of the influence of greenhouse gases on the surface temperature changes over the past 50 years is robust. In some cases, ensembles of simulations have been run to reduce noise in the estimates of the time-dependent response. Some studies have evaluated seasonal variation of the response. Uncertainties in the estimated climate change signals have made it difficult to attribute the observed climate change to one specific combination of anthropogenic and natural influences, but all studies have found a significant anthropogenic contribution is required to account for surface and tropospheric trends over at least the last thirty years.

E.6 A Wider Range of Detection Techniques

Temperature

Evidence of a human influence on climate is obtained over a substantially wider range of detection techniques. A major advance since the SAR is the increase in the range of techniques used and the evaluation of the degree to which the results are independent of the assumptions made in applying those techniques. There have been studies using pattern correlations, optimal detection studies using one or more fixed patterns and time-varying patterns, and a number of other techniques. The increase in the number of studies, breadth of techniques, increased rigour in the assessment of the role of anthropogenic forcing in climate, and the robustness of results to the assumptions made using those techniques, has increased the confidence in these aspects of detection and attribution.

Results are sensitive to the range of temporal and spatial scales that are considered. Several decades of data are necessary to separate forced signals from internal variability. Idealised studies have demonstrated that surface temperature changes are detectable only on scales in the order of 5,000 km. Such studies show that the level of agreement found between simulations and observations in pattern correlation studies is close to what one would expect in theory.

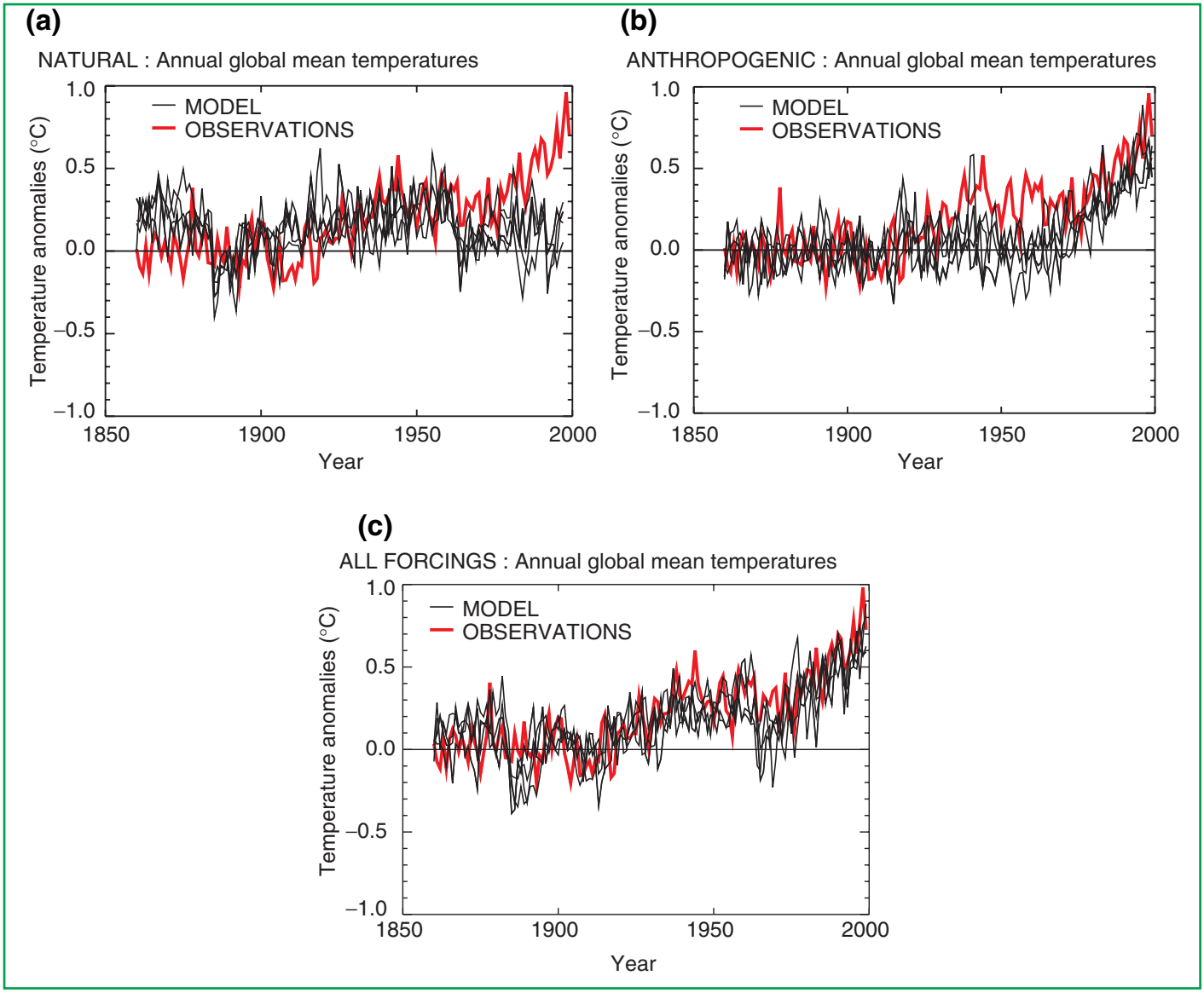

Figure 15: Global mean surface temperature anomalies relative to the 1880 to 1920 mean from the instrumental record compared with ensembles of four simulations with a coupled ocean-atmosphere climate model forced (a) with solar and volcanic forcing only, (b) with anthropogenic forcing including well mixed greenhouse gases, changes in stratospheric and tropospheric ozone and the direct and indirect effects of sulphate aerosols, and (c) with all forcings, both natural and anthropogenic. The thick line shows the instrumental data while the thin lines show the individual model simulations in the ensemble of four members. Note that the data are annual mean values. The model data are only sampled at the locations where there are observations. The changes in sulphate aerosol are calculated interactively, and changes in tropospheric ozone were calculated offline using a chemical transport model. Changes in cloud brightness (the first indirect effect of sulphate aerosols) were calculated by an off line simulation and included in the model. The changes in stratospheric ozone were based on observations. The volcanic and solar forcing were based on published combinations of measured and proxy data. The net anthropogenic forcing at 1990 was 1.0 Wm^{-2} including a net cooling of 1.0 Wm^{-2} due to sulphate aerosols. The net natural forcing for 1990 relative to 1860 was 0.5 Wm^{-2}, and for 1992 was a net cooling of 2.0 Wm^{-2} due to Mount Pinatubo. Other models forced with anthropogenic forcing give similar results to those shown in (b). [Based on Figure 12.7]

Most attribution studies find that, over the last 50 years, the estimated rate and magnitude of global warming due to increasing concentrations of greenhouse gases alone are comparable with or larger than the observed warming. Attribution studies address the question of "whether the magnitude of the simulated response to a particular forcing agent is consistent with observations". The use of multi-signal techniques has enabled studies that discriminate between the effects of different factors on climate. The inclusion of the time dependence of signals has helped to distinguish between natural and anthropogenic forcings. As more response patterns are included, the problem of degeneracy (different combinations of patterns yielding near identical fits to the observations) inevitably arises. Nevertheless, even with all the major responses that have been included in the analysis, a distinct greenhouse gas signal remains detectable. Furthermore, most model estimates that take into account both greenhouse gases and sulphate aerosols are consistent with observations over this period. The best agreement between model simulations and observations over the last 140 years is found when both anthropogenic and natural factors are included (see Figure 15). These results show that the forcings included are sufficient to explain the observed changes, but do not exclude the possibility that other forcings have also contributed. Overall, the magnitude of the temperature response to increasing concentrations of greenhouse gases is found to be consistent with observations on the scales considered (see Figure 16), but there remain discrepies between modelled and observed response to other natural and anthropogenic factors.

Uncertainties in other forcings that have been included do not prevent identification of the effect of anthropogenic greenhouse gases over the last 50 years. The sulphate forcing, while uncertain, is negative over this period. Changes in natural forcing during most of this period are also estimated to be negative. Detection of the influence of anthropogenic greenhouse gases therefore cannot be eliminated either by the uncertainty in sulphate aerosol forcing or because natural forcing has not been included in all model simulations. Studies that distinguish the separate responses to greenhouse gas, sulphate aerosol and natural forcing produce uncertain estimates of the amplitude of the sulphate aerosol and natural signals, but almost all studies are nevertheless able to detect the presence of the anthropogenic greenhouse gas signal in the recent climate record.

The detection and attribution methods used should not be sensitive to errors in the amplitude of the global mean response to individual forcings. In the signal-estimation methods used in this report, the amplitude of the signal is estimated from the observations and not the amplitude of the simulated response. Hence the estimates are independent of those factors determining the simulated amplitude of the response, such as the climate sensitivity of the model used. In addition, if the signal due to a given forcing is estimated individually, the amplitude is largely independent of the magnitude of the forcing used to derive the response. Uncertainty in the amplitude of the solar and indirect sulphate aerosol forcing should not affect the magnitude of the estimated signal.

Sea level

It is very likely that the 20th century warming has contributed significantly to the observed sea level rise, through thermal expansion of sea water and widespread loss of land ice. Within present uncertainties, observations and models are both consistent with a lack of significant acceleration of sea level rise during the 20th century.

E.7 Remaining Uncertainties in Detection and Attribution

Some progress has been made in reducing uncertainty, though many of the sources of uncertainty identified in the SAR still exist. These include:

- *Discrepancies between the vertical profile of temperature change in the troposphere seen in observations and models.* These have been reduced as more realistic forcing histories have been used in models, although not fully resolved. Also, the difference between observed surface and lower-tropospheric trends over the last two decades cannot be fully reproduced by model simulations.
- *Large uncertainties in estimates of internal climate variability from models and observations.* Although as noted above, these are unlikely (bordering on very unlikely) to be large enough to nullify the claim that a detectable climate change has taken place.
- *Considerable uncertainty in the reconstructions of solar and volcanic forcing which are based on proxy or limited observational data for all but the last two decades.* Detection of the influence of greenhouse gases on climate

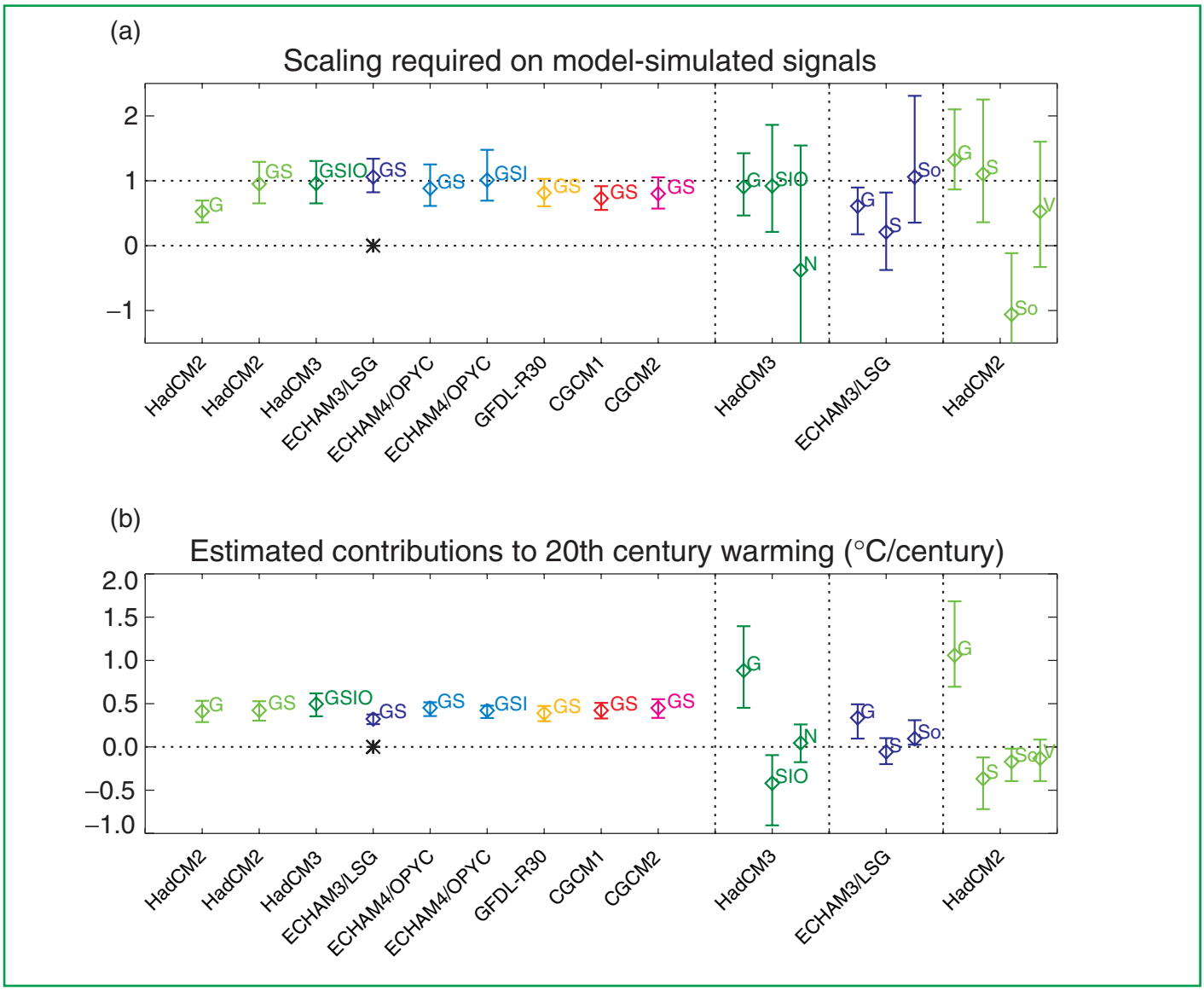

Figure 16: (a) Estimates of the "scaling factors" by which the amplitude of several model-simulated signals must be multiplied to reproduce the corresponding changes in the observed record. The vertical bars indicate the 5 to 95% uncertainty range due to internal variability. A range encompassing unity implies that this combination of forcing amplitude and model-simulated response is consistent with the corresponding observed change, while a range encompassing zero implies that this model-simulated signal is not detectable. Signals are defined as the ensemble mean response to external forcing expressed in large-scale (>5,000 km) near-surface temperatures over the 1946 to 1996 period relative to the 1896 to 1996 mean. The first entry (G) shows the scaling factor and 5 to 95% confidence interval obtained with the assumption that the observations consist only of a response to greenhouse gases plus internal variability. The range is significantly less than one (consistent with results from other models), meaning that models forced with greenhouse gases alone significantly over predict the observed warming signal. The next eight entries show scaling factors for model-simulated responses to greenhouse and sulphate forcing (GS), with two cases including indirect sulphate and tropospheric ozone forcing, one of these also including stratospheric ozone depletion (GSI and GSIO, respectively). All but one (CGCM1) of these ranges is consistent with unity. Hence there is little evidence that models are

appears to be robust to possible amplification of the solar forcing by ozone-solar or solar-cloud interactions, provided these do not alter the pattern or time-dependence of the response to solar forcing. Amplification of the solar signal by these processes, which are not yet included in models, remains speculative.

- *Large uncertainties in anthropogenic forcing are associated with the effects of aerosols.* The effects of some anthropogenic factors, including organic carbon, black carbon, biomass aerosols, and changes in land use, have not been included in detection and attribution studies. Estimates of the size and geographic pattern of the effects of these forcings vary considerably, although individually their global effects are estimated to be relatively small.
- Large differences in the response of different models to the same forcing. These differences, which are often greater than the difference in response in the same model with and without aerosol effects, highlight the large uncertainties in climate change prediction and the need to quantify uncertainty and reduce it through better observational data sets and model improvement.

E.8 Synopsis

In the light of new evidence and taking into account the remaining uncertainties, most of the observed warming over the last 50 years is likely to have been due to the increase in greenhouse gas concentrations.

systematically over- or under predicting the amplitude of the observed response under the assumption that model-simulated GS signals and internal variability are an adequate representation (i.e., that natural forcing has had little net impact on this diagnostic). Observed residual variability is consistent with this assumption in all but one case (ECHAM3, indicated by the asterisk). One is obliged to make this assumption to include models for which only a simulation of the anthropogenic response is available, but uncertainty estimates in these single signal cases are incomplete since they do not account for uncertainty in the naturally forced response. These ranges indicate, however, the high level of confidence with which internal variability, as simulated by these various models, can be rejected as an explanation of recent near-surface temperature change. A more complete uncertainty analysis is provided by the next three entries, which show corresponding scaling factors on individual greenhouse (G), sulphate (S), solar-plus-volcanic (N), solar-only (So) and volcanic-only (V) signals for those cases in which the relevant simulations have been performed. In these cases, multiple factors are estimated simultaneously to account for uncertainty in the amplitude of the naturally forced response. The uncertainties increase but the greenhouse signal remains consistently detectable. In one case (ECHAM3) the model appears to be overestimating the greenhouse response (scaling range in the G signal inconsistent with unity), but this result is sensitive to which component of the control is used to define the detection space. It is also not known how it would respond to the inclusion of a volcanic signal. In cases where both solar and volcanic forcing is included (HadCM2 and HadCM3), G and S signals remain detectable and consistent with unity independent of whether natural signals are estimated jointly or separately (allowing for different errors in S and V responses).

(b) Estimated contributions to global mean warming over the 20th century, based on the results shown in (a), with 5 to 95% confidence intervals. Although the estimates vary depending on which model's signal and what forcing is assumed, and are less certain if more than one signal is estimated, all show a significant contribution from anthropogenic climate change to 20th century warming. [Based on Figure 12.12]

F. The Projections of the Earth's Future Climate

The tools of climate models are used with future scenarios of forcing agents (e.g., greenhouse gases and aerosols) as input to make a suite of projected future climate changes that illustrates the possibilities that could lie ahead. Section F.1 provides a description of the future scenarios of forcing agents given in the IPCC Special Report on Emission Scenarios (SRES) on which, wherever possible, the future changes presented in this section are based. Sections F.2 to F.9 present the resulting projections of changes to the future climate. Finally, Section F.10 presents the results of future projections based on scenarios of a future where greenhouse gas concentrations are stabilised.

F.1 The IPCC Special Report on Emissions Scenarios (SRES)

In 1996, the IPCC began the development of a new set of emissions scenarios, effectively to update and replace the well-known IS92 scenarios. The approved new set of scenarios is described in the IPCC Special Report on Emission Scenarios (SRES). Four different narrative storylines were developed to describe consistently the relationships between the forces driving emissions and their evolution and to add context for the scenario quantification. The resulting set of 40 scenarios (35 of which contain data on the full range of gases required to force climate models) cover a wide range of the main demographic, economic and technological driving forces of future greenhouse gas and sulphur emissions. Each scenario represents a specific quantification of one of the four storylines. All the scenarios based on the same storyline constitute a scenario "family" (See Box 5, which briefly describes the main characteristics of the four SRES storylines and scenario families). The SRES scenarios do not include additional climate initiatives, which means that no scenarios are included that explicitly assume implementation of the United Nations Framework Convention on Climate Change or the emissions targets of the Kyoto Protocol. However, greenhouse gas emissions are directly affected by non-climate change policies designed for a wide range of other purposes (e.g., air quality). Furthermore, government policies can, to varying degrees, influence the greenhouse gas emission drivers, such as demographic change, social and economic development, technological change, resource use, and pollution management. This influence is broadly reflected in the storylines and resulting scenarios.

Since the SRES was not approved until 15 March 2000, it was too late for the modelling community to incorporate the final approved scenarios in their models and have the results available in time for this Third Assessment Report. However, draft scenarios were released to climate modellers earlier to facilitate their input to the Third Assessment Report, in accordance with a decision of the IPCC Bureau in 1998. At that time, one marker scenario was chosen from each of four of the scenario groups based directly on the storylines (A1B, A2, B1, and B2). The choice of the markers was based on which of the initial quantifications best reflected the storyline and features of specific models. Marker scenarios are no more or less likely than any other scenarios, but are considered illustrative of a particular storyline. Scenarios were also selected later to illustrate the other two scenario groups (A1FI and A1T) within the A1 family, which specifically explore alternative technology developments, holding the other driving forces constant. Hence there is an illustrative scenario for each of the six scenario groups, and all are equally plausible. Since the latter two illustrative scenarios were selected at a late stage in the process, the AOGCM modelling results presented in this report only use two of the four draft marker scenarios. At present, only scenarios A2 and B2 have been integrated by more than one AOGCM. The AOGCM results have been augmented by results from simple climate models that cover all six illustrative scenarios. The IS92a scenario is also presented in a number of cases to provide direct comparison with the results presented in the SAR.

The final four marker scenarios contained in the SRES differ in minor ways from the draft scenarios used for the AOGCM experiments described in this report. In order to ascertain the likely effect of differences in the draft and final SRES scenarios, each of the four draft and final marker scenarios were studied using a simple climate model. For three of the four marker scenarios (A1B, A2, and B2) temperature change from the draft and marker scenarios are very similar. The primary difference is a change to the standardised values for 1990 to 2000, which is common to all these scenarios. This results in a higher forcing early in the period.

Box 5: The Emissions Scenarios of the Special Report on Emissions Scenarios (SRES)

A1. The A1 storyline and scenario family describes a future world of very rapid economic growth, global population that peaks in mid-century and declines thereafter, and the rapid introduction of new and more efficient technologies. Major underlying themes are convergence among regions, capacity building and increased cultural and social interactions, with a substantial reduction in regional differences in per capita income. The A1 scenario family develops into three groups that describe alternative directions of technological change in the energy system. The three A1 groups are distinguished by their technological emphasis: fossil intensive (A1FI), non-fossil energy sources (A1T), or a balance across all sources (A1B) (where balanced is defined as not relying too heavily on one particular energy source, on the assumption that similar improvement rates apply to all energy supply and end-use technologies).

A2. The A2 storyline and scenario family describes a very heterogeneous world. The underlying theme is self-reliance and preservation of local identities. Fertility patterns across regions converge very slowly, which results in continuously increasing population. Economic development is primarily regionally oriented and per capita economic growth and technological change more fragmented and slower than other storylines.

B1. The B1 storyline and scenario family describes a convergent world with the same global population, that peaks in mid-century and declines thereafter, as in the A1 storyline, but with rapid change in economic structures toward a service and information economy, with reductions in material intensity and the introduction of clean and resource-efficient technologies. The emphasis is on global solutions to economic, social and environmental sustainability, including improved equity, but without additional climate initiatives.

B2. The B2 storyline and scenario family describes a world in which the emphasis is on local solutions to economic, social and environmental sustainability. It is a world with continuously increasing global population, at a rate lower than A2, intermediate levels of economic development, and less rapid and more diverse technological change than in the A1 and B1 storylines. While the scenario is also oriented towards environmental protection and social equity, it focuses on local and regional levels.

There are further small differences in net forcing, but these decrease until, by 2100, differences in temperature change in the two versions of these scenarios are in the range 1 to 2%. For the B1 scenario, however, temperature change is significantly lower in the final version, leading to a difference in the temperature change in 2100 of almost 20%, as a result of generally lower emissions across the full range of greenhouse gases.

Anthropogenic emissions of the three main greenhouse gases, CO_2, CH_4 and N_2O, together with anthropogenic sulphur dioxide emissions, are shown for the six illustrative SRES scenarios in Figure 17. It is evident that these scenarios encompass a wide range of emissions. For comparison, emissions are also shown for IS92a. Particularly noteworthy are the much lower future sulphur dioxide emissions for the six SRES scenarios, compared to the IS92 scenarios, due to structural changes in the energy system as well as concerns about local and regional air pollution.

F.2 Projections of Future Changes in Greenhouse Gases and Aerosols

Models indicate that the illustrative SRES scenarios lead to very different CO_2 concentration trajectories (see Figure 18). By 2100, carbon cycle models project atmospheric CO_2 concentrations of 540 to 970 ppm for the illustrative SRES scenarios (90 to 250% above the concentration of 280 ppm in 1750). The net effect of land and ocean climate feedbacks as indicated by models is to further increase projected atmospheric CO_2 concentrations by reducing both the ocean and land uptake of CO_2. These projections include the land and ocean climate feedbacks. Uncertainties, especially about the magnitude of the climate feedback from the terrestrial biosphere, cause a variation of about −10 to +30% around each scenario. The total range is 490 to 1260 ppm (75 to 350% above the 1750 concentration).

Measures to enhance carbon storage in terrestrial ecosystems could influence atmospheric CO_2 concentration, but the upper bound for reduction of CO_2 concentration by such means is 40

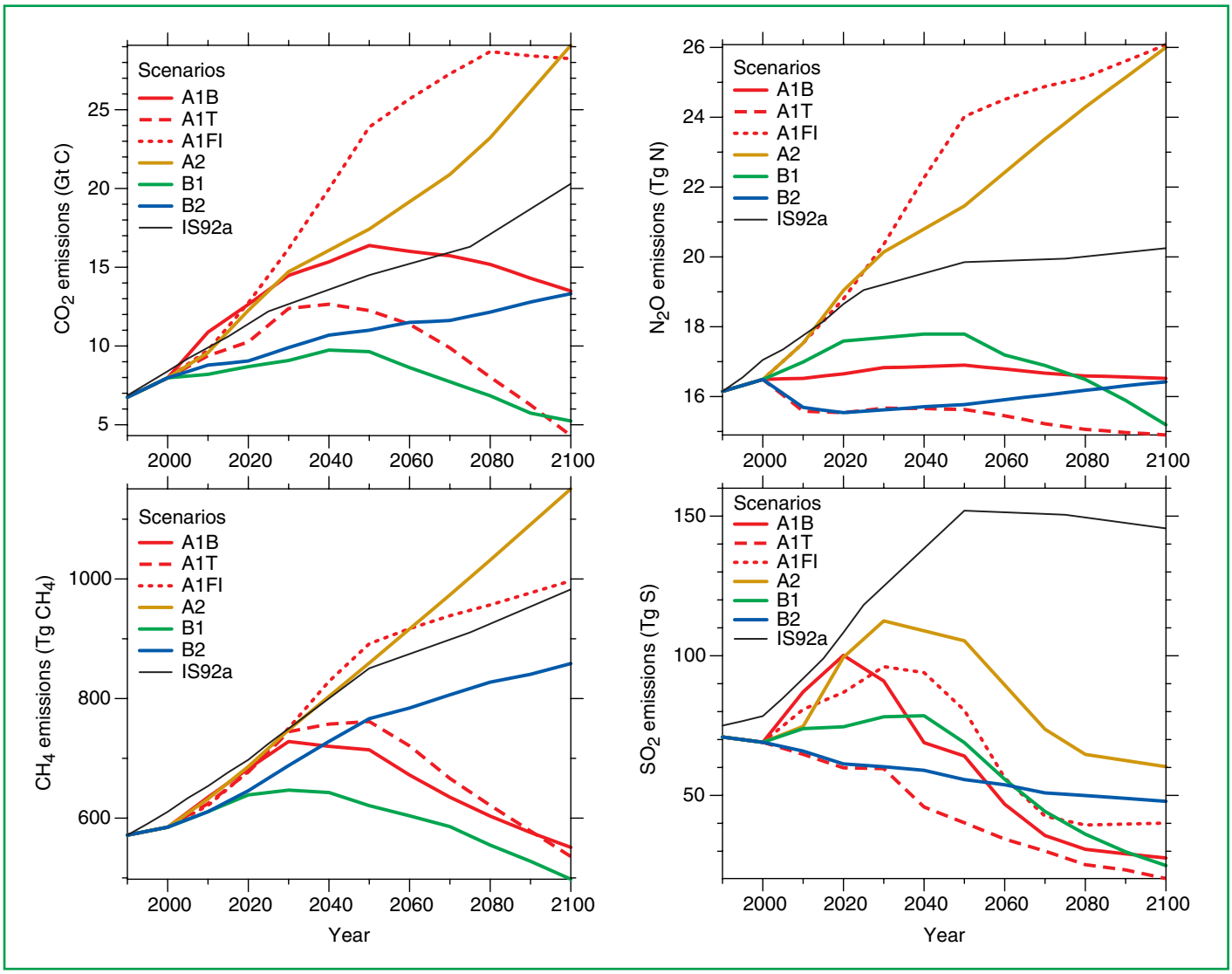

Figure 17: Anthropogenic emissions of CO_2, CH_4, N_2O and sulphur dioxide for the six illustrative SRES scenarios, A1B, A2, B1 and B2, A1FI and A1T. For comparison the IS92a scenario is also shown. [Based on IPCC Special Report on Emissions Scenarios.]

to 70 ppm. If all the carbon released by historic land-use changes could be restored to the terrestrial biosphere over the course of the century (e.g., by reforestation), CO_2 concentration would be reduced by 40 to 70 ppm. Thus, fossil fuel CO_2 emissions are virtually certain to remain the dominant control over trends in atmospheric CO_2 concentration during this century.

Model calculations of the abundances of the primary non-CO_2 greenhouse gases by the year 2100 vary considerably across the six illustrative SRES scenarios. In general A1B, A1T and B1 have the smallest increases, and A1FI and A2, the largest. The CH_4 changes from 1998 to 2100 range from –190 to +1970 ppb (–11 to +112%), and N_2O increases from +38 to +144 ppb (+12 to +46%) (see Figures 17b and c). The HFCs (134a, 143a, and 125) reach abundances of a few hundred to a thousand ppt from negligible levels today. The PFC CF4 is projected to increase to 200 to 400 ppt, and SF_6 is projected to increase to 35 to 65 ppt.

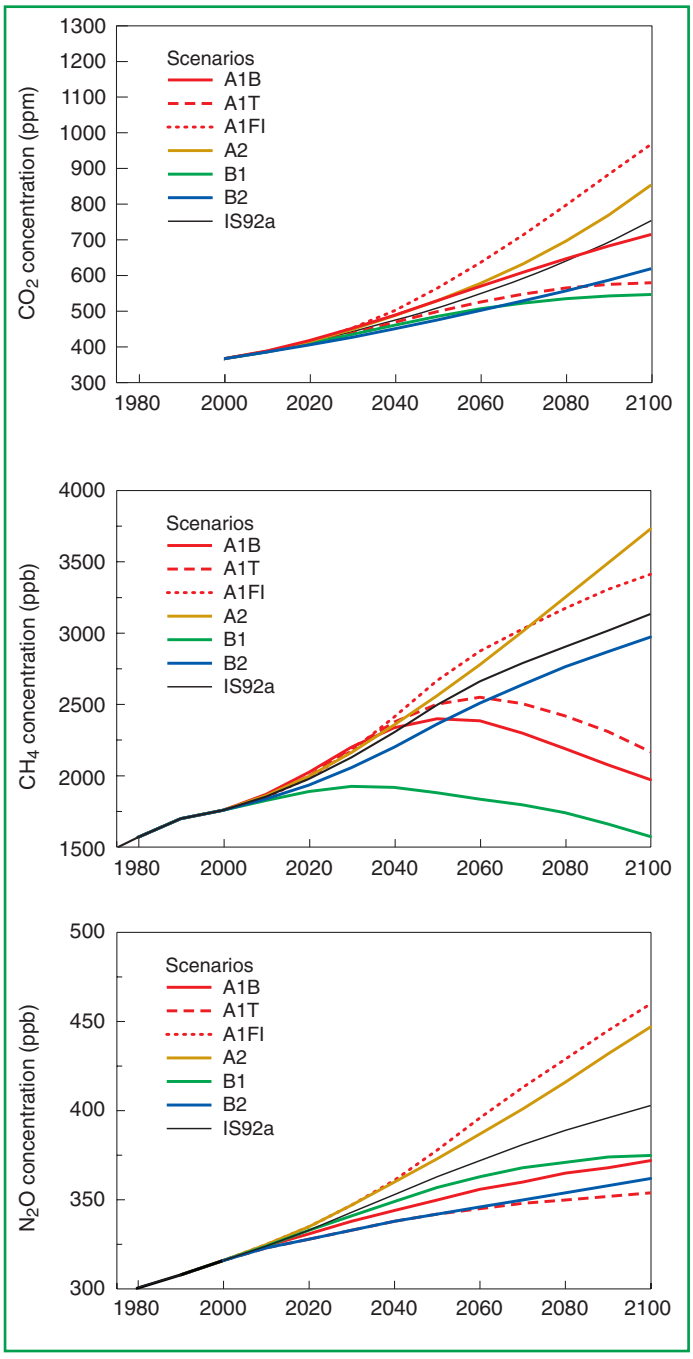

Figure 18: Atmospheric concentrations of CO_2, CH_4 and N_2O resulting from the six SRES scenarios and from the IS92a scenario computed with current methodology. [Based on Figures 3.12 and 4.14]

For the six illustrative SRES emissions scenarios, projected emissions of indirect greenhouse gases (NO_x, CO, VOC), together with changes in CH_4, are projected to change the global mean abundance of the tropospheric hydroxyl radical (OH), by –20% to +6% over the next century. Because of the importance of OH in tropospheric chemistry, comparable, but opposite sign, changes occur in the atmospheric lifetimes of the greenhouse gases CH_4 and HFCs. This impact depends in large part on the magnitude of and the balance between NO_x and CO emissions. Changes in tropospheric O_3 of –12 to +62% are calculated from 2000 until 2100. The largest increase predicted for the 21st century is for scenarios A1FI and A2 and would be more than twice as large as that experienced since the Pre-industrial Era. These O_3 increases are attributable to the concurrent and large increases in anthropogenic NO_x and CH_4 emissions.

The large growth in emissions of greenhouse gases and other pollutants as projected in some of the six illustrative SRES scenarios for the 21st century will degrade the global environment in ways beyond climate change. Changes projected in the SRES A2 and A1FI scenarios would degrade air quality over much of the globe by increasing background levels of tropospheric O_3. In northern mid-latitudes during summer, the zonal average of O_3 increases near the surface are about 30 ppb or more, raising background levels to about 80 ppb, threatening the attainment of current air quality standards over most metropolitan and even rural regions and compromising crop and forest productivity. This problem reaches across continental boundaries and couples emissions of NO_x on a hemispheric scale.

Except for sulphate and black carbon, models show an approximately linear dependence of the abundance of aerosols on emissions. The processes that determine the removal rate for black carbon differ substantially between the models, leading to major uncertainty in the future projections of black carbon. Emissions of natural aerosols such as sea salt, dust, and gas phase precursors of aerosols such as terpenes, sulphur dioxide (SO_2), and dimethyl sulphide oxidation may increase as a result of changes in climate and atmospheric chemistry.

The six illustrative SRES scenarios cover nearly the full range of forcing that results from the full set of SRES scenarios. Estimated total historical anthropogenic radiative forcing from 1765 to 1990 followed by forcing resulting from the six

SRES scenarios are shown in Figure 19. The forcing from the full range of 35 SRES scenarios is shown on the figure as a shaded envelope, since the forcings resulting from individual scenarios cross with time. The direct forcing from biomass-burning aerosols is scaled with deforestation rates. The SRES scenarios include the possibility of either increases or decreases in anthropogenic aerosols (e.g., sulphate aerosols, biomass aerosols, and black and organic carbon aerosols), depending on the extent of fossil fuel use and policies to abate polluting emissions. The SRES scenarios do not include emissions estimates for non-sulphate aerosols. Two methods for projecting these emissions were considered in this report: the first scales the emissions of fossil fuel and biomass aerosols with CO while the second scales the emissions with SO_2 and deforestation. Only the second method was used for climate projections. For comparison, radiative forcing is also shown for the IS92a scenario. It is evident that the range for the new SRES scenarios is shifted higher compared to the IS92 scenarios. This is mainly due to the reduced future SO_2 emissions of the SRES scenarios compared to the IS92 scenarios, but also to the slightly larger cumulative carbon emissions featured in some SRES scenarios.

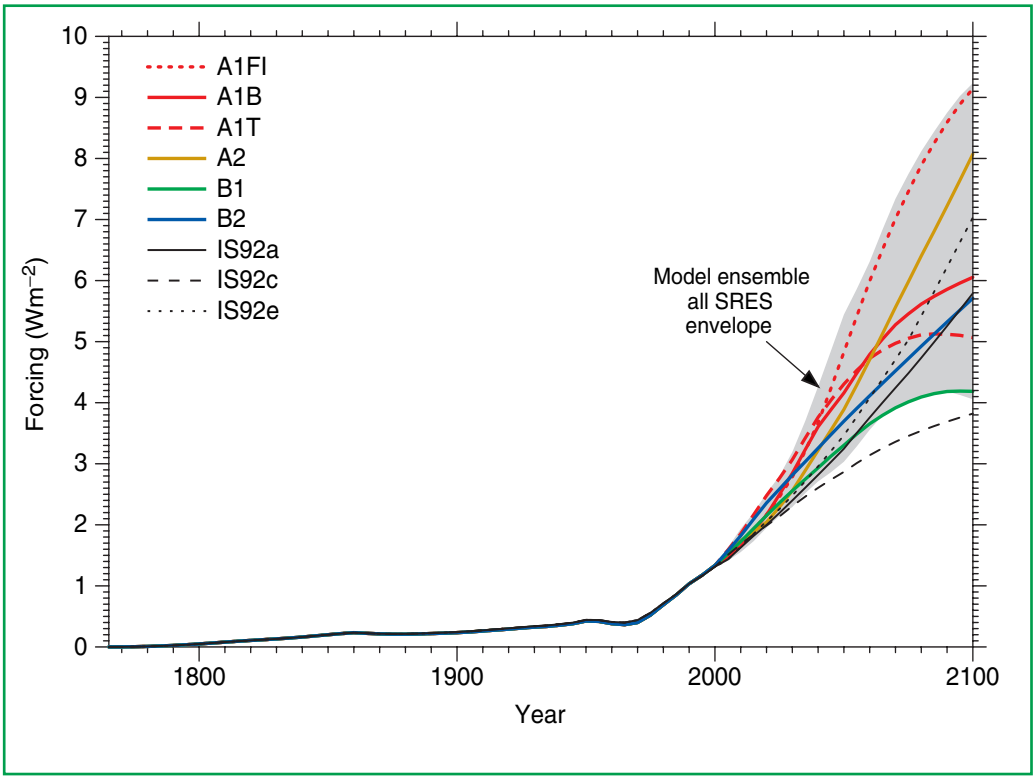

Figure 19: Simple model results: estimated historical anthropogenic radiative forcing up to the year 2000 followed by radiative forcing for the six illustrative SRES scenarios. The shading shows the envelope of forcing that encompasses the full set of thirty five SRES scenarios. The method of calculation closely follows that explained in the chapters. The values are based on the radiative forcing for a doubling of CO_2 from seven AOGCMs. The IS92a, IS92c, and IS92e forcing is also shown following the same method of calculation. [Based on Figure 9.13a]

In almost all SRES scenarios, the radiative forcing due to CO_2, CH_4, N_2O and tropospheric O_3 continue to increase, with the fraction of the total radiative forcing due to CO_2 projected to increase from slightly more than half to about three-quarters of the total. The radiative forcing due to O_3-depleting gases decreases due to the introduction of emission controls aimed at curbing stratospheric ozone depletion. The direct aerosol (sulphate and black and organic carbon components taken together) radiative forcing (evaluated relative to present day, 2000) varies in sign for the different scenarios. The direct plus indirect aerosol effects are projected to be smaller in magnitude than that of CO_2. No estimates are made for the spatial aspects of the future forcings. The indirect effect of aerosols on clouds is included in simple climate model calculations and scaled non-linearly with SO_2 emissions, assuming a present day value of –0.8 Wm^{-2}, as in the SAR.

F.3 Projections of Future Changes in Temperature

AOGCM results

Climate sensitivity is likely to be in the range of 1.5 to 4.5°C. This estimate is unchanged from the first IPCC Assessment Report in 1990 and the SAR. The climate sensitivity is the equilibrium response of global surface temperature to a doubling of equivalent CO_2 concentration. The range of estimates arises from uncertainties in the climate models and their internal feedbacks, particularly those related to clouds and related processes. Used for the first time in this IPCC report is the Transient Climate Response (TCR). The TCR is defined as the globally averaged surface air temperature change, at the time of doubling of CO_2, in a 1%/yr CO_2-increase experiment. This rate of CO_2 increase is assumed to represent the radiative forcing from all greenhouse gases. The TCR combines elements of model sensitivity and factors that affect response (e.g., ocean heat uptake). The range of the TCR for current AOGCMs is 1.1 to 3.1°C.

Including the direct effect of sulphate aerosols reduces global mean mid-21st century warming. The surface temperature response pattern for a given model, with and without sulphate aerosols, is more similar than the pattern between two models using the same forcing.

Models project changes in several broad-scale climate variables. As the radiative forcing of the climate system changes, the land warms faster and more than the ocean, and there is greater relative warming at high latitudes. Models project a smaller surface air temperature increase in the North Atlantic and circumpolar southern ocean regions relative to the global mean. There is projected to be a decrease in diurnal temperature range in many areas, with night-time lows increasing more than daytime highs. A number of models show a general decrease of daily variability of surface air temperature in winter and increased daily variability in summer in the Northern Hemisphere land areas. As the climate warms, the Northern Hemisphere snow cover and sea-ice extent are projected to decrease. Many of these changes are consistent with recent observational trends, as noted in Section B.

Multi-model ensembles of AOGCM simulations for a range of scenarios are being used to quantify the mean climate change and uncertainty based on the range of model results. For the end of the 21st century (2071 to 2100), the mean change in global average surface air temperature, relative to the period 1961 to 1990, is 3.0°C (with a range of 1.3 to 4.5°C) for the A2 draft marker scenario and 2.2°C (with a range of 0.9 to 3.4°C) for the B2 draft marker scenario. The B2 scenario produces a smaller warming that is consistent with its lower rate of increased CO_2 concentration.

On time-scales of a few decades, the current observed rate of warming can be used to constrain the projected response to a given emissions scenario despite uncertainty in climate sensitivity. Analysis of simple models and intercomparisons of AOGCM responses to idealised forcing scenarios suggest that, for most scenarios over the coming decades, errors in large-scale temperature projections are likely to increase in proportion to the magnitude of the overall response. The estimated size of and uncertainty in current observed warming rates attributable to human influence thus provides a relatively model-independent estimate of uncertainty in multi-decade projections under most scenarios. To be consistent with recent observations, anthropogenic warming is likely to lie in the range 0.1 to 0.2°C/decade over the next few decades under the IS92a scenario. This is similar to the range of responses to this scenario based on the seven versions of the simple model used in Figure 22.

Most of the features of the geographical response in the SRES scenario experiments are similar for different scenarios (see Figure 20) and are similar to those for idealised 1% CO_2-increase integrations. The biggest difference between the 1% CO_2-increase experiments, which have no sulphate aerosol, and the SRES experiments is the regional moderating of the warming over industrialised areas, in the SRES experiments, where the negative forcing from sulphate aerosols is greatest. This regional effect was noted in the SAR for only two models, but this has now been shown to be a consistent response across the greater number of more recent models.

It is very likely that nearly all land areas will warm more rapidly than the global average, particularly those at northern high latitudes in the cold season. Results (see Figure 21) from recent AOGCM simulations forced with SRES A2 and B2 emissions scenarios indicate that in winter the warming for all high-latitude northern regions exceeds the global mean warming in each model by more than 40% (1.3 to 6.3°C for the range of models and scenarios considered). In summer, warming is in excess of 40% above the global mean change in central and northern Asia. Only in south Asia and southern South America in June/July/August, and Southeast Asia for both seasons, do the models consistently show warming less than the global average.

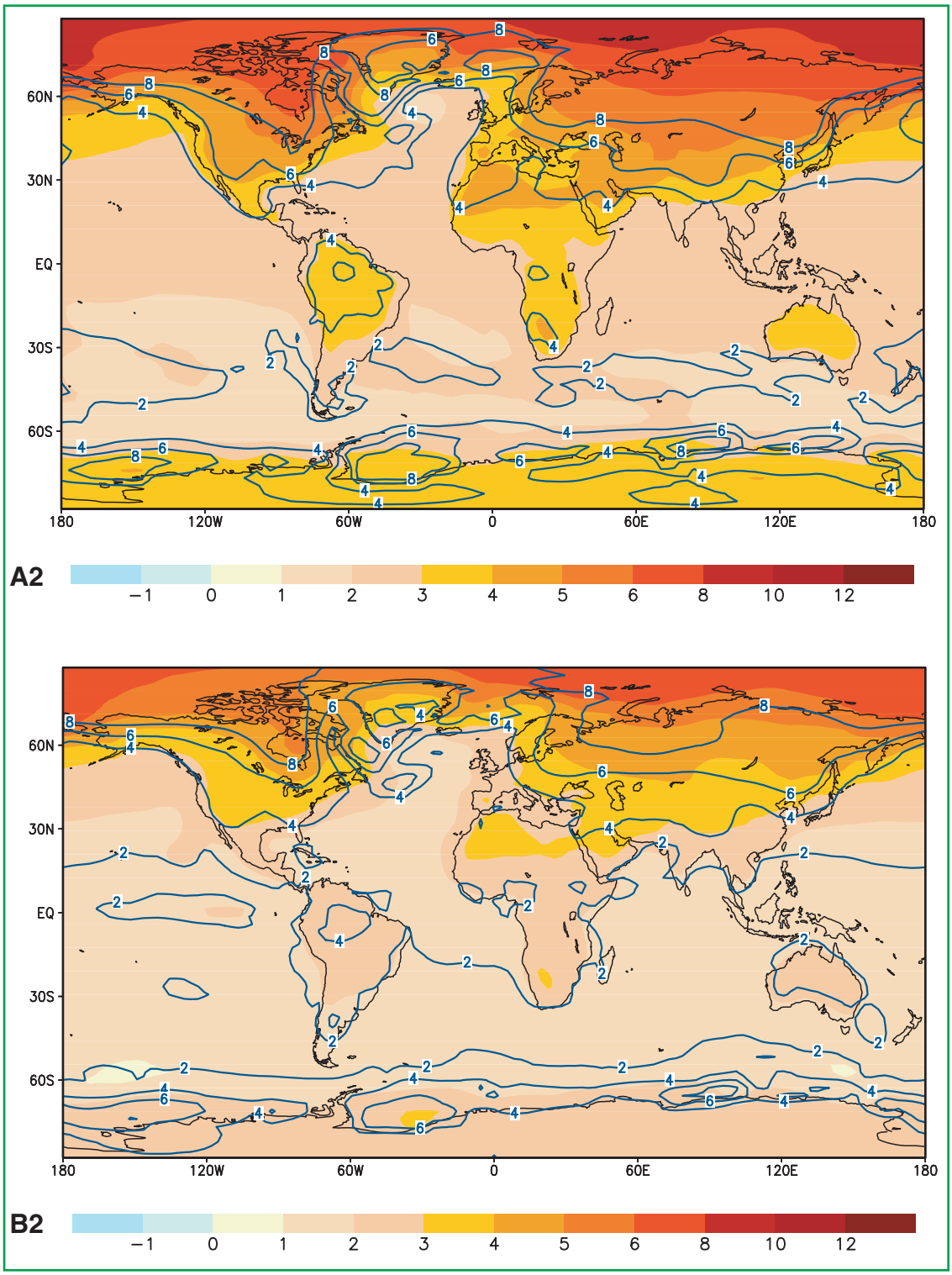

Figure 20: The annual mean change of the temperature (colour shading) and its range (isolines) (Unit: °C) for the SRES scenario A2 (upper panel) and the SRES scenario B2 (lower panel). Both SRES scenarios show the period 2071 to 2100 relative to the period 1961 to 1990 and were performed by OAGCMs. [Based on Figures 9.10d and 9.10e]

Simple climate model results

Due to computational expense, AOGCMs can only be run for a limited number of scenarios. A simple model can be calibrated to represent globally averaged AOGCM responses and run for a much larger number of scenarios.

The globally averaged surface temperature is projected to increase by 1.4 to 5.8°C (Figure 22(a)) over the period 1990 to 2100. These results are for the full range of 35 SRES scenarios, based on a number of climate models.[6,7] Temperature increases are projected to be greater than those in the SAR, which were about 1.0 to 3.5°C based on six IS92 scenarios. The higher projected temperatures and the wider range are due primarily to the lower projected SO_2 emissions in the SRES scenarios relative to the IS92 scenarios. The projected rate of warming is much larger than the observed changes during the 20th century and is very likely to be without precedent during at least the last 10,000 years, based on palaeoclimate data.

The relative ranking of the SRES scenarios in terms of global mean temperature changes with time. In particular, for scenarios with higher fossil fuel use (hence, higher carbon dioxide emissions, e.g., A2), the SO_2 emissions are also higher. In the near term (to around 2050), the cooling effect of

[6] Complex physically based climate models are the main tool for projecting future climate change. In order to explore the range of scenarios, these are complemented by simple climate models calibrated to yield an equivalent response in temperature and sea level to complex climate models. These projections are obtained using a simple climate model whose climate sensitivity and ocean heat uptake are calibrated to each of 7 complex climate models. The climate sensitivity used in the simple model ranges from 1.7 to 4.2°C, which is comparable to the commonly accepted range of 1.5 to 4.5°C.

[7] This range does not include uncertainties in the modelling of radiative forcing, e.g. aerosol forcing uncertainties. A small carbon cycle climate feedback is included.

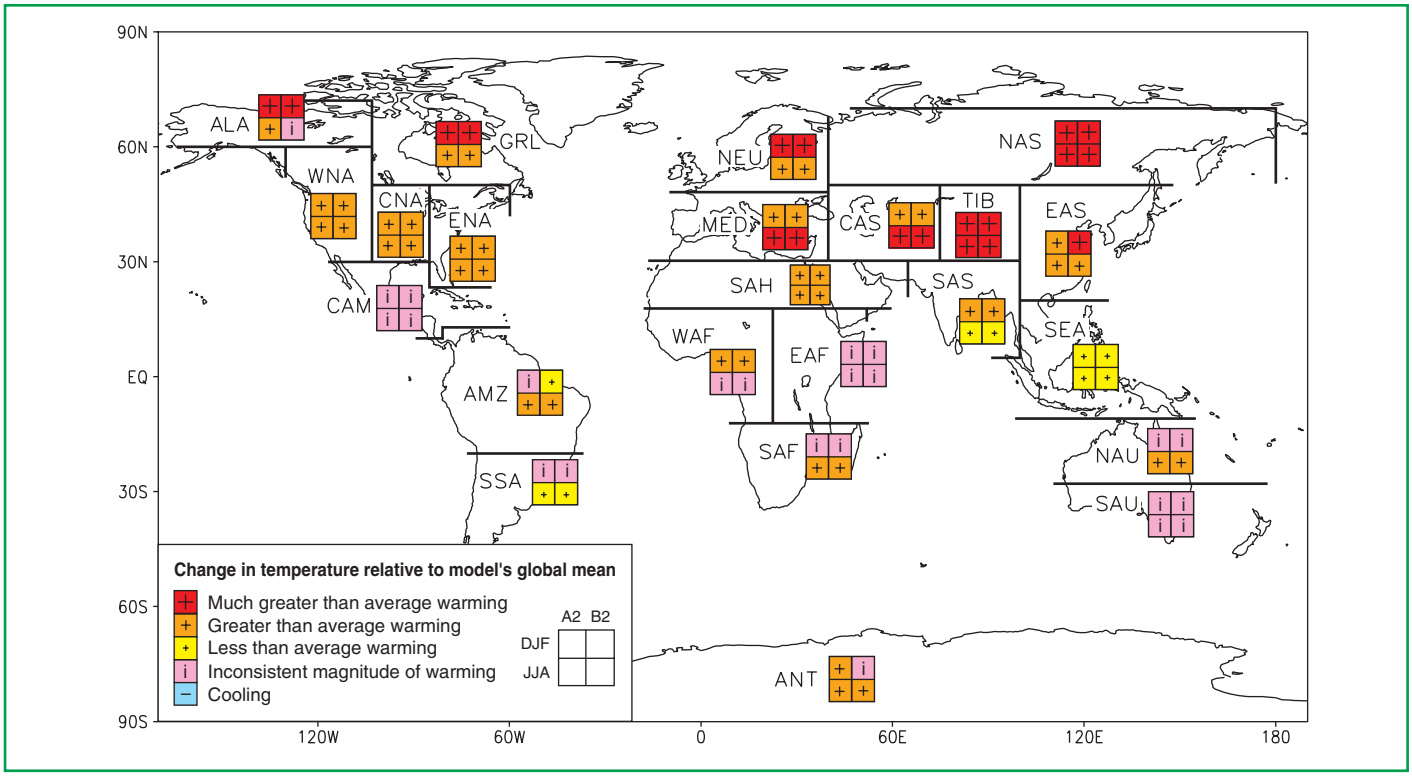

Figure 21: Analysis of inter-model consistency in regional relative warming (warming relative to each model's global average warming). Regions are classified as showing either agreement on warming in excess of 40% above the global average ('Much greater than average warming'), agreement on warming greater than the global average ('Greater than average warming'), agreement on warming less than the global average ('Less than average warming'), or disagreement amongst models on the magnitude of regional relative warming ('Inconsistent magnitude of warming'). There is also a category for agreement on cooling (which never occurs). A consistent result from at least seven of the nine models is deemed necessary for agreement. The global annual average warming of the models used span 1.2 to 4.5°C for A2 and 0.9 to 3.4°C for B2, and therefore a regional 40% amplification represents warming ranges of 1.7 to 6.3°C for A2 and 1.3 to 4.7°C for B2. [Based on Chapter 10, Box 1, Figure 1]

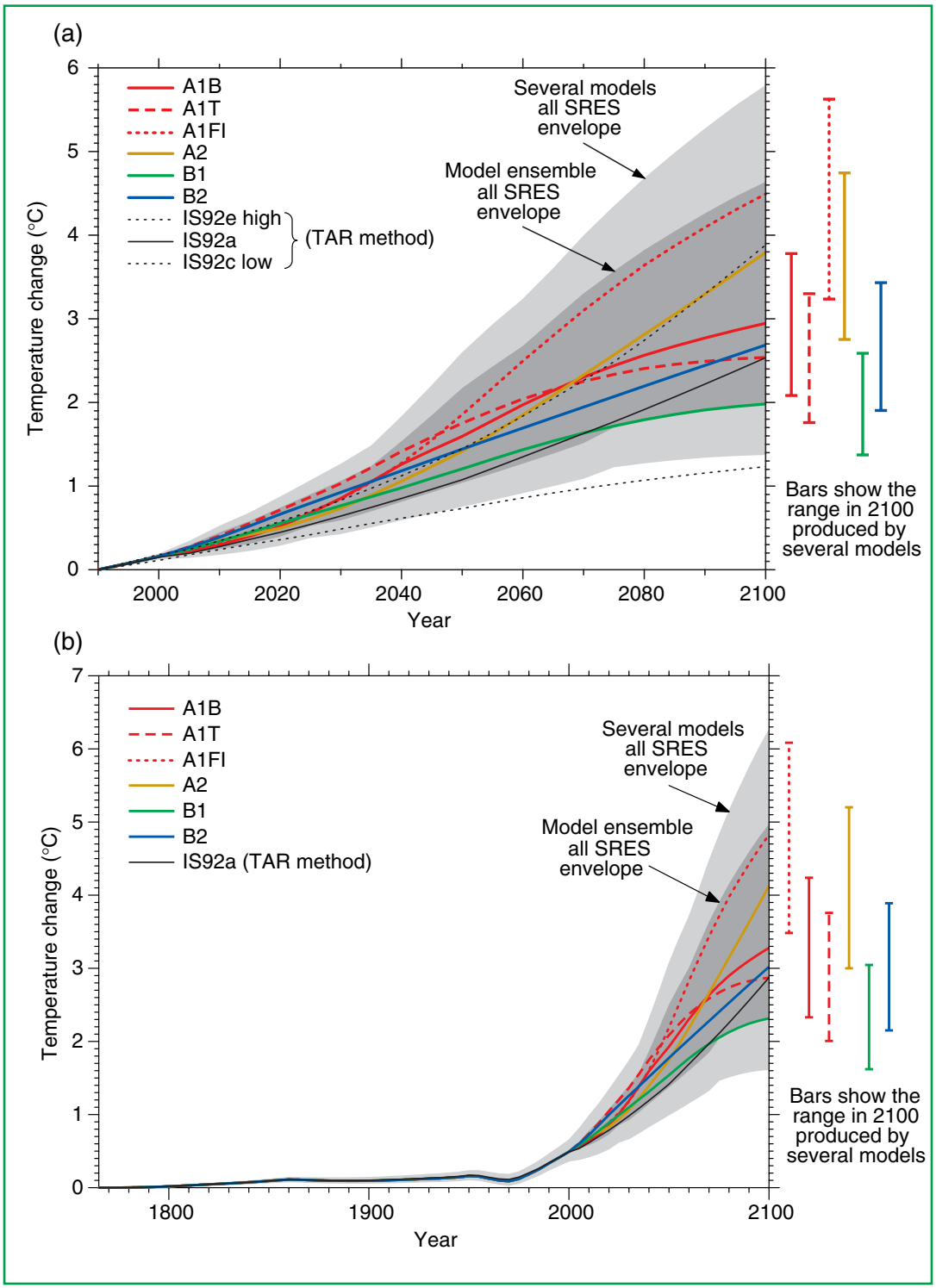

Figure 22: Simple model results: (a) global mean temperature projections for the six illustrative SRES scenarios using a simple climate model tuned to a number of complex models with a range of climate sensitivities. Also for comparison, following the same method, results are shown for IS92a. The darker shading represents the envelope of the full set of thirty-five SRES scenarios using the average of the model results (mean climate sensitivity is 2.8°C). The lighter shading is the envelope based on all seven model projections (with climate sensitivity in the range 1.7 to 4.2°C). The bars show, for each of the six illustrative SRES scenarios, the range of simple model results in 2100 for the seven AOGCM model tunings. (b) Same as (a) but results using estimated historical anthropogenic forcing are also used. [Based on Figures 9.14 and 9.13b]

higher sulphur dioxide emissions significantly reduces the warming caused by increased emissions of greenhouse gases in scenarios such as A2. The opposite effect is seen for scenarios B1 and B2, which have lower fossil fuel emissions as well as lower SO_2 emissions, and lead to a larger near-term warming. In the longer term, however, the level of emissions of long-lived greenhouse gases such as CO_2 and N_2O become the dominant determinants of the resulting climate changes.

By 2100, differences in emissions in the SRES scenarios and different climate model responses contribute similar uncertainty to the range of global temperature change. Further uncertainties arise due to uncertainties in the radiative forcing. The largest forcing uncertainty is that due to the sulphate aerosols.

F.4 Projections of Future Changes in Precipitation

Globally averaged water vapour, evaporation and precipitation are projected to increase. At the regional scale both increases and decreases in precipitation are seen. Results (see Figure 23) from recent AOGCM simulations forced with SRES A2 and B2 emissions scenarios indicate that it is likely for precipitation to increase in both summer and winter over high-latitude regions. In winter, increases are also seen over northern mid-latitudes, tropical Africa and Antarctica, and in summer in southern and eastern Asia. Australia, central America, and southern Africa show consistent decreases in winter rainfall.

Based on patterns emerging from a limited number of studies with current AOGCMs, older GCMs, and regionalisation studies, there is a strong correlation between precipitation

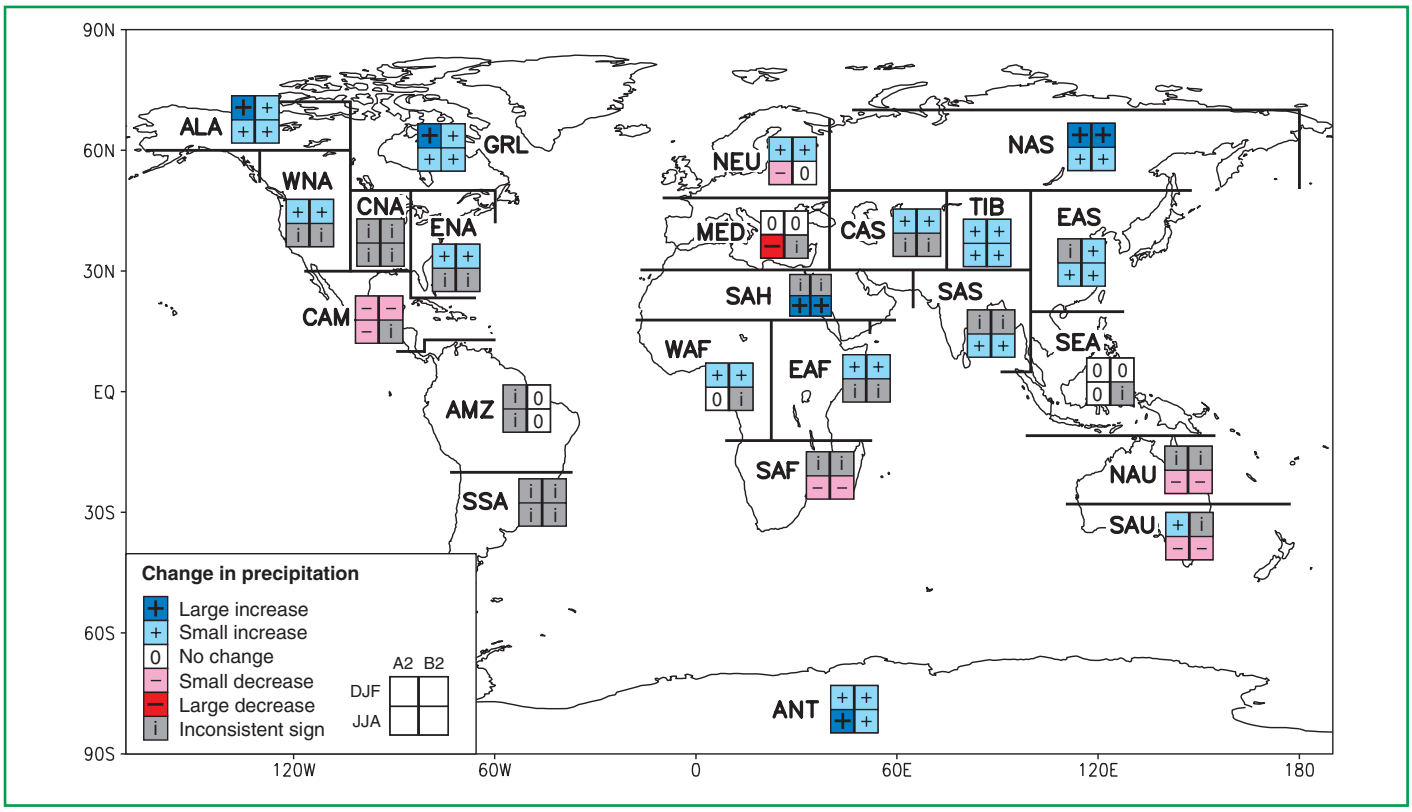

Figure 23: Analysis of inter-model consistency in regional precipitation change. Regions are classified as showing either agreement on increase with an average change of greater than 20% ('Large increase'), agreement on increase with an average change between 5 and 20% ('Small increase'), agreement on a change between –5 and +5% or agreement with an average change between –5 and 5% ('No change'), agreement on decrease with an average change between –5 and –20% ('Small decrease'), agreement on decrease with an average change of less than –20% ('Large decrease'), or disagreement ('Inconsistent sign'). A consistent result from at least seven of the nine models is deemed necessary for agreement. [Based on Chapter 10, Box 1, Figure 2]

interannual variability and mean precipitation. Future increases in mean precipitation will likely lead to increases in variability. Conversely, precipitation variability will likely decrease only in areas of reduced mean precipitation.

F.5 Projections of Future Changes in Extreme Events

It is only recently that changes in extremes of weather and climate observed to date have been compared to changes projected by models (Table 4). More hot days and heat waves are very likely over nearly all land areas. These increases are projected to be largest mainly in areas where soil moisture decreases occur. Increases in daily minimum temperature are projected to occur over nearly all land areas and are generally larger where snow and ice retreat. Frost days and cold waves are very likely to become fewer. The changes in surface air temperature and surface absolute humidity are projected to result in increases in the heat index (which is a measure of the combined effects of temperature and moisture). The increases in surface air temperature are also projected to result in an increase in the "cooling degree days" (which is a measure of the amount of cooling required on a given day once the temperature exceeds a given threshold) and a decrease in "heating degree days". Precipitation extremes are projected to increase more than the mean and the intensity of precipitation events are projected to increase. The frequency of extreme

Table 4: Estimates of confidence in observed and projected changes in extreme weather and climate events. The table depicts an assessment of confidence in observed changes in extremes of weather and climate during the latter half of the 20th century (left column) and in projected changes during the 21st century (right column)[a]. This assessment relies on observational and modelling studies, as well as physical plausibility of future projections across all commonly used scenarios and is based on expert judgement (see Footnote 4). [Based upon Table 9.6]

Confidence in observed changes (latter half of the 20th century)	Changes in Phenomenon	Confidence in projected changes (during the 21st century)
Likely	**Higher maximum temperatures and more hot days over nearly all land areas**	Very likely
Very likely	**Higher minimum temperatures, fewer cold days and frost days over nearly all land areas**	Very likely
Very likely	**Reduced diurnal temperature range over most land areas**	Very likely
Likely, over many areas	**Increase of heat index[8] over land areas**	Very likely, over most areas
Likely, over many Northern Hemisphere mid- to high latitude land areas	**More intense precipitation events[b]**	Very likely, over many areas
Likely, in a few areas	**Increased summer continental drying and associated risk of drought**	Likely, over most mid-latitude continental interiors (Lack of consistent projections in other areas)
Not observed in the few analyses available	**Increase in tropical cyclone peak wind intensities[c]**	Likely, over some areas
Insufficient data for assessment	**Increase in tropical cyclone mean and peak precipitation intensities[c]**	Likely, over some areas

[a] For more details see Chapter 2 (observations) and Chapters 9, 10 (projections).

[b] For other areas there are either insufficient data of conflicting analyses.

[c] Past and future changes in tropical cyclone location and frequency are uncertain.

[8] Heat index: A combination of temperature and humidity that measures effects on human comfort

precipitation events is projected to increase almost everywhere. There is projected to be a general drying of the mid-continental areas during summer. This is ascribed to a combination of increased temperature and potential evaporation that is not balanced by increases of precipitation. There is little agreement yet among models concerning future changes in mid-latitude storm intensity, frequency, and variability. There is little consistent evidence that shows changes in the projected frequency of tropical cyclones and areas of formation. However, some measures of intensities show projected increases, and some theoretical and modelling studies suggest that the upper limit of these intensities could increase. Mean and peak precipitation intensities from tropical cyclones are likely to increase appreciably.

For some other extreme phenomena, many of which may have important impacts on the environment and society, there is currently insufficient information to assess recent trends, and confidence in models and understanding is inadequate to make firm projections. In particular, very small-scale phenomena such as thunderstorms, tornadoes, hail, and lightning are not simulated in global models. Insufficient analysis has occurred of how extra-tropical cyclones may change.

F.6 Projections of Future Changes in Thermohaline Circulation

Most models show weakening of the Northern Hemisphere Thermohaline Circulation (THC), which contributes to a reduction of the surface warming in the northern North Atlantic. Even in models where the THC weakens, there is still a warming over Europe due to increased greenhouse gases. In experiments where the atmospheric greenhouse gas concentration is stabilised at twice its present day value, the North Atlantic THC is projected to recover from initial weakening within one to several centuries. The THC could collapse entirely in either hemisphere if the rate of change in radiative forcing is large enough and applied long enough. Models indicate that a decrease of the THC reduces its resilience to perturbations, i.e., a once reduced THC appears to be less stable and a shut-down can become more likely. However, it is too early to say with confidence whether an irreversible collapse in the THC is likely or not, or at what threshold it might occur and what the climate implications could be. None of the current projections with coupled models exhibits a complete shut-down of the THC by 2100. Although the North Atlantic THC weakens in most models, the relative roles of surface heat and fresh water fluxes vary from model to model. Wind stress changes appear to play only a minor role in the transient response.

F.7 Projections of Future Changes in Modes of Natural Variability

Many models show a mean El Niño-like response in the tropical Pacific, with the central and eastern equatorial Pacific sea surface temperatures projected to warm more than the western equatorial Pacific and with a corresponding mean eastward shift of precipitation. Although many models show an El Niño-like change of the mean state of tropical Pacific sea surface temperatures, the cause is uncertain. It has been related to changes in the cloud radiative forcing and/or evaporative damping of the east-west sea surface temperature gradient in some models. Confidence in projections of changes in future frequency, amplitude, and spatial pattern of El Niño events in the tropical Pacific is tempered by some shortcomings in how well El Niño is simulated in complex models. Current projections show little change or a small increase in amplitude for El Niño events over the next 100 years. However, even with little or no change in El Niño amplitude, global warming is likely to lead to greater extremes of drying and heavy rainfall and increase the risk of droughts and floods that occur with El Niño events in many regions. It also is likely that warming associated with increasing greenhouse gas concentrations will cause an increase of Asian summer monsoon precipitation variability. Changes in monsoon mean duration and strength depend on the details of the emission scenario. The confidence in such projections is limited by how well the climate models simulate the detailed seasonal evolution of the monsoons. There is no clear agreement on changes in frequency or structure of naturally occurring modes of variability, such as the North Atlantic Oscillation, i.e., the magnitude and character of the changes vary across the models.

F.8 Projections of Future Changes in Land Ice (Glaciers, Ice Caps and Ice Sheets), Sea Ice and Snow Cover

Glaciers and ice caps will continue their widespread retreat during the 21st century and Northern Hemisphere snow cover and sea ice are projected to decrease further. Methods have been developed recently for estimating glacier melt from

seasonally and geographically dependent patterns of surface air temperature change, that are obtained from AOGCM experiments. Modelling studies suggest that the evolution of glacial mass is controlled principally by temperature changes, rather than precipitation changes, on the global average.

The Antarctic ice sheet is likely to gain mass because of greater precipitation, while the Greenland ice sheet is likely to lose mass because the increase in runoff will exceed the precipitation increase. The West Antarctic Ice Sheet (WAIS) has attracted special attention because it contains enough ice to raise sea level by 6 m and because of suggestions that instabilities associated with its being grounded below sea level may result in rapid ice discharge when the surrounding ice shelves are weakened. However, loss of grounded ice leading to substantial sea level rise from this source is now widely agreed to be very unlikely during the 21st century, although its dynamics are still inadequately understood, especially for projections on longer time-scales.

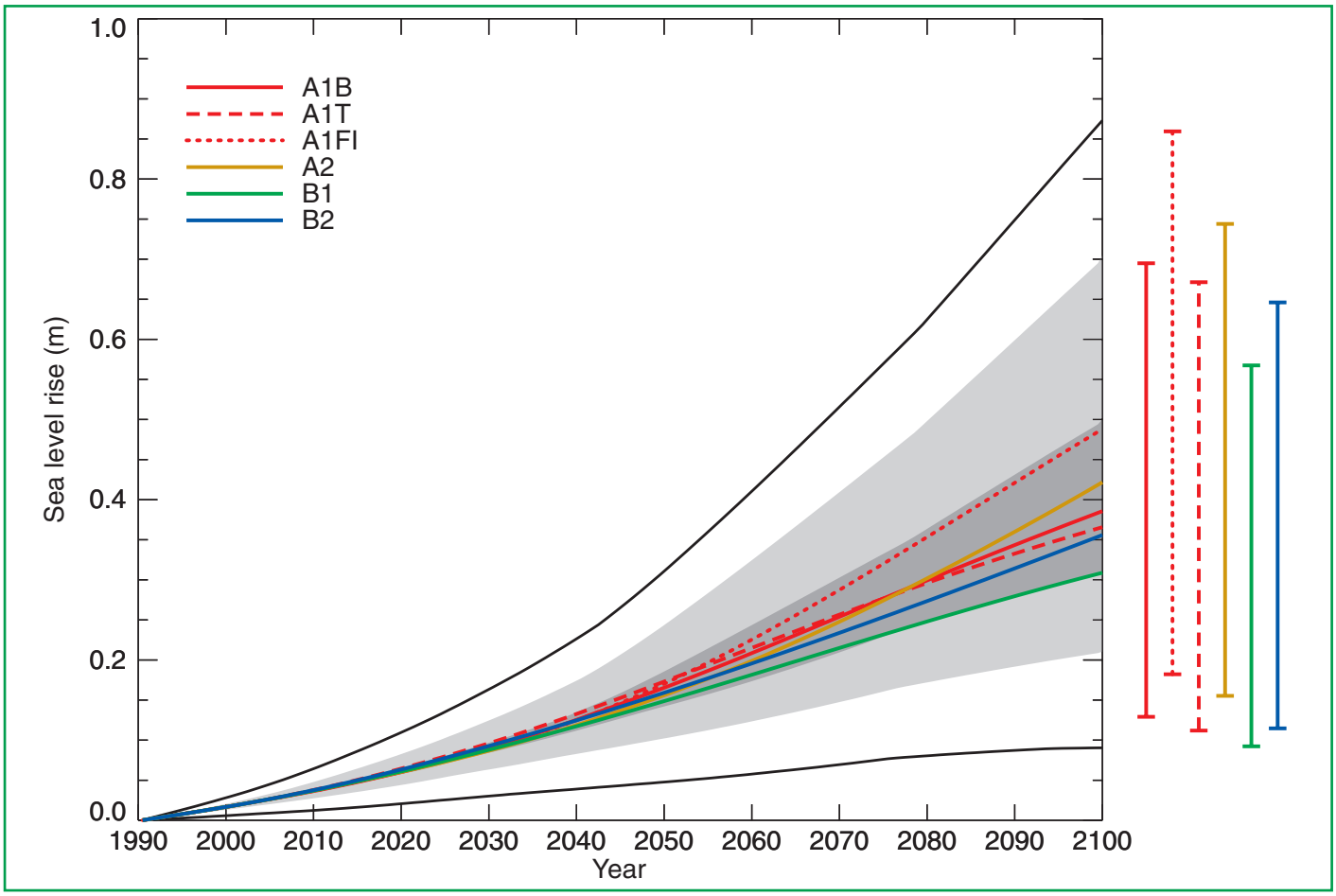

Figure 24: Global average sea level rise 1990 to 2100 for the SRES scenarios. Thermal expansion and land ice changes were calculated using a simple climate model calibrated separately for each of seven AOGCMs, and contributions from changes in permafrost, the effect of sediment deposition and the long-term adjustment of the ice sheets to past climate change were added. Each of the six lines appearing in the key is the average of AOGCMs for one of the six illustrative scenarios. The region in dark shading shows the range of the average of AOGCMs for all thirty five SRES scenarios. The region in light shading shows the range of all AOGCMs for all thirty five scenarios. The region delimited by the outermost lines shows the range of all AOGCMs and scenarios including uncertainty in land-ice changes, permafrost changes and sediment deposition. Note that this range does not allow for uncertainty relating to ice-dynamic changes in the West Antarctic ice sheet. [Based on Figure 11.12]

F.9 Projections of Future Changes in Sea Level

Projections of global average sea level rise from 1990 to 2100, using a range of AOGCMs following the IS92a scenario (including the direct effect of sulphate aerosol emissions), lie in the range 0.11 to 0.77 m. This range reflects the systematic uncertainty of modelling. The main contributions to this sea level rise are:

- a thermal expansion of 0.11 to 0.43 m, accelerating through the 21st century;
- a glacier contribution of 0.01 to 0.23 m;
- a Greenland contribution of –0.02 to 0.09 m; and
- an Antarctic contribution of –0.17 to +0.02 m.

Also included in the computation of the total change are smaller contributions from thawing of permafrost, deposition of sediment, and the ongoing contributions from ice sheets as a result of climate change since the Last Glacial Maximum. To establish the range of sea level rise resulting from the choice of different SRES scenarios, results for thermal expansion and land-ice change from simple models tuned to several AOGCMs are used (as in Section F.3 for temperature).

For the full set of SRES scenarios, a sea level rise of 0.09 to 0.88 m is projected for 1990 to 2100 (see Figure 24), primarily from thermal expansion and loss of mass from glaciers and ice caps. The central value is 0.48 m, which corresponds to an average rate of about two to four times the rate over the 20th century. The range of sea level rise presented in the SAR was 0.13 to 0.94 m based on the IS92 scenarios. Despite higher temperature change projections in this assessment, the sea level projections are slightly lower, primarily due to the use of improved models which give a smaller contribution from glaciers and ice sheets. If terrestrial storage continues at its current rates, the projections could be changed by –0.21 to 0.11 m. For an average of the AOGCMs, the SRES scenarios give results that differ by 0.02 m or less for the first half of the 21st century. By 2100, they vary over a range amounting to about 50% of the central value. Beyond the 21st century, sea level rise depends strongly on the emissions scenario.

Models agree on the qualitative conclusion that the range of regional variation in sea level change is substantial compared to global average sea level rise. However, confidence in the regional distribution of sea level change from AOGCMs is low because there is little similarity between models, although nearly all models project greater than average rise in the Arctic Ocean and less than average rise in the Southern Ocean. Further, land movements, both isostatic and tectonic, will continue through the 21st century at rates that are unaffected by climate change. It can be expected that by 2100, many regions currently experiencing relative sea level fall will instead have a rising relative sea level. Lastly, extreme high water levels will occur with increasing frequency as a result of mean sea level rise. Their frequency may be further increased if storms become more frequent or severe as a result of climate change.

F.10 Projections of Future Changes in Response to CO_2 Concentration Stabilisation Profiles

Greenhouse gases and aerosols

All of the stabilisation profiles studied require CO_2 emissions to eventually drop well below current levels. Anthropogenic CO_2 emission rates that arrive at stable CO_2 concentration levels from 450 to 1,000 ppm were deduced from the prescribed CO_2 profiles (Figure 25a). The results (Figure 25b) are not substantially different from those presented in the SAR; however, the range is larger, mainly due to the range of future terrestrial carbon uptake caused by different assumptions in the models. Stabilisation at 450, 650 or 1,000 ppm would require global anthropogenic emissions to drop below 1990 levels within a few decades, about a century, or about two centuries, respectively, and continue to steadily decrease thereafter. Although there is sufficient uptake capacity in the ocean to incorporate 70 to 80% of foreseeable anthropogenic CO_2 emissions to the atmosphere, this process takes centuries due to the rate of ocean mixing. As a result, even several centuries after emissions occurred, about a quarter of the increase in concentration caused by these emissions is still present in the atmosphere. To maintain constant CO_2 concentration beyond 2300 requires emissions to drop to match the rate of carbon sinks at that time. Natural land and ocean sinks with the capacity to persist for hundreds or thousands of years are small (<0.2 PgC/yr).

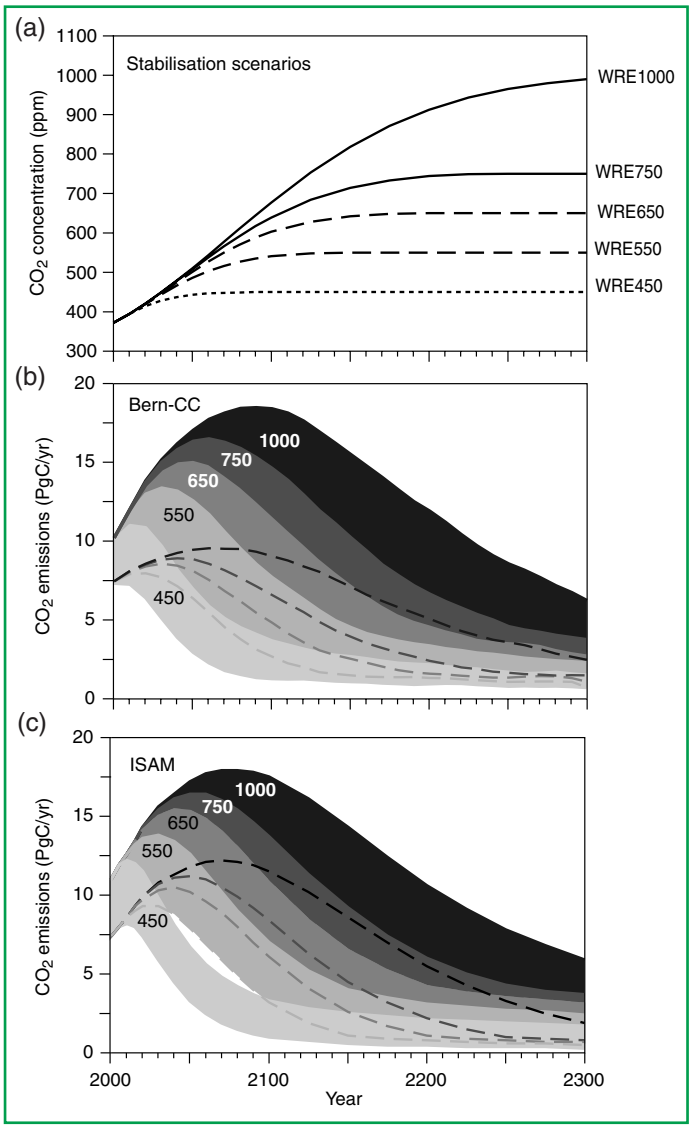

Figure 25: Projcted CO_2 emissions permitting stabilisation of atmospheric CO_2 concentrations at different final values. Panel (a) shows the assumed trajectories of CO_2 concentration (WRE scenarios) and panels (b) and (c) show the implied CO_2 emissions, as projected with two fast carbon cycle models, Bern-CC and ISAM. The model ranges for ISAM were obtained by tuning the model to approximate the range of responses to CO_2 and climate from model intercomparisons. This approach yields a lower bound on uncertainties in the carbon cycle response. The model ranges for Bern-CC were obtained by combining different bounding assumptions about the behaviour of the CO_2 fertilization effect, the response of heterotrophic respiration to temperature and the turnover time of the ocean, thus approaching an upper bound on uncertainties in the carbon cycle response. For each model, the upper and lower bounds are indicated by the top and bottom of the shaded area. Alternatively, the lower bound (where hidden) is indicated by a hatched line. [Based on Figure 3.13]

Temperature

Global mean temperature continues to increase for hundreds of years at a rate of a few tenths of a degree per century after concentrations of CO_2 have been stabilised, due to long time-scales in the ocean. The temperature implications of CO_2 concentration profiles leading to stabilisation from 450 ppm to 1,000 ppm were studied using a simple climate model tuned to seven AOGCMs with a mean climate sensitivity of 2.8°C. For all the pathways leading to stabilisation, the climate system shows considerable warming during the 21st century and beyond (see Figure 26). The lower the level at which concentrations stabilise, the smaller the total temperature change.

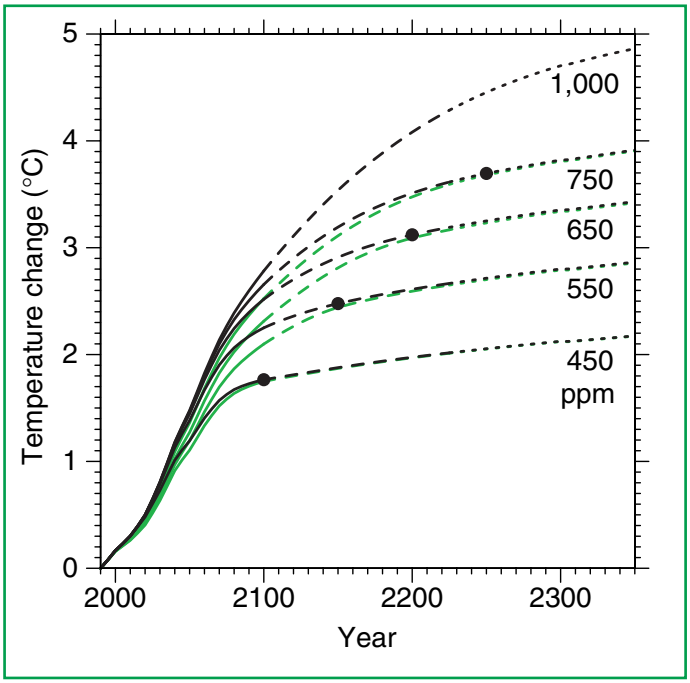

Figure 26: Simple model results: Projected global mean temperature changes when the concentration of CO_2 is stabilised following the WRE profiles (see Chapter 9 Section 9.3.3). For comparison, results based on the S profiles in the SAR are also shown in green (S1000 not available). The results are the average produced by a simple climate model tuned to seven AOGCMs. The baseline scenario is scenario A1B, this is specified only to 2100. After 2100, the emissions of gases other than CO_2 are assumed to remain constant at their A1B 2100 values. The projections are labelled according to the level of CO_2 stabilisation. The broken lines after 2100 indicate increased uncertainty in the simple climate model results beyond 2100. The black dots indicate the time of CO_2 stabilisation. The stabilisation year for the WRE1000 profile is 2375. [Based on Figure 9.16]

Sea level

If greenhouse gas concentrations were stabilised (even at present levels), sea level would nonetheless continue to rise for hundreds of years. After 500 years, sea level rise from thermal expansion may have reached only half of its eventual level, which models suggest may lie within a range of 0.5 to 2.0 m and 1 to 4 m for CO_2 levels of twice and four times pre-industrial, respectively. The long time-scale is characteristic of the weak diffusion and slow circulation processes that transport heat into the deep ocean.

The loss of a substantial fraction of the total glacier mass is likely. Areas that are currently marginally glaciated are most likely to become ice-free.

Ice sheets will continue to react to climatic change during the next several thousand years, even if the climate is stabilised. Together, the present Antarctic and Greenland ice sheets contain enough water to raise sea level by almost 70 m if they were to melt, so that only a small fractional change in their volume would have a significant effect.

Models project that a local annual average warming of larger than 3°C, sustained for millennia, would lead to virtually a complete melting of the Greenland ice sheet with a reulting sea level rise of about 7 m. Projected temperatures over Greenland are generally greater than globally averaged temperatures by a factor of 1.2 to 3.1 for the range of models used in Chapter 11. For a warming over Greenland of 5.5°C, consistent with mid-range stabilisation scenarios (see Figure 26), the Greenland ice sheet is likely to contribute about 3 m in 1,000 years. For a warming of 8°C, the contribution is about 6 m, the ice sheet being largely eliminated. For smaller warmings, the decay of the ice sheet would be substantially slower (see Figure 27).

Current ice dynamic models project that the West Antarctic ice sheet (WAIS) will contribute no more than 3 mm/yr to sea level rise over the next thousand years, even if significant changes were to occur in the ice shelves. Such results are strongly dependent on model assumptions regarding climate change scenarios, ice dynamics and other factors. Apart from the possibility of an internal ice dynamic instability, surface melting will affect the long-term viability of the Antarctic ice sheet. For warmings of more than 10ºC, simple runoff models predict that a zone of net mass loss would develop on the ice sheet surface. Irreversible disintegration of the WAIS would result because the WAIS cannot retreat to higher ground once its margins are subjected to surface melting and begin to recede. Such a disintegration would take at least a few millennia. Thresholds for total disintegration of the East Antarctic ice sheet by surface melting involve warmings above 20ºC, a situation that has not occurred for at least 15 million years and which is far more than predicted by any scenario of climate change currently under consideration.

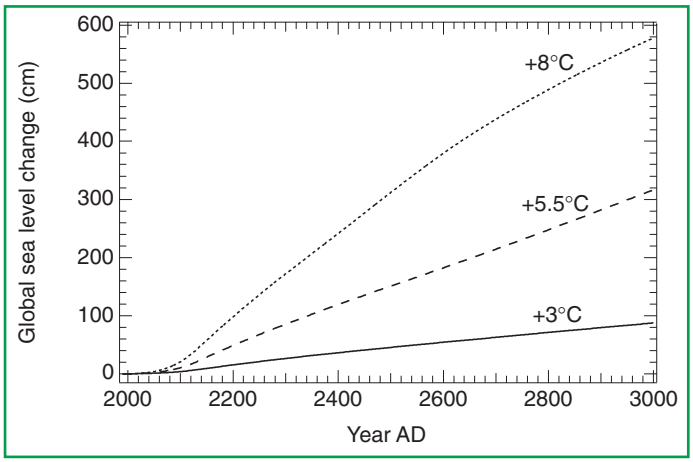

Figure 27: Response of the Greenland ice sheet to three climatic warming scenarios during the third millennium expressed in equivalent changes of global sea level. The curve labels refer to the mean annual temperature rise over Greenland by 3000 AD as predicted by a two-dimensional climate and ocean model forced by greenhouse gas concentration rises until 2130 AD and kept constant after that. Note that projected temperatures over Greenland are generally greater than globally averaged temperatures by a factor of 1.2 to 3.1 for the range of models used in Chapter 11. [Based on Figure 11.16]

G. Advancing Understanding

The previous sections have contained descriptions of the current state of knowledge of the climate of the past and present, the current understanding of the forcing agents and processes in the climate system and how well they can be represented in climate models. Given the knowledge possessed today, the best assessment was given whether climate change can be detected and whether that change can be attributed to human influence. With the best tools available today, projections were made of how the climate could change in the future for different scenarios of emissions of greenhouse gases.

This Section looks into the future in a different way. Uncertainties are present in each step of the chain from emissions of greenhouse gases and aerosols, through to the impacts that they have on the climate system and society (see Figure 28). Many factors continue to limit the ability to detect, attribute, and understand current climate change and to project what future climate changes may be. Further work is needed in nine broad areas.

G.1 Data

Arrest the decline of observational networks in many parts of the world. Unless networks are significantly improved, it may be difficult or impossible to detect climate change in many areas of the globe.

Expand the observational foundation for climate studies to provide accurate, long-term data with expanded temporal and spatial coverage. Given the complexity of the climate system and the inherent multi-decadal time-scale, there is a need for long-term consistent data to support climate and environmental change investigations and projections. Data from the present and recent past, climate-relevant data for the last few centuries, and for the last several millennia are all needed. There is a particular shortage of data in polar regions and data for the quantitative assessment of extremes on the global scale.

G.2 Climate Processes and Modelling

Estimate better future emissions and concentrations of greenhouse gases and aerosols. It is particularly important that improvements are realised in deriving concentrations from emissions of gases and particularly aerosols, in addressing biogeochemical sequestration and cycling, and specifically, and in determining the spatial-temporal distribution of CO_2 sources and sinks, currently and in the future.

Understand and characterise more completely dominant processes (e.g., ocean mixing) and feedbacks (e.g., from clouds and sea ice) in the atmosphere, biota, land and ocean surfaces, and deep oceans. These sub-systems, phenomena, and processes are important and merit increased attention to improve prognostic capabilities generally. The interplay of observation and models will be the key for progress. The rapid forcing of a non-linear system has a high prospect of producing surprises.

Address more completely patterns of long-term climate variability. This topic arises both in model calculations and in the climate system. In simulations, the issue of climate drift within model calculations needs to be clarified better in part because it compounds the difficulty of distinguishing signal and noise. With respect to the long-term natural variability in the climate system per se, it is important to understand this variability and to expand the emerging capability of predicting patterns of organised variability such as ENSO.

Explore more fully the probabilistic character of future climate states by developing multiple ensembles of model calculations. The climate system is a coupled non-linear chaotic system, and therefore the long-term prediction of future exact climate states is not possible. Rather the focus must be upon the prediction of the probability distribution of the system's future possible states by the generation of ensembles of model solutions.

Improve the integrated hierarchy of global and regional climate models with emphasis on improving the simulation of regional impacts and extreme weather events. This will require improvements in the understanding of the coupling between the major atmospheric, oceanic, and terrestrial systems, and extensive diagnostic modelling and observational studies that evaluate and improve simulative performance. A particularly important issue is the adequacy of data needed to attack the question of changes in extreme events.

G.3 Human Aspects

Link more formally physical climate-biogeochemical models with models of the human system and thereby provide the basis for expanded exploration of possible cause-effect-cause patterns linking human and non-human components of the Earth system. At present, human influences generally are treated only through emission scenarios that provide external forcings to the climate system. In future more comprehensive models are required in which human activities need to begin to interact with the dynamics of physical, chemical, and biological sub-systems through a diverse set of contributing activities, feedbacks and responses.

G.4 International Framework

Accelerate internationally progress in understanding climate change by strengthening the international framework that is needed to co-ordinate national and institutional efforts so that research, computational, and observational resources may be used to the greatest overall advantage. Elements of this framework exist in the international programmes supported by the International Council of Scientific Unions (ICSU), the World Meteorological Organization (WMO), the United Nations Environment Programme (UNEP), and the United Nations Education, Scientific and Cultural Organisation (UNESCO). There is a corresponding need for strengthening the co-operation within the international research community, building research capacity in many regions and, as is the goal of this assessment, effectively describing research advances in terms that are relevant to decision making.

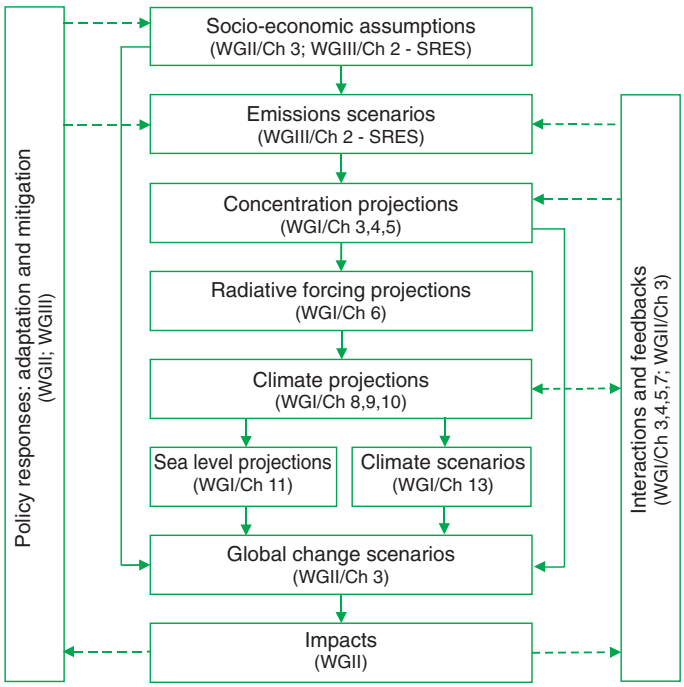

Figure 28: The cascade of uncertainties in projections to be considered in developing climate and related scenarios for climate change impact, adaptation, and mitigation assessment. [Based on Figure 13.2]

Source Information: Technical Summary

This Appendix provides the cross-reference of the topics in the Technical Summary (page and section) to the sections of the chapters that contain expanded information about the topic.

Section A: Introduction

TS Page	Technical Summary Section and Topic – Chapter Section
22	*A.1 The IPCC and its Working Groups* Introduction to the Intergovernmental Panel on Climate Change (from the IPCC Secretariat, Geneva) or the IPCC web page at http://www.ipcc.ch
22 – 23	*A.2 The First and Second Assessment Reports of Working Group I* IPCC, 1990a: Climate Change: The IPCC Scientific Assessment. J.T. Houghton, G.J. Jenkins and J.J. Ephraums (eds.), Cambridge University Press, Cambridge, United Kingdom, 365 pp. IPCC, 1992: Climate Change 1992: The Supplementary Report to the IPCC Scientific Assessment. J.T. Houghton, B.A. Callander and S.K. Varney (eds.), Cambridge University Press, Cambridge, United Kingdom, 198 pp. IPCC, 1994: Climate Change 1994: Radiative Forcing of Climate Change and an Evaluation of the IPCC IS92 Emission Scenarios. J.T. Houghton, L.G. Meira Filho, J. Bruce, Hoesung Lee, B.A. Callander, E. Haites, N. Harris and K. Maskell (eds.), Cambridge University Press, Cambridge, United Kingdom, 339 pp. IPCC, 1996a: Climate Change 1995: The Science of Climate Change. Contribution of Working Group I to the Second Assessment Report of the Intergovernmental Panel on Climate Change [Houghton, J.T., L.G. Meira Filho, B.A. Callander, N Harris, A. Kattenberg, and K. Maskell (eds.)]. Cambridge University Press, Cambridge, United Kingdom and New York, NY, USA, 572 pp.
23 – 24	*A.3 The Third Assessment Report: This Technical Summary* Background to these questions is in Chapter 1. Box 1: What drives changes in climate? – Chapter 1.

Section B: The Observed Changes in the Climate System

TS Page	Technical Summary Section and Topic – Chapter Section
26 – 29	*B.1 Observed Changes in Temperature* Temperatures in the instrumental record for land and oceans – Chapter 2.2.2 and 2.3. Temperatures above the surface layer from satellite and weather balloon records – Chapter 2.2.3 and 2.2.4. Surface temperatures during the pre-instrumental record from the proxy record Last 1,000 years – Chapter 2.3. Last glacial and deglaciation – Chapter 2.4.
30	*B.2 Observed Changes in Precipitation and Atmospheric Moisture* Annual land-surface precipitation – Chapter 2.5.2. Water vapour – Chapter 2.5.3. Cloud amounts – Chapter 2.5.5.
30	*B.3 Observed Changes in Snow Cover and Land- and Sea-Ice Extent* Snow cover and land-ice extent – Chapter 2.2.5. Sea-ice extent – Chapter 2.2.5. Arctic sea-ice thickness – Chapter 2.2.5.
31 – 32	*B.4 Observed Changes in Sea Level* Changes During the Instrumental Record Tide gauge data for the 20th century – Chapter 11.3.2. Box 2: What causes sea level to change? – Chapter 11.2. Changes during the pre-instrumental record – Chapter 11.3.1.
32 – 33	*B.5 Observed Changes in Atmospheric and Oceanic Circulation Patterns* El Niño-Southern Oscillation (ENSO) – Chapter 2.6.2 and 2.6.3. North Atlantic, Arctic, and Antarctic oscillations – Chapter 2.6.5 and 2.6.6.
33	*B.6 Observed Changes in Climate Variability and Extreme Weather and Climate Events* Heavy and extreme precipitation – Chapter 2.7.2. Tropical and extra-tropical storms – Chapter 2.7.3.
33	*B.7 The Collective Picture: A Warming World and Other Changes in the Climate System* A warming world – Chapter 2.8. Little or no change – Chapter 2.2.5 and 2.7.3.

Section C: The Forcing Agents That Cause Climate Change

Section D: The Simulation of the Climate System and Its Changes

Section E: The Identification of a Human Influence on Climate Change

Section F: The Projections of the Earth's Future Climate

Section G: Advancing Understanding